"Molecular mechanisms of shikonin and its derivatives in cancer therapy"

Dissertation

zur Erlangung des Grades

"Doktor der Naturwissenschaften" im

Promotionsfach Pharmazie

am Fachbereich Chemie, Pharmazie und Geowissenschaften der
Johannes Gutenberg-Universität in Mainz

vorgelegt von Qiaoli Zhao

geboren am ███████████████████

Mainz, August 2015

Betreuer: ███████████████

Gutachter der Arbeit: ██████████████

██████████████████

Datum der mündlichen Prüfung: 16.09.2015

Prüfer: ██████████████

████████████████

█████████████

D77 (Dissertation Universität Mainz)

Erklärung

Hiermit erkläre ich an Eides statt, dass ich diese Arbeit selbständig verfasst und keine anderen als die angegebenen Quellen und Hilfsmittel verwendet habe.

Mainz, 10.08.2015   Keine Unterschrift zwecks Datenschutz

———————————————   ———————————————

Ort, Datum   Qiao Zhao

Acknowledgement

My deepest gratitude goes first and foremost to ██████████████, my supervisor. The acceptance letter from him to a PhD position opened the door for me to study in an excellent group full of scientific and international atmosphere and to experience a different life in a great and beautiful country – Germany where the people are friendly and intelligent. The way to completion of this thesis is never easy. He has walked me through all the stages of my PhD projects. Without his constant guidance, illuminating views and encouragement during the crossroads and challenges in the research projects, this dissertation could not have reached its present form.

I would like to thank ██████████████ and ██████████████ for reviewing my thesis and taking part in my defense.

Many thanks to ██████████████ and ██████████████ for providing us with the substances and for valuable suggestion on my paper. I also thank ██████████████ and ██████████████ for their kind offer of cell lines being required.

I am thankful for ██████████ at the IMB for his help and patience in answering my questions concerning flow cytometry.

I express my warmest gratitude to all team members of the Department of Pharmaceutical Biology. Thanks to ██████████ who taught me the first lesson in cell culture and put great effort to establish and maintain a favorable experimental circumstances in cell culture lab for us. Thank ██████████ for her willing to help whenever asked for and our secretary ████ for her help with university registration and housing problem, as well as ██████████ for his support in camera and computer problems. Many thanks to ██████████, ██████, ██████████, ██████████, ████████, ██████████████ and ██████████ for sharing their expertise and instructive opinions on a number of issues related to my work. Special thanks go to ██████████ and ██████████g for the numerous pleasant and inspiring discussions, for the sincere and valuable advices and motivation, and for all the fun we have had in the last years. The friendship between us is a true harvest for my life and something I could always count on.

I thank the diploma student ███████████ for her help in the lab.

Much gratitude is entitled to the ████████████████████ for the financial support throughout my PhD.

I am also grateful for ██████████ who gave me a lot of help at the beginning of my life in Germany. Her trustful translation and precious suggestion have made my initial time abroad much more smooth and easier. And she has become an important and good friend of mine since then.

I owe my heartfelt thanks to my beloved parents and my family. Your endless love, support and confidence for me were what sustained me thus far. Much sincere gratitude also goes to my friends ██████████, ██████, ██████████, ████████████ and ████████████. The talk with you always added much joy and comfort to my life, which later on filled me with plenty of enthusiasm and courage to strive towards my goal.

Last but not least, I would like to express appreciation to my better half ████████ who spent sleepless nights, patience and understanding with me. Thank you for sharing my journey with true soul companions.

Abstract

The identification of molecular processes involved in cancer development and prognosis opened avenues for targeted therapies, which made treatment more tumor-specific and less toxic than conventional therapies. One important example is the epidermal growth factor receptor (EGFR) and EGFR-specific inhibitors (i.e. erlotinib). However, challenges such as drug resistance still remain in targeted therapies. Therefore, novel candidate compounds and new strategies are needed for improvement of therapy efficacy. Shikonin and its derivatives are cytotoxic constituents in traditional Chinese herbal medicine *Zicao (Lithospermum erythrorhizin).* In this study, we investigated the molecular mechanisms underlying the anti-cancer effects of shikonin and its derivatives in glioblastoma cells and leukemia cells. Most of shikonin derivatives showed strong cytotoxicity towards erlotinib-resistant glioblastoma cells, especially U87MG.ΔEGFR cells which overexpressed a deletion-activated EGFR (ΔEGFR). Moreover, shikonin and some derivatives worked synergistically with erlotinib in killing EGFR-overexpressing cells. Combination treatment with shikonin and erlotinib overcame the drug resistance of these cells to erlotinib. Western blotting analysis revealed that shikonin inhibited ΔEGFR phosphorylation and led to corresponding decreases in phosphorylation of EGFR downstream molecules. By means of Loewe additivity and Bliss independence drug interaction models, we found erlotinb and shikonin or its derivatives corporately suppressed ΔEGFR phosphorylation. We believed this to be a main mechanism responsible for their synergism in U87MG.ΔEGFR cells. In leukemia cells, which did not express EGFR, shikonin and its derivatives exhibited even greater cytotoxicity, suggesting the existence of other mechanisms. Microarray-based gene expression analysis uncovered the transcription factor c-MYC as the commonly deregulated molecule by shikonin and its derivatives. As validated by Western blotting analysis, DNA-binding assays and molecular docking, shikonin and its derivatives bound and inhibited c-MYC. Furthermore, the deregulation of ERK, JNK MAPK and AKT activity was closely associated with the reduction of c-MYC, indicating the involvement of these signaling molecules in shikonin-triggered c-MYC inactivation. In conclusion, the inhibition of EGFR signaling, synergism with erlotinib and targeting of c-MYC illustrate the multi-targeted feature of natural naphthoquinones such as shikonin and derivatives. This may open attractive possibilities for their use in a molecular targeted cancer therapy.

Zusammenfassung

Die Identifizierung molekularer Prozesse der Krebsentstehung und -prognose eröffnet zahlrahlreiche Möglichkeiten für zielgerichtete Therapien, welche Tumor-spezifischer und weniger toxisch sind als konventionelle Methoden. Ein wichtiges Beispiel ist der epidermale Wachstumsfaktor-Rezeptor (EGFR) und EGFR-spezifische Hemmstoffe (z.B. Erlotinib). Jedoch bleibt das Problem der Medikamentenresistenz auch bei zielgerichteten Therapien bestehen. Deshalb weden neue Kandidatensubstanzen und neue Strategien zur Verbesserung der Therapieeffizienz benötigt. Shikonin und seine Derivate sind zytotoxische Inhaltsstoffe der traditional chinesischen Heilpflanze *Zicao* (*Lithospermum erythrorhizon*). In dieser Dissertation untersuchten wir die zugrundeliegenden molekularen Mechanismen der antitumoralen Wirkung von Shikonin und seinen Derivaten in Glioblastom- und Leukämiezellen. Die meisten Shikoninderivate zeigten eine starke Zytotoxizität gegenüber Erlotinib-resistenten Glioblastomzellen-besonders gegenüber U87.MGΔEGFR Zellen, welche einen deletions-aktivierten EGFR (ΔEGFR) exprimierten. Darüber hinaus wirkten Shikonin und einige Derivate zusammen mit Erlotinib synergistisch bei der Abtötung von U87.MGΔEGFR Zellen. Die Kombinationsbehandlung mit Shikonin und Erlotinib überwand die Resistenz dieser Zellen zu Erlotinib. Western-Blot Analysen zeigten, dass Shikonin die ΔEGFR-Phosphorylierung hemmte und dass die Phosphorylierung EGFR-nachgeschalteter Moleküle ebenfalls sank. Mittels Loewe Additivitäts- und Bliss unabhängige Medikamenten-Interaktions-Modellen fanden wir, dass Erlotinib und Shikonin (bzw. seine Derivate) gemeinsam die ΔEGFR-Phosphorylierung hemmten. Wir glauben, dass das der Hauptmechanismus ist, welcher für den Synergismus in U87.MGΔEGFR Zellen verantwortlich ist. In Leukämiezellen, welche kein EGFR exprimieren, wiesen Shikonin und seine Derivate sogar noch höhere Zytotoxizitäten auf, was auf die Existenz anderer Mechanimen hindeutet. Microarray-basierte Genexpressionsanalysen deckten den Transkriptionsfaktor c-MYC als gemeisam dereguliertes Molekül durch Shikonin und seine Detivate auf. Wie durch Western-Blot Analysen, DNA-Bindungs-Assays und molekulares Docking bestätigt wurde, banden und hemmten Shikonin und Derivate c-MYC. Weiterhin war eine Deregulation der ERK, JNK, MAPK und AKT Aktivität eng assoziiert mit einer c-MYC Reduktion. Dies weist auf eine Einbindung dieser Signalmoleküle in die Shikonin-gesteuerte c-MYC Inaktivierung hin. Zusammenfassend veranschaulicht die Hemmung von EGFR-Signalwegen, der Synergismus mit Erlotinib sowie die zielgerichtete Bindung an c-MYC die multi-*Target* Eigenschaften natürlich vorkommender Naphthochinone wie Shikonin und seine Derivate. Dies eröffnet attraktive Möglichkeiten für deren Gebrauch in der molekularen, zielgerichteten Krebstherapie.

Table of Contents

List of Abbreviations

Abbreviation	Connotation
ABC	ATP binding cassette
ABCB1	ATP-binding cassette sub-family B member 1/P-glycoprotein/MDR1
Abl	Abelson tyrosine protein kinase
ADP	Adenosine diphosphate
Akt	Murine thymoma viral oncogene homolog
AML	Acute myeloid leukemia
ALL	Acute lymphocytic leukemia
APS	Ammonium persulfate
ARF	ADP Ribosylation Factors
ATCC	American Type Culture Collection
ATP	Adenosine triphosphate
Bax	Bcl-2-associated X protein
Bcl-2	B-cell CLL/lymphoma 2
BCR	Breakpoint cluster region
BD	Becton Dickinson
BET	Bromodomain and extraterminal domain
BH3	Bcl-2 homology 3
bHLH-Lz	Basic helix-loop-helix leucine zipper
BSA	Bovine serum albumin
C lobe	Carboxy-terminal lobe
CAK	CDK-activating kinase
CD	Cluster of differentiation
CDC25	Cell division cycle 25
CDK	Cyclin dependent kinases
cDNA	Complementary DNA
cRNA	Complementary RNA
CI	Combination index
CTD	Carboxy-termianl domain
CTLA4	Cytotoxic T-lymphocyte-associated protein 4
DAG	Diacylglycerol
DKFZ	German Cancer Research Center
DMEM	Dulbecco's modified eagle medium
DMSO	Dimethyl sulfoxide
DNA	Deoxyribonucleic acid
DPBS	Dulbecco's phoshpate-buffered saline
E2F	E2 promoter binding factor
E-box	Enhancer box
EDTA	Ethylene diamine tetraacetic acid
EGFR	Epidermal growth factor receptor

ELISA	Enzyme linked immunosorbent assay
ERK	Extracellular signal-regulated kinases
FACS	Fluorescence-activated cell sorting
FBS	Fetal bovine serum
FDA	US Food and Drug Administration
FITC	Fluorescein isothiocyanate
GBM	Glioblastoma multiforme
GSK-3	Glycogen synthase kinase-3
HER1	Human epidermal growth factor receptor type 1/EGFR/ErbB1
HER2/neu	Human epidermal growth factor receptor type 2
HGF	Hepatocyte growth factor
HIV	Human Immunodeficiency Virus
HRP	Horseradish peroxidase
IC_{50}	Half maximal inhibitory concentration
IPA	Ingenuity Pathway Analysis
JAK	Janus-activated kinase
JNK	Jun N-terminal Kinase
MAD	Median absolute deviation
MAD1	Mitotic arrest deficient 1
MAPK	Mitogen-activated protein kinase
MAX	Myc-associated factor X
MDM2	Mouse double minute 2 homolog
MDR	Multidrug resistance
MDR1	Multidrug resistance protein 1/ABCB1/P-glycoprotein
MEK	Mitogen-activated protein kinase kinase
MGMT	O^6-methylguanine-DNA-methyltransferase
mRNA	Messenger ribonucleic acid
MS4A3	Membrane-spanning 4-domains, subfamily A, member 3
mTOR	Mammalian target of rapamycin
MYB	v-myb Avian myeloblastosis viral oncogene homolog
MYC	c-myc Avian myelocytomatosis viral oncogene homolog
Nec-1	Necrostatin-1
NF-kB	Nuclear factor of kappa light polypeptide gene enhancer in B-cells
NK	Natural killer
NSCLC	Non-small-cell lung cancer
P53	Tumor protein 53/TP53
PARP	Poly (ADP-ribose) polymerase
PCNA	Proliferating cell nuclear antigen
PCR	Polymerase chain reaction
PDB	Protein data bank
P-gp	P-glycoprotein
PI	Propidium iodide

PI3K	Phosphatidylinositol 3-kinase
PKC	Protein kinase C
PLC	Phospholipase C
PS	Phosphatidylserine
PTEN	Phosphatase and tensin homolog
PVDF	Polyvinyl difluoride
RAC1	Ras-related C3 botulinum toxin substrate 1
Raf	Rapidly accelerated fibrosarcoma proto-oncogene
Ras	Rat sarcoma viral oncogene homolog
RIP	Receptor interacting protein
RNA	Ribonucleic acid
ROS	Reactive oxygen species
RPMI 1640	Roswell Park Memorial Institute 1640
RT-PCR	Reverse transcription PCR
S-180	Sarcoma 180
SAPK	Stress-activated protein kinases
SDS-PAGE	Sodium dodecyl sulfate-polyacrilamide gel electrophoresis
SEM	Standard error of mean
SNP	Single nucleotide polymorphism
Src	Sarcoma proto-oncogene tyrosine-protein kinase
STAT	Signal transducer and activator of transcription
STR	Short tandem repeat
TAD	Transcriptional activation domain
TBST	Tris-buffered saline-Tween20
TCM	Traditional Chinese Medicine
TEMED	Tetramethylenediamine
TGF	Transforming growing factor
TK	Tyrosine kinase
TKIs	Tyrosine kinase inhibitors
Tris	Tris (hydroxymethyl) aminomethane
ULBP	UL-16 binding proteins
VEGF	Vascular endothelial growth factor
VMD	Visual Molecular Dynamics
WHO	World Health Organization

1   Introduction

1.1   General information about Cancer

According to the World Cancer Report 2014 published by the World Health Organization (WHO), cancer is now the leading cause of morbidity and mortality worldwide, accounting for 14.1 million new cases and 8.2 million deaths in 2012, among which about a quarter of the incidence burden and mortality proportions occur in Europe and China [1]. With the continuing growth and aging of the world's population, the predicted global cancer burden is expected to exceed 20 million new cancer cases and 12 million deaths annually by 2025 [2].
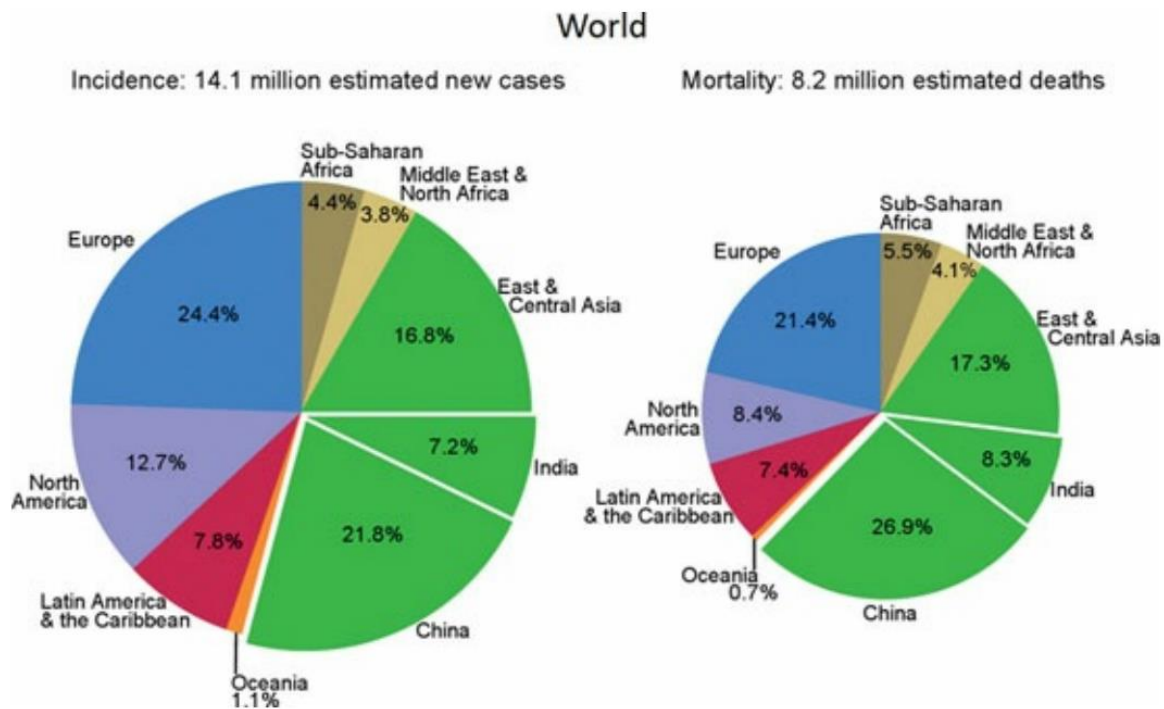
Figure 1: Estimated world cancer incidence and mortality proportions by major world regions, in both sexes combined, 2012. Image taken from Stewart and Wild [1].

Cancer, also known as malignant neoplasm, has more than 100 different types, which roughly fall into two categories: solid and hematological malignancies. Solid tumors are abnormal mass of tissue usually free of cysts or liquid areas and formed by cells which may stem from different tissue types such as brain, breast, lung or liver. They initially grow in the organ of its cellular origin and may spread to other organs through metastatic growth in advanced stages. Hematological malignancies are cancer types that occur in cells of the immune system like

lymph nodes or in blood-forming tissues including bone marrow. Examples of hematologic cancers are acute and chronic leukemia, lymphomas, multiple myeloma [3]. All various types of cancers are fundamentally characterized by uncontrolled growth and spread of abnormal cells. Carcinogenesis, the term for formation of a cancer, is a complex, multistep, multipath process that usually initiates with a genetic alteration, which causes either the activation of proto-oncogenes or the inactivation of tumor-suppressor genes, leading to abnormal proliferation of a single cell [4]. By the selective clonal expansion of initiated cells and further several genetic mutations, tumor cells continuously become more aggressive, rapid-growing and increasingly malignant, ultimately the invasion of cancerous cells into regional tissues as well as metastatic spread of cancerous cells to distant locations result in life-threatening consequences overtime [5]. The causes responsible for initial genetic mutations and cancer development lie in inherited genetic defects but mostly in environmental factors, such as exposure to radiation, chemicals, smoke and pollution, or infection by viruses, *e.g.* hepatitis B [6]. The rising tendency of cancer incidence and mortality forces the humanity to work more on the cancer prevention and treatments.
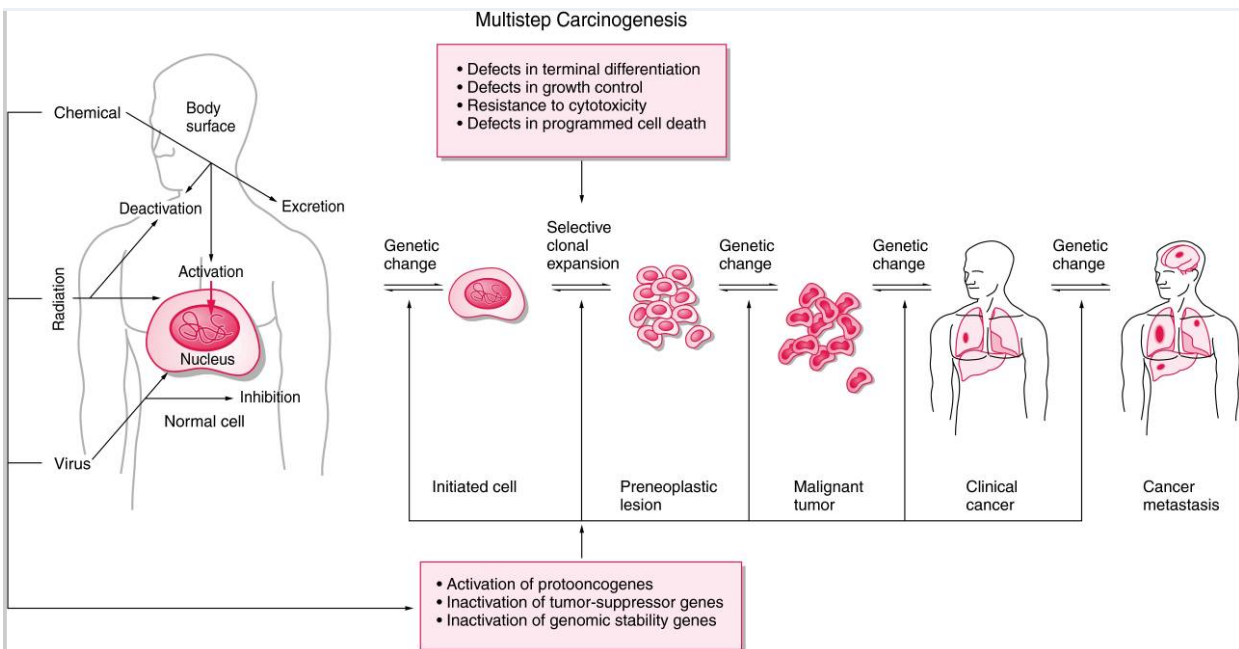
Figure 2: Multistage carcinogenesis. Conceptually four stages involved: tumor initiation, tumor promotion, malignant conversion, and tumor progression. Image taken from Kufe *et al* [5].

1.2   Cancer treatment

Cancer is not a new disease, during centuries of struggle against it, especially in the last hundred years, various treatment modalities containing surgery, radiation therapy, chemotherapy, immunotherapy, hormone therapy and new option targeted therapy had been discovered and developed to effectively counterattack cancers. Which strategy to use for a certain cancer lies on the type, localization and grade of the cancer as well as the patient's health and wishes. Usually a combination of treatments, such as surgery with chemotherapy and/or radiation therapy, is applied in clinic to fulfill the ultimate goal of curing the disease, prolonging life and improving quality of life [7]. The following paragraphs will focus on the chemotherapy and the recently emerged mechanism-based target therapy.

1.2.1 Chemotherapy

The use of chemicals to treat disease was termed 'chemotherapy' in 1914 by the famous German chemist Paul Ehrlich [8]. However, it is not until 1940s when a compound called nitrogen mustard was found to work against lymphoma and make marked regression in lymphoma patients, the chemotherapy stepped into the landscape of cancer treatment and ended the age when surgery and radiotherapy were the only effective way to fight tumor growth [8]. More importantly, the appearance of cancer chemotherapy enabled metastatic cancers curable for the first time. Over the years, more than one hundred chemotherapy drugs have been successfully developed and available now in clinics to treat many types of cancers. They are often used as an adjuvant treatment after surgery or radiation therapy to maintain and strengthen the therapeutic effect by destroying any remaining cancer cells in the body. When applied before surgery or irradiation therapy as neoadjuvant treatment, they help to shrink tumors for further operation. The general principle for classic chemotherapeutic agents is to interrupt with cell division-related metabolic processes such as DNA, RNA, and protein biosynthesis [9]. Based on their specific biochemical structure and mode of action, cancer chemotherapy drugs fall into a small number of broad categories including: alkylating agents (e.g. cyclophosphamide and mitozolomide), heavy metals (e.g. cisplatin and oxaliplatin), antimetabolites (e.g. pyrimidine analogues), cytotoxic antibiotics (e.g. anthracyclines), spindle poisons (e.g. *Vinca* alkaloids), toxoids and topoisomerase inhibitors [10]. Due to wide effect in the treatment of cancer,

chemotherapy remains the backbone of current treatment. But there are also a number of limitations in their safety profile and efficacy. Because these chemotherapeutic agents mainly affect rapidly dividing cells, some normal cells that grow actively (e.g. blood, mouth, intestines and hair) will also be compromised by chemotherapy drugs. Consequently, the resulting severe side effect such as bleeding problems, mucositis, gastrointestinal distress, dramatic hair loss and so on, lead to a narrow therapeutic index for most chemotherapeutic agents [11]. Therefore, a new generation of anti-cancer drugs with more tumor-specificity and fewer side effects has been designed over the past decades, beginning the era of 'targeted therapy'.

1.2.2 Targeted cancer therapy

The advent of targeted therapy is inseparable from the tremendous advances in understanding of the molecular biology of cancers. The hallmarks that are necessary for tumor growth and progression include resistance to cell death, self-dependence on positive regulatory signals, avoidance of growth suppressors and immune destruction, limitless replicative potential, capability of inducing angiogenesis and deregulating cellular energetics, and the ability to invade and establish distant metastasis [12]. Treatment with drugs that target certain specific molecules or signaling pathways that play a crucial role in these hallmarks is so called targeted therapy. Currently more than 30 targeted therapy drugs are available in clinical use. They have become an important component of treatment for many types of cancer, such as breast, colorectal, lung, and pancreatic cancers, as well as lymphoma, leukemia, and multiple myeloma[13]. Most of them counter cancer cell growth by targeting members from epidermal receptor family (e.g. EGFR and HER2/neu), pro-angiogenic factors (e.g. VEGF), proteasomes, the fusion protein BCR-Abl or cluster of differentiation (CD) system. Meanwhile, there is a deep pipeline of candidate drugs under development for either these proven valuable targets or some new promising targets, such as c-MYC [14, 15], PI3K pathway [16], PARP [17] and so on [18]. Figure 3 gives an overview of some targeted therapy drugs that are in clinical trials or have been approved for clinical use against the therapeutic targeting of the hallmarks of cancer [12]. Detailed introductions to two attractive molecules, EGFR and c-MYC, as drug targets for cancer therapy can be found in chapter 1.4 and 1.5.
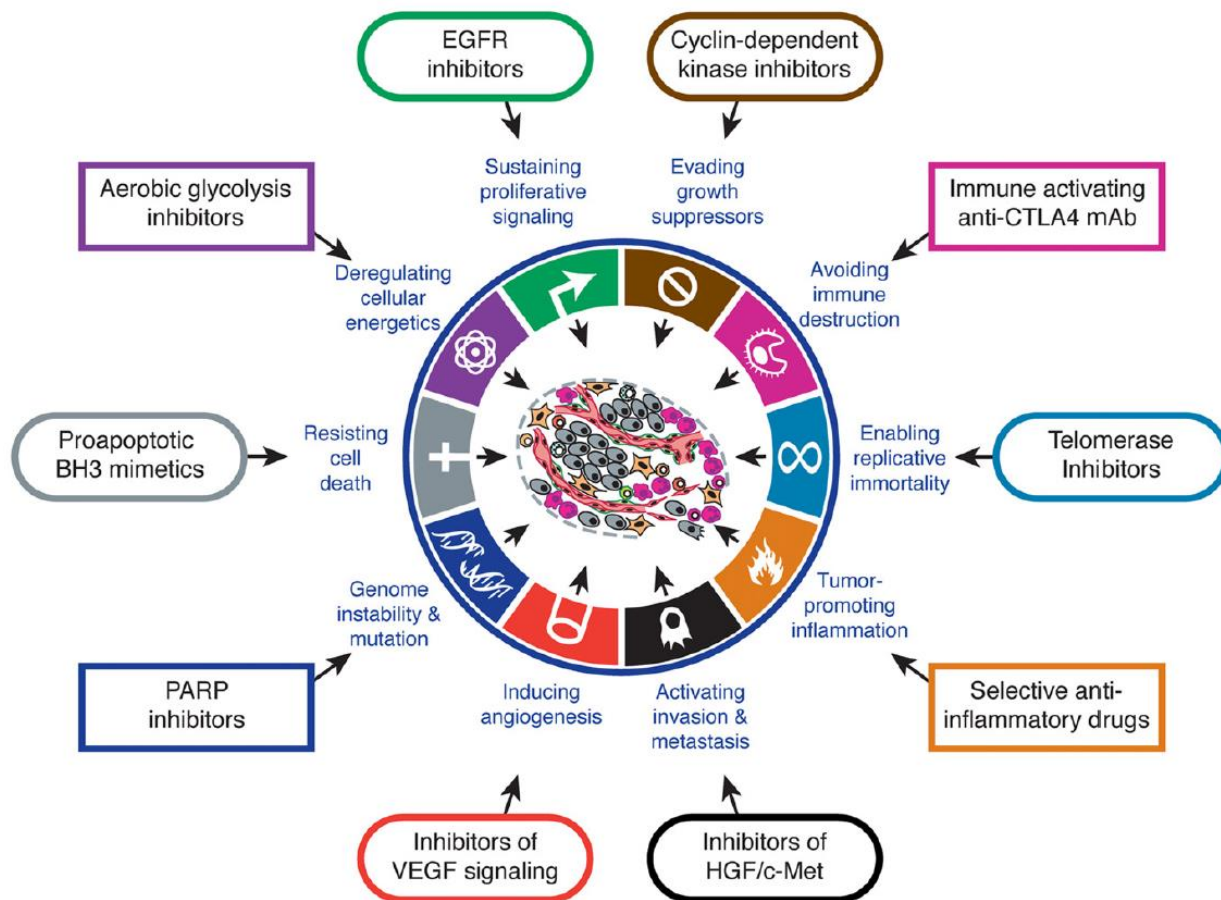
Figure 3: Categories for targeted therapeutics according to their respective effects on the hallmark capabilities of cancer cell. Image taken from Hanahan and Weinberg [12].

1.2.3 Drug resistance and combination cancer therapy

Despite targeted cancer therapy drugs have achieved great successes in the last 20 years, they also suffer from a considerable failure rate as chemotherapeutic agents, in large part due to the development of drug resistance, which is a fundamental problem and limitation facing all successful cancer therapies [19]. In nearly 50% of all cancer types, resistance to chemotherapy/targeted therapy is already present prior to drug administration (intrinsic resistance), and the large proportion of the remaining half will develop resistance during treatment (acquired resistance) [20]. The mechanisms of acquired drug resistance to classic chemotherapies and targeted drugs are generally similar and can be broadly divided into two groups: genetic and non-genetic [21, 22]. Genetic mechanisms virtually result from tumor cell

heterogeneity. Under the selective pressure (e.g. drug treatment), they readily develop mutations that can confer resistance in their genome and rapidly equip this resistance for whole population by clonal expansion, leading to lack of response to treatment. Genetic alterations responsible for drug resistance mainly include mutation to drug targets, activation or loss of downstream signaling components and activation of alternative compensatory signaling pathways [22]. For example, advanced non-small-cell lung cancer (NSCLC) patients who initially show marked responses to EGFR tyrosine kinase inhibitors (TKIs) develop resistance to them within ∼12 months due to a secondary mutation in the EGFR kinase domain (T790M), which increases the affinity for ATP and weakens the affinity for ATP-competitive inhibitors, and the activation of an alternative oncogene able to compensate for the inhibited signaling pathways [23-25]. Although remaining less characterized, a number of non-genetic mechanisms also contribute to the acquisition of resistance to cancer drugs, among which tumor microenvironment and cancer stem cells play the most significant roles [22].

Another most prevalent and important resistance mechanism for both chemotherapies and targeted therapies is increased drug efflux, which is mainly mediated by the ATP-binding cassette (ABC) transporters. These transporters are transmembrane proteins utilizing the energy of ATP hydrolysis to regulate drug efflux and thus reduce intracellular drug levels below their therapeutic threshold. A large number of structurally and mechanistically unrelated anti-cancer drugs such as taxanes, topoisomerase inhibitors, antimetabolites and EGFR inhibitors, can be recognized and excluded from cells by ABC transporters [21], therefore they are considered to be the principle mechanism of multidrug resistance (MDR) [26]. P-glycoprotein (P-gp, also known as multidrug resistance protein 1, MDR1 and ABCB1) is the first identified and best characterized member of all 49 ABC transporters [27]. Overexpression of P-gp, is frequently associated with the intrinsic resistance in many cancers, such as hepatoma, lung and colon carcinomas [28]. Moreover, the expression of P-gp can be induced by anti-cancer agents, thus also leading to the acquired development of MDR [29]. Figure 4 illustrates the major mechanisms of cancer cells against anticarcinogens.
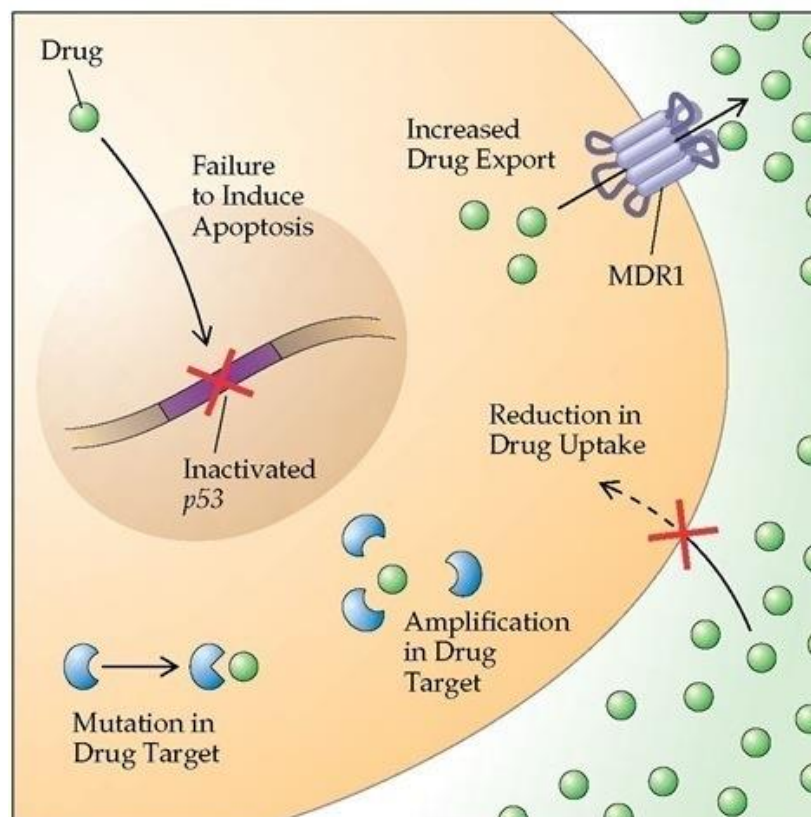
Figure 4: Resistance mechanisms of tumor cells to anti-cancer agents. Genetic alterations such as mutations in the target and inactivated p53 gene, which inhibits apoptotic signaling pathways and repairs of drug induced DNA-damage; decreased drug influx; increased drug efflux by MDR1-related proteins or a compensatory amplification in the amounts of the cellular drug target contribute to the development of drug resistant. Image taken from http://what-when-how.com/acp-medicine/molecular-genetics-of-cancer-part-4/.

To conquer polygenic cancer drug resistance, rational combination therapy, which in this context refers to the use of two or more drugs to fight the same disease, may be the best solution. The rationale for combination therapy is to use drugs that act by different mechanisms, thereby broadening target spectrum and increasing therapeutic effectiveness while decreasing the likelihood of drug resistance [30]. When treated with one drug alone, a cancer cell that develops a mutation that confers resistance to the drug will acquire proliferative advantage, which finally leads to the tumor relapses. By that time switching to a second drug is likely to no avail since a cell resistant to both drugs may have already emerged. But during combination therapy (using both drugs simultaneously), cells that are singly resistant to either drug will be eliminated by the other drug immediately, which therefore reduces the chance of a doubly mutated cell emerging

and improves the cure rates [31]. (Figure 5) A classic example of combination therapy is using a 'drug cocktail' to treat HIV, which successfully tackle the drug resistance problem in HIV [32]. In cancer therapy, the application of combination therapy was inspired in the 1960s when doctors successfully combined the antifolate methotrexate, tubulin inhibitor vincristine, the purine nucleotide synthesis inhibitor 6-mercaptoturine and the steroidal agent prednisone to treat pediatric leukemia [30]. Later on, it extended to and became the standard of care for Hodgkin's lymphoma, testicular cancer and epithelial malignancies [32].
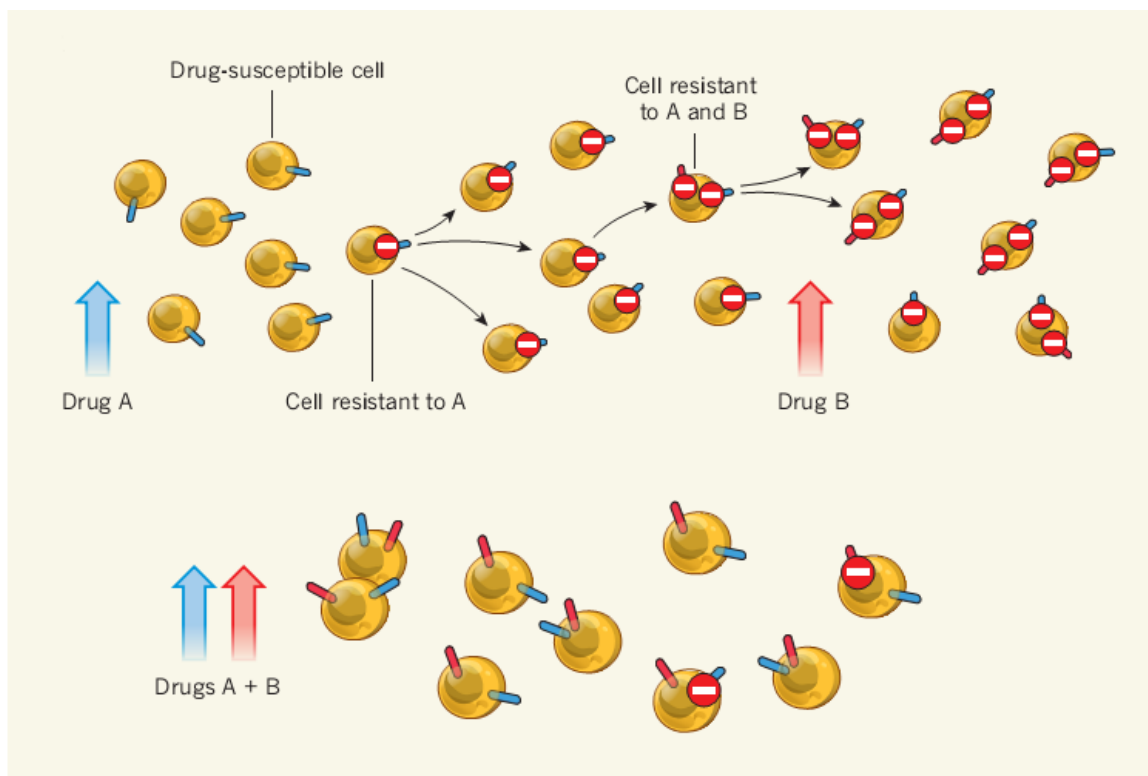
Figure 5: Single-drug versus combination therapy. Combination therapy lowers the likelihood of drug resistance development compared to using of single drug sequentially and increases treatment effectiveness. Image taken from Komarova and Boland [31].

However, the majority of previously accumulated clinical protocols for combination therapies are mainly obtained empirically [33]. They include the consideration on tolerability and possible pharmacokinetic interactions but lack supporting biochemical and molecular mechanisms underlining them, therefore it's hard to estimate the response of a patient to a combination therapy or identify patients who are likely to respond well to it [30, 33]. Powered by genomic technologies, advances in understanding of the biology of cancers, and the

discovery of molecularly targeted therapies, it is now becoming feasible to match patients with appropriate therapies that are more likely to be effective and safe [30, 34]. In view of this, the rationally-designed drug combination therapy such as combing targeted drugs that inhibit the same receptor in more than one way or attack multiple cancer hallmarks is now imperative. The synergistic effect and circumvention of drug resistance it brings will definitely benefit personalized cancer treatment.

1.2.4   Natural products for cancer therapy

Natural products are defined as chemical compounds or substances produced naturally by living organisms, mainly including terrestrial and marine plants and microbes [35]. The great majority of natural products do not appear to participate directly in growth and development of those living organisms themselves but influence ecological interactions between them and their environment, therefore regarded as secondary metabolism[36]. They have evolved for billion years in response to needs and challenges of the natural environment, such as defense against competitors, herbivores and pathogens. The biological and geographical diversity results in the chemical and pharmacological diversity of natural products [37].

A thousand years long history exists of natural products that have been used for the treatment and prevention of human diseases [38]. In the context of cancer treatment, it can trace back to American Indians, who used extracts from the roots of mayapple (*Podophyllum peltatum*) to combat skin cancers and other malignant neoplasms [39]. The major constituent of this extract is podophyllotoxin, which was the first in a group of effective anticancer agents known as podophyllins [40]. Nowadays, natural products play a leading role in the discovery and the development of drugs for cancer treatment. Natural products or natural-products-derived drugs comprise over 60% of all anticancer agents approved since 1940 [37]. Representative examples of plant-derived anticancer agents are *Vinca* alkaloids from *Vinca rosea*, the earliest example, and taxanes originating from Pacific yew bark, the most recent example, which are presently considered as the most effective antitumor agent [38]. Other anticancer agents derived from natural sources contain actinomycin D, rapamycin, daunorubicin that are produced by microbes, as well as cytarabine, trabectedin, aplidine contributed by marine organisms.

Due to the diversity of natural products, their anticancer mechanisms are numerous and distinctive in different components [35]. For example, both vinblastine and taxol act on microtubules, but the former destabilize microtubules while the latter stabilizes them during cell division to inhibit cell growth. In case of camptothecin and podophyllotoxin, they function as DNA topoisomerase inhibitors. Other mechanisms include interruption of angiogenesis, induction of apoptosis, mitochondrial permeabilization, *etc*. With the deepening of studies, many potential anticancer natural products, *e.g.* curcumin and resveratrol, as well as the known compounds mentioned above have been reported to exert their effect by interfering multiple cellular signaling pathways rather than a single target [40]. Since cancer is a multifactorial disease, this feature of natural products may be favorable for the fight against cancers. Therefore natural products have to be considered not only as a source of cytotoxicity-inducing agents, but also for their use as molecularly targeted agents and potential partners in combination therapy [41, 42].

The search for novel drugs is still a priority goal for cancer therapy [37]. Traditional medicines such as traditional Chinese medicine (TCM), Ayurveda and others, which have utilized numerous natural products and developed over centuries, serve as rich resources for modern drug discovery [40]. Combination of this valuable knowledge with modern cutting-edge technologies such as genomics, proteomics, combinatorial chemistry and high throughput screening, provides an attractive and efficient approach for the development of novel and improved cancer therapeutics. One group of promising anticancer agents derived from TCM and major subject of this study is the natural naphthoquinones–shikonin and its derivatives.

1.3   Naphthoquinones: shikonin and its derivatives

1.3.1   Sources, structures and biological activities

The naphtoquinones shikonin and its derivatives are the main active molecules present in traditional Chinese herbal medicine *Zicao*, which is made from the dried root of *Lithospermum erythrorhizon* Sieb et Zucc. (Boraginaceae) [43]. (Figure 6) The application of *Zicao* in traditional Chinese medicine can be traced back with certainty to the latter 16th century, as it was included in the classic compilation of traditional Chinese medicine *Pen Ts'ao Kang Mu*

[44]. It is believed to be able to remove heat from the blood and possess properties of detoxification, and it has been used for centuries as an effective treatment for a variety of inflammatory and infectious diseases, including burns, anal ulcers, macular eruptions, measles, sore-throat, carbuncles and oozing dermatitis [45].
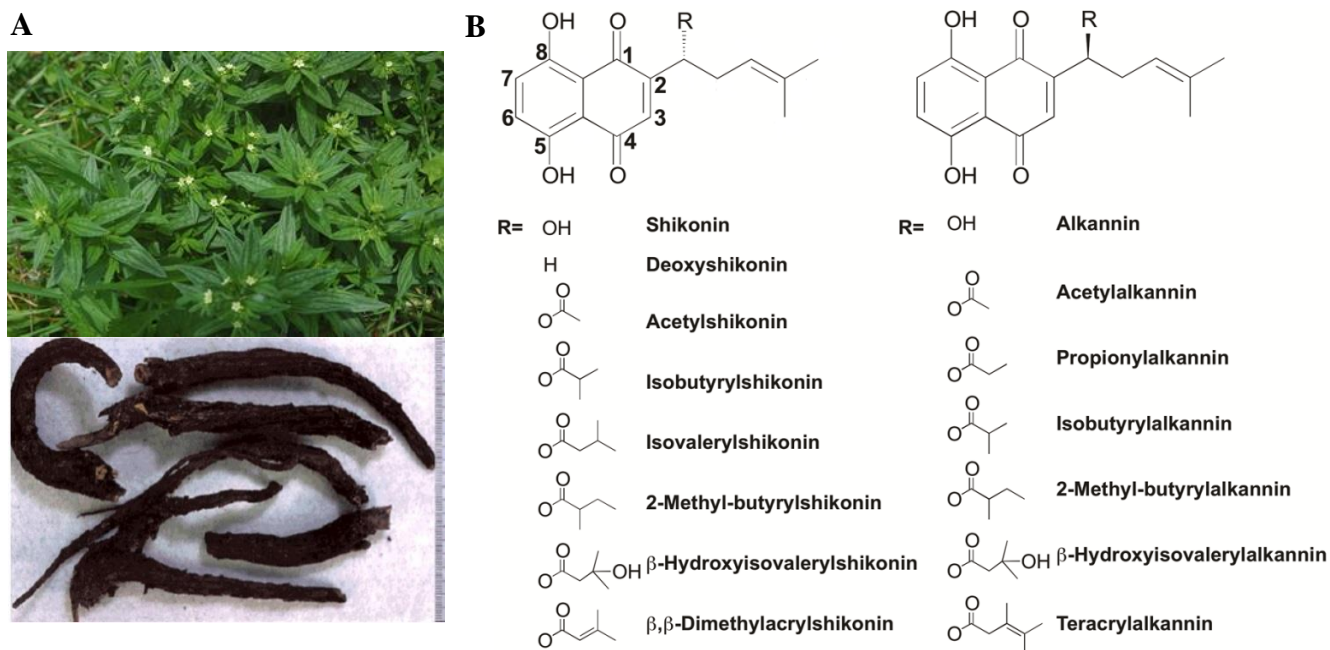
Figure 6: A, Pictures of the plant *Lithospermum erythrorhizon* (ja.wikipedia.org) and its dried roots (taken from Vassilios P. Papageorgiou [44]); B, The chemical structures of shikonin and its derivatives studied in the thesis.

Shikonin was first isolated as acetylshikonin from the roots of *Lithospermum erythrorhizon* by Majima and Kurodain in 1922 [46]. Later on, Brockmann and Liebigs were the first to define the correct structure of this molecule as 5, 8-dihydroxy-2-[(1*R*)-1-hydroxy-4-methyl-3-pentenyl]-1,4-naphthoquinone and identify shikonin's enantiomer alkannin in 1936 [44]. In addition to being mostly isolated in the root of *Lithospermum erythrorhizon*, shikonin, along with alkannin and other derivate compounds can also be found in many other species of Boraginaceae family, such as *Arnebia euchroma*, *Echium lycoris*, *Eritrichium sericeum* and *Onosma armeniacum*, among others [43]. New strategies such as cell tissue cultures and total synthesis have been successfully applied in production of shikonin and its derivatives. However, for mass commercial use of shikonin, we still have to rely upon extraction and isolation form plants at present [44].

Biological investigations over the last 40 years have demonstrated a wide spectrum of pharmacological activities for shikonin and its derivatives, including antioxidant, anti-inflammatory, anti-cancer, antimicrobial, neuro-/cardio-protective and wound healing effects [43]. Their diversely beneficial properties stand for a sound scientific basis for the use of *Zicao* in folk medicine to treat a variety of inflammatory and infectious diseases. The focus of this study is their antitumor activities, which will be discussed in more details in the next paragraph.

1.3.2   Anticancer effect

Shikonin and its derivatives were first found exhibiting *in vitro* cytotoxicity against cancer cells in 1974 during a mass screening programs of natural products conducted by the National Cancer Institute of the USA [44]. Three years later, the anti-tumorigenic effects of shikonin and its derivatives were scientifically confirmed *in vivo* animal models. They showed complete tumour growth inhibition and increase in life span at a dose of 5–10mg/kg/day in mice with sarcoma 180 (S-180) ascites cells [47, 48]. Since then, an increasing body of *in vitro* and *in vivo* studies have demonstrated the antitumor activities of shikonin and its derivatives towards various types of cancer cells, such as leukemia cells [49, 50], breast cancer cells [51, 52], glioma cells [53, 54], bladder cancer cells [55] and lung cancer cells [56] .

The molecular mechanisms underlying shikonin and its derivatives' antitumor activities vary depending on the cell type and treatment method [57]. Primarily they exert their antitumor effects by inhibiting cell growth and inducing apoptosis through a classic caspases-dependent pathway [57]. A wide spectrum of anticancer mechanisms are involved and play a role in shikonins-induced apoptosis, such as generation of reactive oxygen species (ROS), suppression of nuclear factor (NF)-κB-regulated gene products, activation of caspases-9, -8 and -3, release of the mitochondrial proteins cytochrome c, cleavage of poly (ADP-ribose) polymerase (PARP), upregulation of p53, cell cycle arrest with concomitant downregulation of cyclin-dependent proteins, decreased Bcl-2 expression and increased Bax expression, *etc*. [43] Besides, shikonin and its derivatives have been shown to induce a non-apoptotic cell death known as necroptosis to bypass apoptotic/drug resistance [58, 59]. Additionally, shikonin also functions as a topoisomerase I inhibitor [60] and proteasome inhibitor [61].

Studies have demonstrated that shikonin selectively kills tumor cells but not normal cells [57]. A clinical trial using a medicinal mixtures containing purified shikonin in 19 patients with late-stage lung cancer revealed that it was effective for the treatment of late stage cancer and had no harmful effects on the heart, kidneys, liver, or peripheral blood [62]. The specificity of shikonin's cytotoxic effects towards tumor cells and modulation of multiple cancer-associated cellular targets indicate that this type phytochemical is a promising candidate for targeted cancer therapy.

1.4   Targeting EGFR for cancer therapy

The epidermal growth factor receptor (EGFR) is among the most studied receptor protein-tyrosine kinases owing to its general role in signal transduction and in oncogenesis [63]. It is also an example of a target against which several anti-cancer small-molecule inhibitors and monoclonal antibodies have been successfully developed [64]. Therefore, in the following paragraphs, function, structure, and importance of EGFR in cancer therapy will be thoroughly discussed.

1.4.1   Function, structure and downstream signaling pathways

EGFR, also referred to as ErbB1 or HER1, is a 170-kDa transmembrane glycoprotein belonging to the ERBB/HER superfamily of receptor tyrosine kinase (TK), which comprises four proteins (ERBB/HER 1 ~ 4) encoded by the *c-erbB* proto oncogene [63]. These growth factor receptors are predominantly located on cell surface and play important roles in modulating cell division, proliferation and differentiation [65]. The structure of EGFR is composed of a cysteine-rich extracellular region, a single transmembrane region and an intracellular domain containing an ATP-binding site and TK activity. The extracellular portion has been subdivided into four domains: domains I and III are cysteine-poor and conformationally contain the site for ligand (e.g. EGF and transforming growing factor (TGF) α) binding. Cysteine-rich domains II and IV contain N-linked glycosylation sites and disulfide bonds, which determine the tertiary conformation of the external domain of the molecule [66]. Upon binding of ligand to its extracellular domain, EGFR is known to homodimerize or heterodimerize with HER2, resulting

in a conformational change that leads to auto-phosphorylation of the intracellular tyrosine kinase domain. Figure 7 shows the structure and activation of EGFR.
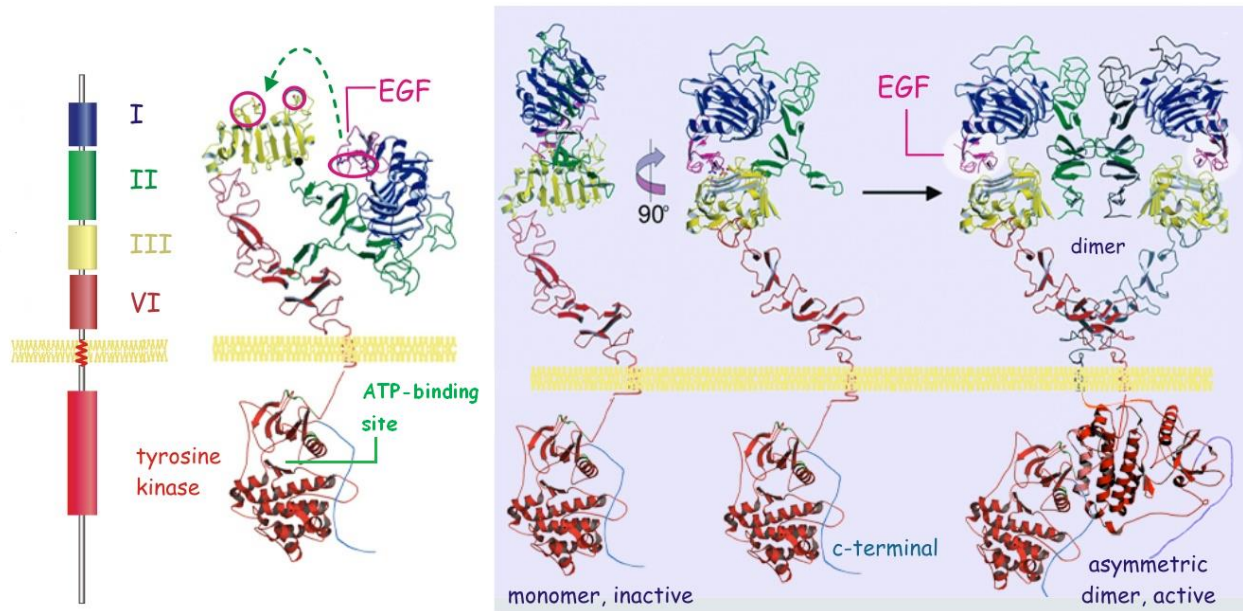
Figure 7: Modelled structures and dimerization process of EGFR. Image adapted from Gomperts, Kramer and Tatham [67].

Phosphorylated TK residues serve as binding sites for the recruitment of signal transducers and activators of intracellular substrates, which then initiate numbers of intracellular signaling pathways, including Ras-Raf mitogen-activated protein kinase (MAPK), Src, STAT3/5, the phospholipase C (PLCγ), protein serine/threonine kinase C (PKC), and the phosphatidylinositol 3-kinase (PI3K)/Akt [65, 68]. The activation of PLCγ causes calcium release from intracellular stores and the generation of diacylglycerol (DAG), the activator of PKC, which is responsible for transformation, differentiation and apoptosis [69]. Activated Ras binds to Raf, which in turn triggers the phosphorylation of mitogen-activated protein kinase 1/2 (MEK1/2) and extracellular signal-regulated kinases 1/2 (ERK1/2). Phosphorylated ERK1/2 translocates into the nucleus and activates various transcription factors involving in cell-cycle progression and cell proliferation [70]. EGFR activates PI3K, which then phosphorylates Akt, a well-established anti-apoptotic kinase that has several cell effects related to cell survival, angiogenesis and so on [71]. Figure 8 displays the main downstream signaling pathways regulated by EGFR.
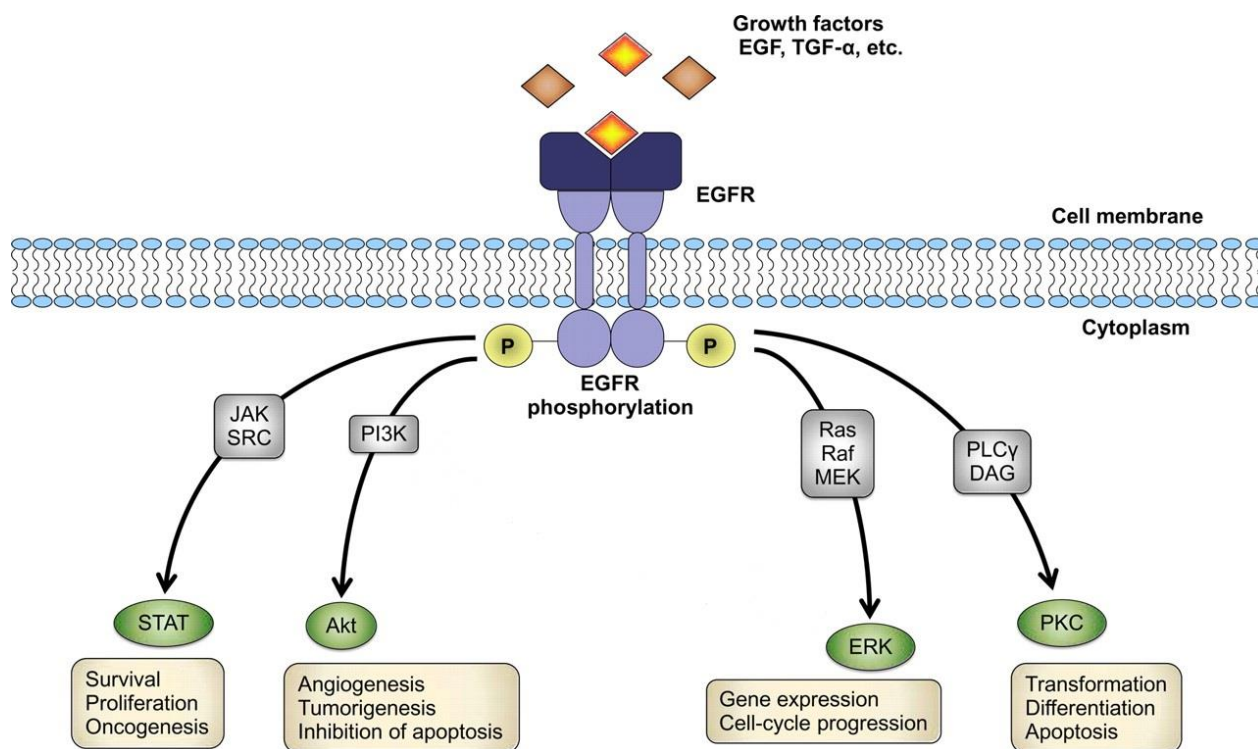
Figure 8: The EGFR signaling pathway. The figure shows signaling pathways that are activated by EGFR. Important signaling pathways regulated by EGFR are represented with important functions highlighted in colored boxes. Image taken from Lee and Moon [72].

1.4.2   Role in cancer and mutations

Although present in normal cells, EGFR is overexpressed in a broad spectrum of solid tumors, including glioblastoma (GBM), breast cancer, head-and-neck cancer, non–small-cell lung cancer (NSCLC), renal cancer, ovarian cancer, and colon cancer, which classifies it as one of the most frequently implicated cell-surface markers for human cancers [65, 66]. Such overexpression has been associated with tumor progression and poor prognosis, as it produces intense signal and activates downstream signaling pathways, leading to more aggressive and invasive cell proliferation. For example, up to 90% of high-grade GBM express EGFR, which is associated with EGFR gene amplification in 40–50% of GBM [66]. In NSCLC, EGFR is overexpressed in 40% to 80% of cases and correlated with a high metastatic rate, poor tumor differentiation, and a high rate of tumor growth [65]. The overexpression of EGFR is presumably caused by multiple epigenetic mechanisms, gene amplification, and oncogenic viruses [73].

Originally, it was thought that EGFR amplification promoted tumor development only by increasing ligand-activated, growth-stimulatory signaling through wild-type EGFR (EGFRwt). However, it is now known that in some cancer cells with EGFR amplification have EGFR mutations, which also play their corresponding roles in contribution to tumor development [66]. Mutations can happen in the extracellular, juxtamembrane regions or kinase domain of EGFR. Although several EGFR mutations have been documented, the best described and the most common mutation is EGFRvIII (also known as de2-7EGFR and ΔEGFR), which was first identified in primary human glioblastoma tumors [66]. EGFRvIII was encoded by *EGFRvIII* gene that has an in-frame deletion of 801 base pairs spanning exons 2–7 in the mRNA [74]. This deletion leads to the loss of amino acids 6–273 that include ligand-binding site in the extracellular domain and decreased molecular mass (145 kDa) of EGFRvIII. The mutated receptor possesses ligand-independent, constitutive TK activity, which promotes EGFR-mediated pro-survival and anti-apoptotic signals through the key downstream pathways as mentioned above. It has been suggested by substantial evidence that EGFRvIII plays a key role in increase the tumorigenicity of diverse cancer cells, including breast, lung, prostate and ovarian cancers, especially GBM [66, 74]. More than 50% GBMs with EGFR gene amplification express EGFRvIII, which is a poor prognostic factor and correlates with decreased overall survival in GBM patients [75]. Introduction of EGFRvIII into GBM cell lines results in an increased proliferation, angiogenesis and invasiveness, as well as reduced apoptosis compared with matched parental cell lines [74]. Moreover, EGFRvIII is specifically found in malignancies and has not been found in normal tissues [69], representing a truly tumor-specific target for drug development.

1.4.3 EGFR inhibitors

A large number of potentially therapeutic agents have been developed directly against EGFR/ΔEGFR for cancer treatment, including monoclonal antibodies (mAbs), tumor-antigen specific vaccines, TK inhibitors (TKIs) and RNA-based therapies [76, 77]. Out of these approaches, only TKIs are orally active and therefore become the focus of current anti-cancer drug research. TKIs are small molecules that mechanistically compete for the ATP-binding site in the TK domain of EGFR, thereby resulting in the ablation of both phosphorylation of the

receptor and downstream signaling [78]. Several TKIs (e.g. erlotinib, gefitinib, PKI166, lapatanib, pelitinib and canertinib) have been found to have effective anti-tumor activity and have been approved or are in clinical trials [68].

Erlotinib, as a representative of best explored TKIs, is a quinazoline derivative which reversibly inhibits the tyrosine kinase activity of EGFR and exerts anti-proliferative effects, cell cycle arrest, as well as induction of apoptosis in preclinical studies [79]. It has been applied in treatment of NSCLC, pancreatic cancer and several other types of cancer. A recent study reported that a subset of GBM patients with MGMT promoter methylation and PTEN positivity showed significantly longer survival with the treatment of erlotinib in combination with radiotherapy and temozolomide [80]. However, most studies have shown very modest or no significant survival benefit from TKIs due to the recurrent problem of resistance caused by mutations in EGFR or tumor heterogeneity [76, 81]. Thus, new treatment strategies are urgently needed to overcome drug resistance and improve the efficacy of EGFR TKIs. One promising approach might be the combination treatment with EGFR TKIs and natural products [82]. For example, results of this study indicated that shikonin and its derivatives synergistically inhibit EGFR activity and kill cancer cells in combination with erlotinib.

1.5 Targeting c-MYC for cancer therapy

1.5.1 Structure, transcriptional activity and target genes

c-MYC is a 65 kDa oncoprotein transcription factor encoded by the proto-oncogene *c-myc*, which belongs to the family of *myc* genes that also include *N-myc* and *L-myc* [83]. c-MYC protein consists of an amino-terminal domain where lies its transcriptional activation domain (TAD), a carboxy-termianl domain (CTD) and a central region. The carboxy terminus of c-Myc is a basic helix-loop-helix leucine zipper (bHLH-Lz) region that is homologous to those found in characterized transcription factors and functioning as its DNA-binding domain and dimerization interface for its binding partner Myc-associated factor X (MAX) [84, 85]. c-MYC heterodimerizes with MAX, which is also a member of bHLH-Lz protein family, to recognize a consensus sequence "CACGTG", which is termed the "Enhancer box" (E-box), in the promoters of its target genes. Thereby, it exerts most of its fundamental biological

activities. Figure 9 shows the crystal structure of a MYC/MAX heterodimer bound to a canonical E-box.
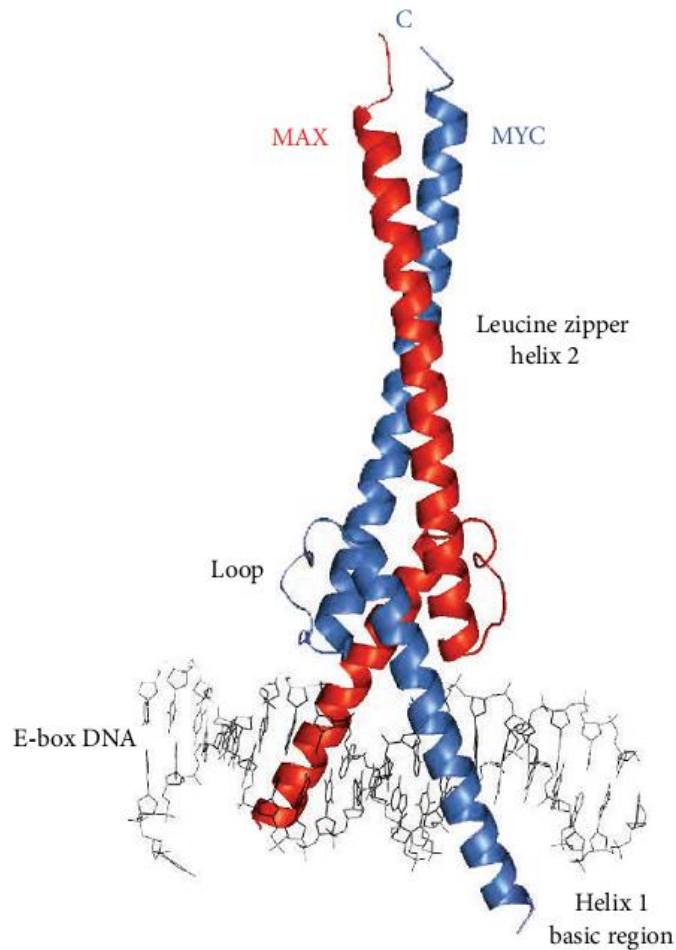
Figure 9: Crystal structure of the bHLH-Lz region of a MYC/MAX heterodimer bound to a canonical E-box. Image taken from Tansey [85].

c-MYC is a global transcriptional regulator, unlike other transcription factors, c-MYC can bind to as many as 15% of the genomes and can regulate both genes encoding proteins and those encoding non-coding RNA products of several functional classes [86, 87]. c-MYC can activate or repress target genes in transcriptional regulation. Although there is still considerable controversy over the precise regulation mode of c-MYC responsive genes, the role of c-MYC in specific classes of genes and various cellular functions has been well known based on the phenotypic consequences of ectopic c-MYC function on the cell [85, 87]. It plays a pivotal role in modulating a broad range of cellular events relevant to tumorigenesis, including cell cycle control, differentiation, genomic stability, metabolism and apoptosis [83].

For example, cell cycle progression from the G0/G1 into the S phase is tightly controlled by c-MYC by regulating the expression of cyclins, cyclin dependent kinases (CDK), CDK inhibitors and the pRb-binding transcription factor E2F [88]. Five of most high-profile tumor relevant processes that influenced by c-MYC are displayed in Figure 10.

In normal cells, the expression of c-MYC is under the stringent control so that typically there are only a few thousand molecules per cell [85]. But under cancerous conditions, c-MYC is usually deregulated and overexpressed due to several mechanisms, such as insertional mutagenesis, chromosomal translocation, gene amplifications, and constitutive activation of upstream signaling pathways [86]. Deregulated expression of c-MYC is a hallmark feature of cancer and essential for certain tumor initiation and maintenance [89]. Averagely, 50% of both blood-borne and solid human cancers overexpress c-MYC protein, which is frequently correlated with a poor clinical outcome, aggressive biological behavior, increased likelihood of relapse, and advanced stage of disease [85, 89]. The following paragraph will emphasize on the role of c-MYC in hematopoietic malignancies.
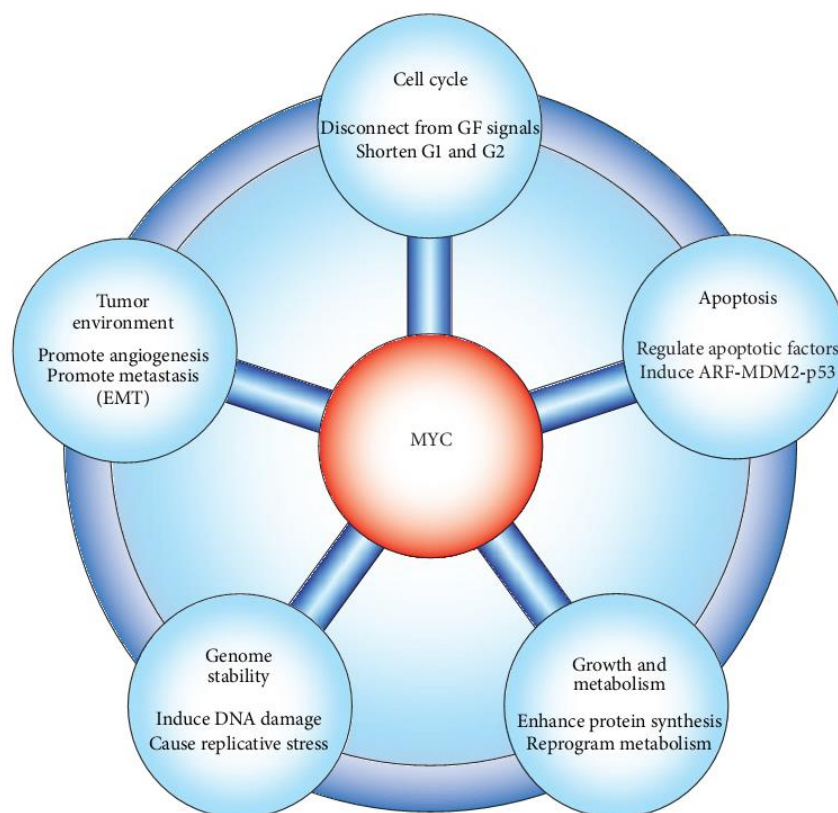
Figure 10: MYC-regulated key tumor-relevant activities. Image taken from Tansey [85].

1.5.2   Deregulation in hematopoietic malignancies

c-MYC deregulation is closely associated to hematopoietic malignancies [90, 91]. In fact, the retroviral form, v-MYC was first discovered to cause myelocytomatosis (a type of myeloid leukemia) in chicken and the oncogene was named after this tumor [85]. Later, the cellular pendant, c-MYC, was found to be translocated in aggressive Burkitt's lymphoma. The important role for c-MYC on leukemogenesis was subsequently confirmed in animal models. Conditional overexpression of c-MYC in hematopoietic cells in transgenic mice led to the formation of malignant T-cell lymphomas and acute myeloid leukemias, which were reverted by inactivation of the c-MYC transgene [92, 93]. Later on, mounting evidence has been accumulated showing that c-MYC is a key player in hematopoiesis and leukemia [91]. It is noteworthy that a pristine form of c-MYC or a small expression change of c-MYC is sufficient to promote tumorigenesis. For instance, in Burkitt lymphoma, which is the paradigm of MYC-dependent human cancer, expression of c-MYC can be only 2-fold more than normal lymphocytes [85, 91]. The c-MYC alteration in human hematological malignancies mainly results from *MYC* gene translocation, amplification, rearrangement and mRNA overexpression [91]. Recently, c-MYC is closely correlated to drug resistance in leukemia cells. Leukemic cell lines resistant to cytarabine displayed a c-MYC-dependent overexpression of the natural killer (NK) group 2, member D (NKG2D) ligands (NKG2DL) UL-16 binding proteins 1-3 (ULBP1-3) [94]. Up-regulated expression of c-MYC in leukemia cells promoted the colony formation ability and maintained poor differentiation leading to drug resistance [95]. In addition, c-MYC contributed to microenvironment-mediated drug resistance in AML [96]. The role of c-MYC in regulating various pro-tumorigenic functions, together with its extensive deregulation in human cancer, speaks for the potential of c-MYC as therapeutic target in the quest to cure cancer. Inactivation of c-MYC represents as a novel approach to improve clinical outcome and prognosis in hematopoietic malignancies treatment.

1.5.3   Strategies to inhibit MYC

Several strategies have been developed to inhibit c-MYC over the past decade, including direct inhibition of c-MYC, inhibition of c-MYC-dependent transcription signaling, modulation of c-MYC stability and its upstream pathways [89]. Since interaction of c-MYC with MAX is

absolutely required for MYC's oncogenicity, it also provides an important point for c-MYC regulation. A straightforward strategy to inhibit c-MYC functions is to block its DNA binding activity by either interfering with c-MYC–MAX dimerization or disrupting the interaction of transcriptionally-active c-MYC–MAX dimers with DNA [97, 98]. In this context, several small-molecule c-MYC inhibitors have been identified from large chemical libraries. For some of them, e.g. 10058-F4 and 10074-G5, the actual binding modes have been elaborately illustrated [99, 100]. At the level of c-MYC gene transcription, compounds such as bromodomain and extraterminal domain (BET) inhibitors and G-quadruplex stabilizers have been developed that attenuate c-MYC transcription by inducing unique and inhibitory DNA structures at the c-MYC promoter [83]. Another mechanism of c-MYC inactivation involves the interference of signal transduction pathways that down-regulate c-MYC expression. Many signaling pathways, including phosphatidylinositol 3-kinase (PI3K)/AKT, Ras-Raf-MEK-ERK mitogen-activated protein kinase (MAPK), regulate c-MYC mRNA expression and promote c-MYC stability [86, 101]. Marampon et al demonstrated that the inhibition of the MEK/ERK pathway dramatically decreased c-MYC expression and thus inhibited in cancer cell growth [102].

Numerous studies have proven that c-MYC inhibition or even transient inactivation of c-MYC leads to tumor collapse in many mouse model systems [103-105]. Furthermore, effective killing of cancer cells in such models does not require complete blockade of c-MYC activity, but only attenuating MYC below a certain threshold [85]. This could be a distinct advantage for c-MYC inhibitors, as they may have a relatively large therapeutic window that could kill tumors without harming normal cells. However, although several small molecules have been described as c-MYC inhibitors, none of them is clinically used as of yet. Therefore, novel c-MYC-targeting drugs are urgently needed. The results of this study reveal that shikonin and its derivatives exert a strong inhibitory effect on c-MYC and deregulate its upstream signal pathways in killing leukemia cells, raising the possibility of these compounds to be attractive c-MYC inhibitors.

2   Aim of the thesis

As the primary active molecules present in traditional Chinese herbal medicine *Zicao*, the naphtoquinones shikonin and its derivatives had been shown to possess significant anti-inflammatory and antimicrobial activities, which stand for a sound scientific basis for the long-history use of *Zicao* in folk medicine to treat various infectious diseases. Recently, increasing evidence revealed that this type compounds have strong antitumor activities towards various types of cancer cells by influencing several cancer hallmarks, indicating the potential of them as new anticancer agents in molecular targeted therapy. EGFR is one of the most important therapeutic targets, against which several small-molecule inhibitors, *e.g.* erlotinib, have been developed. However, the rapid development of drug resistance severely limits the efficacy of these agents. Novel EGFR inhibitors or new strategies such as combination therapy are urgently needed in order to overcome drug resistance and improve treatment effect. Thus, the first aim of this thesis was:

- ● *Analysis of the effect of shikonin and its derivatives alone and in combination with erlotinib on the EGFR signaling pathway.*

During the cytotoxicity screen of shikonin towards a panel of various tumor cell lines, leukemia cell lines were found more sensitive to shikonin compared to solid tumor cell lines. Since EGFR expression was not detected in leukemia cells, the particularly effective of shikonin and its derivatives against leukemia cells should lie in other mechanisms. This was leading to the second aim of this thesis:

- ● *Investigation of new molecular targets and mode of action of shikonin and its dervatives in leukemia cells.*

3 Results

3.1 Inhibition of EGFR signaling and synergism with erlotinib in glioblastoma cells

As previously mentioned, shikonin, its derivatives and erlotinib are known for their activities against tumor cells *in vitro* and *in vivo*. However, there is no report about the effectiveness of a combination treatment and the underlying molecular mechanisms of cellular response. Moreover, as new treatment strategies are urgently needed to overcome drug resistance against EGFR TKIs and one promising approach might be the combination treatment with EGFR TKIs and natural products [82]. Therefore, the first aim of the thesis was to investigate whether and how the combination of erlotinib with shikonin or its derivatives exert synergic activities in cancer cells. For this purpose, shikonin and 14 derivatives were analyzed in combination with erlotinib in the parental human glioblastoma cell line U87MG and its transfected U87MG.EGFR subline, which overexpresses constitutively active ΔEGFR. Furthermore, three other EGFR-expressing cell lines were tested for the combined cytotoxic effect of shikonin and erlotinib to obtain the translational relevance.[1]

3.1.1 Cytotoxicity towards glioblastoma cells

As a starting point, the sensitivities of the parental U87MG and transfected U87MG.ΔEGFR cells to erlotinib, shikonin and its derivatives were determined. Both cell lines were treated with varying concentrations of these compounds for 72 h. The results are summarized in **Table 1**.

---

[1] The results presented in this section were recently published in a peer-reviewed scientific journal:

Zhao Q, Kretschmer N, Bauer R and Efferth T. Shikonin and its derivatives inhibit the epidermal growth factor receptor signaling and synergistically kill glioblastoma cells in combination with erlotinib. *International journal of cancer*. 2015; 137(6):1446-1456.

All text passages, tables and figures of this publication that are used in a modified form in this dissertation were prepared or written by myself.

Table 1: IC$_{50}$ values (mean ± SEM) of erlotinib, shikonin and 14 derivatives for U87MG and U87MG.ΔEGFR cells after 72 h as measured by resazurin assay. Results shown are mean values and standard deviation of at least two independent experiments with each 6 parallel measurements.

Compounds	IC$_{50}$ [µM]	
	U87MG	U87MG.ΔEGFR
Erlotinib	>10[a]	>10[b]
Shikonin	4.11±0.18	2.14±0.07
β-β-Dimethylacrylshikonin	3.63±0.42	1.11±0.02
2-Methyl-butyrylshikonin	3.61±0.46	1.49±0.04
Deoxyshikonin	14.50±1.00	2.58±0.38
Isobutyrylshikonin	16.18±1.37	4.46±2.01
Isovaltryshikonin	14.67±0.39	10.91±6.26
β-Hydroxyisovalerylshikonin	21.62±1.02	14.72±1.99
Acetylshikonin	18.59±6.66	17.38±2.93
Acetylalkannin	26.00±2.52	21.21±3.11
Teracrylalkannin	50.63±3.87	21.89±1.34
Isobutyrylalkannin	51.97±6.96	24.64±3.38
2-Methyl-butyrylalkannin	39.37±1.61	25.53±0.68
Propionylalkannin	>100	>100
Alkannin	>100	>100
β-Hydroxyisovalerylalkannin	>100	>100

a. Maximal growth inhibition by 10 µM erlotinib on U87MG cells is 32.5±0.5%.
b. Maximal growth inhibition by 10 µM erlotinib on U87MG.ΔEGFR cells is 35.4±1.5%.

Both cell lines displayed similar sensitivities to growth inhibition by erlotinib, but no cell line showed maximal growth inhibition > 50% by 10 µM erlotinib indicating that both cell lines were considered to be resistant to erlotinib. Ten micromol was the maximum concentration achieved in our culture medium and this concentration also had clinical and biological relevance, as it was reported to represent a plasma concentration that was achievable in non-smoking patients and growth inhibition by 10 µM erlotinib *in vitro* closely reflected the percent tumor growth inhibition derived from *in vivo* xenograft experiments [106, 107].

However, shikonin inhibited cell growth at lower concentrations. Moreover, it preferentially inhibited U87MG.ΔEGFR cells with an IC$_{50}$ value of 2.1 µM, which was 2-fold lower than the IC$_{50}$ value of U87MG cells (4.1 µM). Interestingly, hypersensitivity of shikonin towards U87MG.ΔEGFR cells compared to U87MG cells was also observed for most derivatives of

shikonin. Except for three alkannin derivatives, which were inactive by both cell lines ($IC_{50} >$ 100 µM), the IC_{50} values of all other compounds were 5.6~1.1 folds lower for U87MG.ΔEGFR cells than those for U87MG cells. Representative dose-response curves used to calculate IC_{50} values were shown in **Figure 11**.
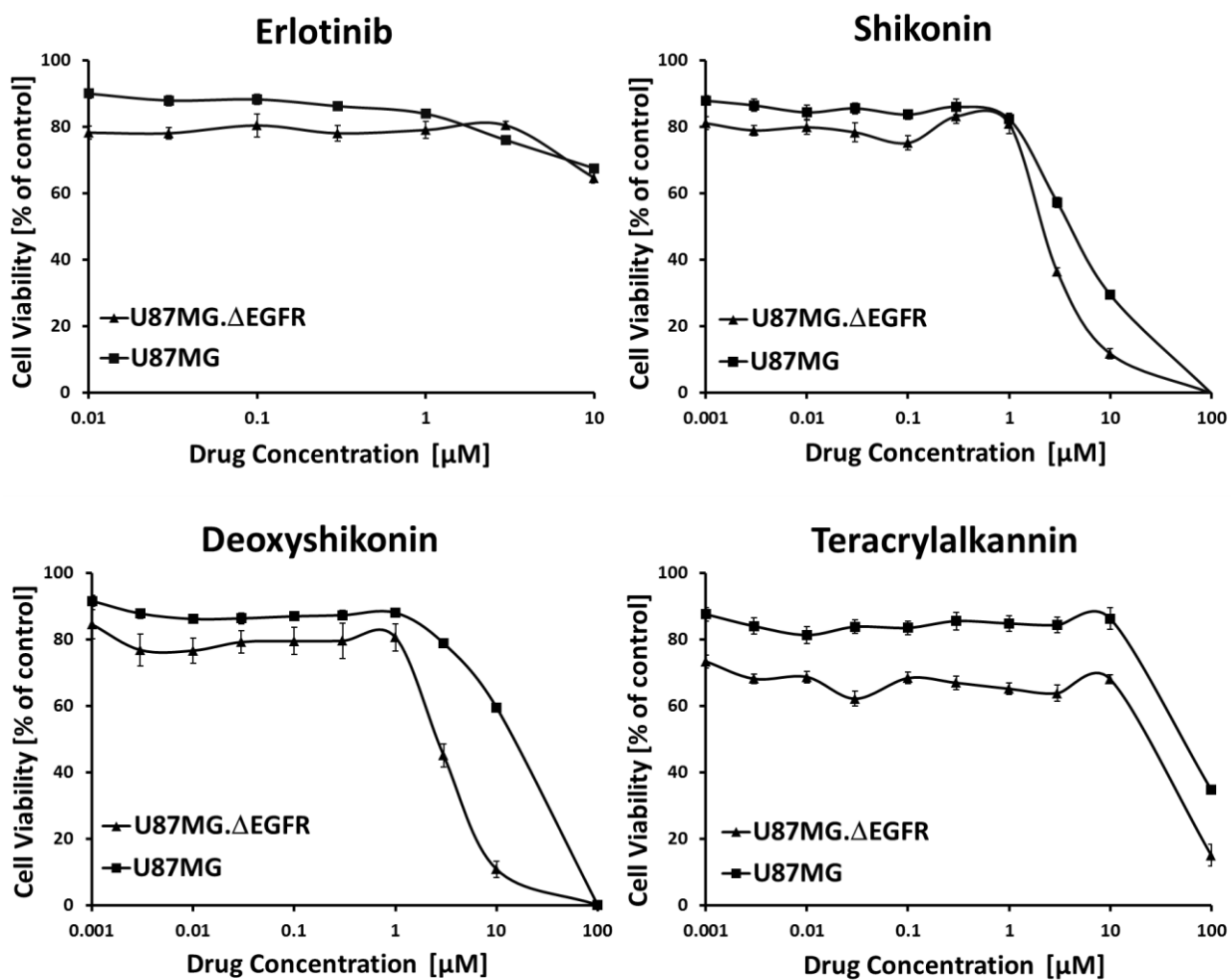
Figure 11: Shikonin and derivatives showed preferential cytotoxicity towards EGFR-mutated erlotinib-resistant transfected cells. U87MG and U87MG.ΔEGFR cell lines were treated with varying concentrations of erlotinib, shikonin and 14 derivatives for 72 h. Cell viability was measured by resazurin assay and representative pairs of cell viability curves are shown. Results shown are mean values and standard deviation of at least two independent experiments with each 6 parallel measurements.

3.1.2 Cytotoxicity of combination treatments

The initial cytotoxicity experiments gave us a good hint that shikonin and its derivatives were not resisted by EGFR-mutated U87MG.ΔEGFR cells. Next, in order to investigate whether the combination of shikonin or its derivatives with erlotinib may render additive or synergistic growth inhibitory interactions on glioblastoma cells, two classic methods for assessment of drug interaction, namely Bliss independence model and Loewe additivity model, were applied to analyze the combination effect.

3.1.2.1 Assessment by Bliss independence model

Shikonin as lead compound was first examined. The effects of varying concentrations of shikonin on growth inhibition of the two cell lines in the presence or absence of 10 µM erlotinib are shown in Figure 12. The Bliss independence model was first utilized, as it allows to assess the nature of drug interactions even in cases, where the maximal inhibition by erlotinib as single agent was low enough so that a reliable IC_{50} value could not be obtained. For cell lines that were less sensitive to erlotinib as single agent, the IC_{50} value is often > 10 µM. This approach has previously been used for drug combination studies in erlotinib-insensitive cell lines [108]. In Figure 12, the Bliss analysis showed a theoretical curve (dashed line) that would be expected, if the combination of erlotinib and shikonin was solely additive in nature. For U87MG wild-type cells, the Bliss analysis showed a slight antagonism for the combination of shikonin with erlotinib. However, in U87MG.ΔEGFR cells the combination was synergistic, as reflected by an increase in potency. The dose-response curve shifted nearly 4-fold in potency (1.2~0.3), when shikonin was combined with erlotinib.
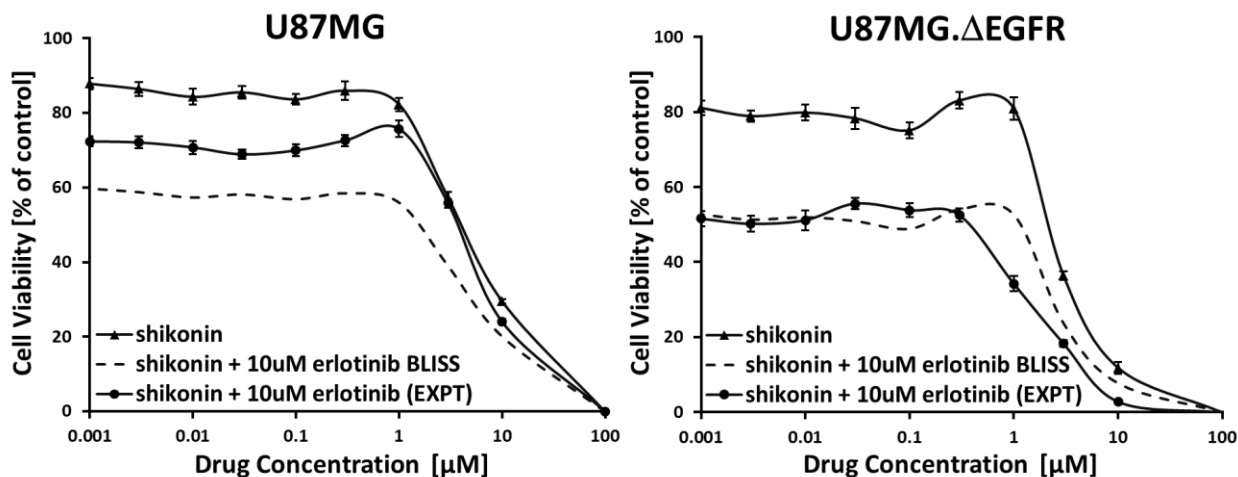
Figure 12: Effect of varying concentrations of shikonin on the proliferation of U87MG, U87MG.ΔEGFR cells in the absence or presence of 10 µM erlotinib. Dashed line, Bliss additivity curve, represents the theoretical expectation, if the combined effect of shikonin with erlotinib was exactly additive. Results shown are mean values and standard deviation of at least three independent experiments with each 6 parallel measurements.

Next, we tested the combined effect of erlotinib with 14 shikonin derivatives on U87MG.ΔEGFR cells to further analyze possible synergistic interactions. Based on the dose-response curves of shikonin combined with erlotinib, which demonstrated maximal synergistic effects at 10 µM erlotinib and IC_{50} of shikonin, the further experiments were therefore performed with combinations of 10 µM erlotinib with single concentrations selected around the IC_{50} values of the other 14 shikonin derivatives. Figure 13 shows the summary of the Bliss analyses for the combination treatments.
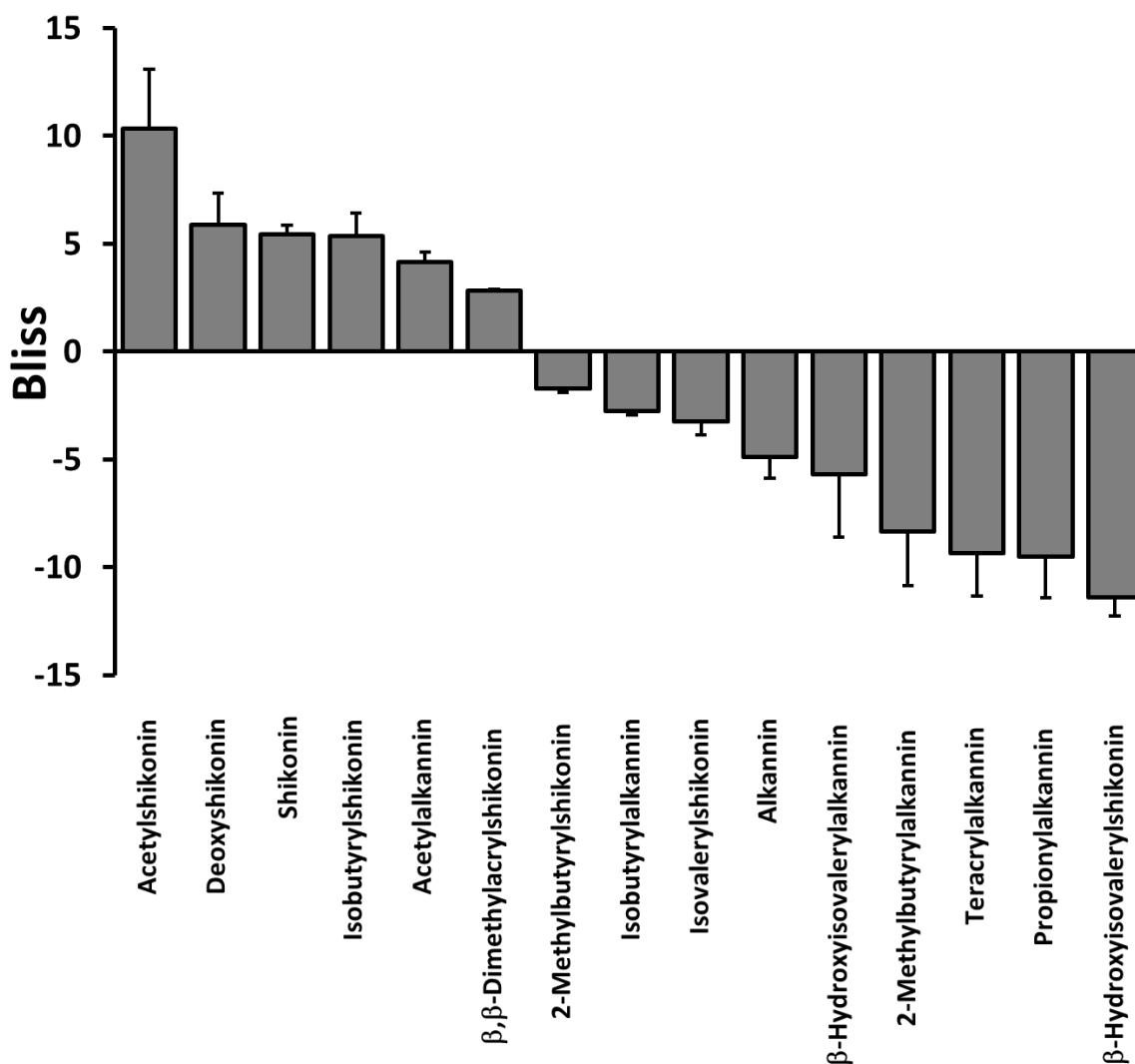
Figure 13: Sensitivity of U87MG.ΔEGFR to the combination of 10 μM erlotinib with shikonin and 14 derivatives. Synergy, as noted by a positive Bliss value, was observed in 6 of 14 compounds. Results shown are mean values and standard deviation of at least three independent experiments with each 6 parallel measurements.

Here, the Bliss values are expressed as percentage change in fractional inhibitions of cell growth. They were calculated by the formula $E_{expt} - E_{bliss}$. Bliss = 0, which meant that $E_{expt} = E_{bliss}$ indicated additive effects. Bliss > 0 meant $E_{expt} > E_{bliss}$ indicated a percentage increase in fractional inhibitions above additivity (synergy). Bliss < 0 meant $E_{expt} < E_{bliss}$ indicated a percentage decrease in fractional inhibitions below additivity (antagonism) [106]. Besides shikonin, synergy was also observed with 5 of 14 derivatives, including deoxyshikonin, isobutyrylshikonin, acetylshikonin, β,β-dimethylacrylshikonin and acetylalkannin.

In addition to the U87MG cell line transfected with a deletion-activated *EGFR*, we tried another glioma cell line BS153 with a mutated *EGFR* to prove [109], whether or not shikonin and erlotinib also exert synergism in cell lines expressing the EGFR variant. BS153 cells were also resistant to erlotinib, the IC_{50} value was > 10 µM, while shikonin inhibited them with an IC_{50} value of 1.57 µM (Figure 15A). Therefore, we also took Bliss model to analyze the combined effect of shikonin and erlotinib. In Figure 14, the dose-response curve of shikonin plus 10 µM erlotinib, similar to the curve of U87MG.ΔEGFR cell line and even better, shifted significantly from the shikonin alone curve and the theoretically additive curve, indicating the combination was synergistic on BS153 as well.
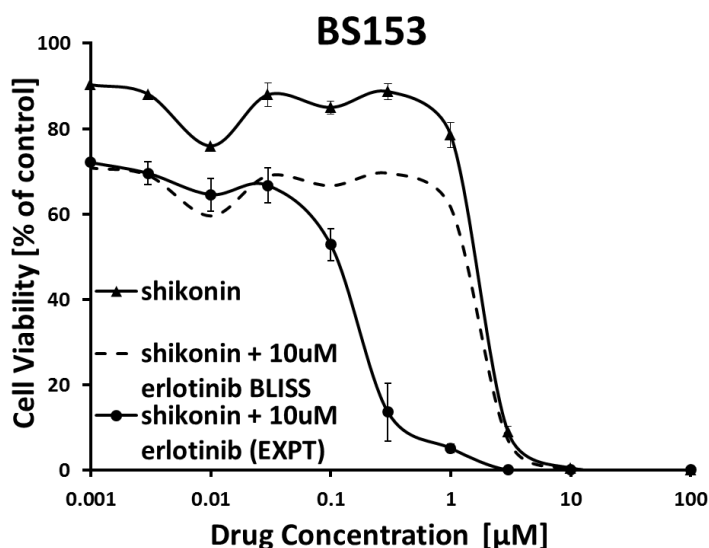
Figure 14: Effect of varying concentrations of shikonin on the proliferation of BS153 in the absence or presence of 10 µM erlotinib. Dashed line, Bliss additivity curve, represents the theoretical expectation, if the combined effect of shikonin with erlotinib was exactly additive. Results shown are mean values and standard deviation of at least three independent experiments with each 6 parallel measurements.

3.1.2.2 Assessment by Loewe additivity model

Because Bliss independence model was not a final proof for synergistic interaction, we wanted to apply another universal reference model used for evaluating the effects of drug interaction, namely Loewe additivity model, which is regarded as 'gold standard' in pharmacology to further confirm our observation [110]. To perform Loewe model, normally a reliable IC_{50} value

is needed for each of compounds in combination. However, all of U87MG, U87MG.ΔEGFR and BS153 cells did not reveal IC$_{50}$ values for erlotinib, therefore we further analyzed other 10 EGFR-expressing cell lines with shikonin and erlotinib alone. Shikonin inhibited all of the 10 cell lines with the IC$_{50}$ values ranged from 0.5 to 5.2 μM, but only two cell lines, DK-MG and A431, were inhibited by erlotinib and provided IC$_{50}$ values below 10 μM (Figure 15A).

A

Shikonin

Cell lines	IC$_{50}$ (μM)
A172	2.88 ± 1.74
A431	1.46 ± 0.14
A498	5.20 ± 0.04
BS153	1.57 ± 0.1
BT-20	4.49 ± 0.1
Calu6	2.54 ± 0.94
DK-MG	0.51 ± 0.02
MDA-MB-436	1.36 ± 0.48
SNB-19	3.93 ± 0.38
T98G	4.83 ± 0.15
U251	1.46 ± 0.09

Erlotinib

Cell lines	IC$_{50}$ (μM)
A172	>10
A431	2.34 ± 0.38
A498	>10
BS153	>10
BT-20	>10
Calu6	>10
DK-MG	5.87 ± 0.43
MDA-MB-436	>10
SNB-19	>10
T98G	>10
U251	>10
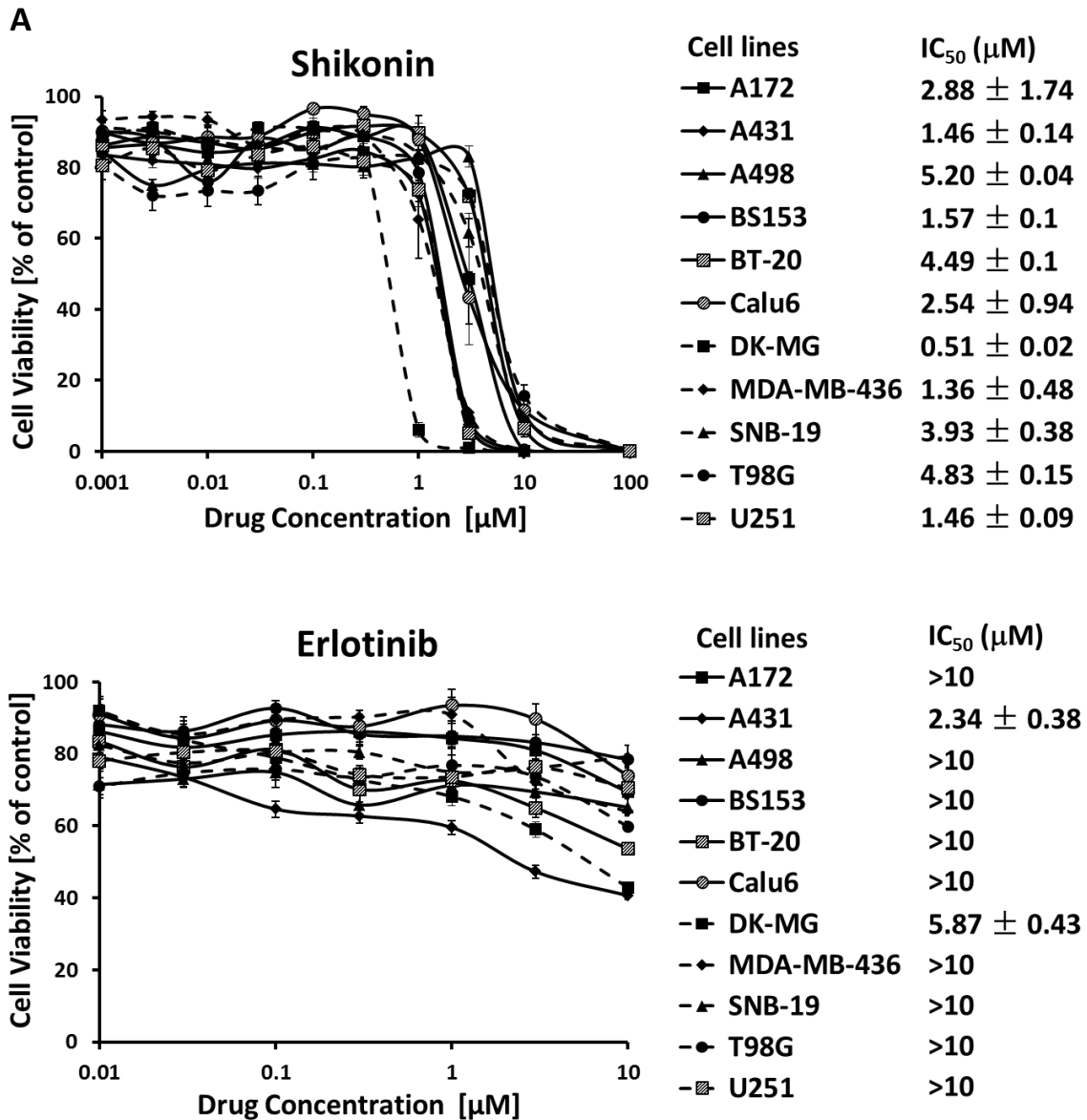
B
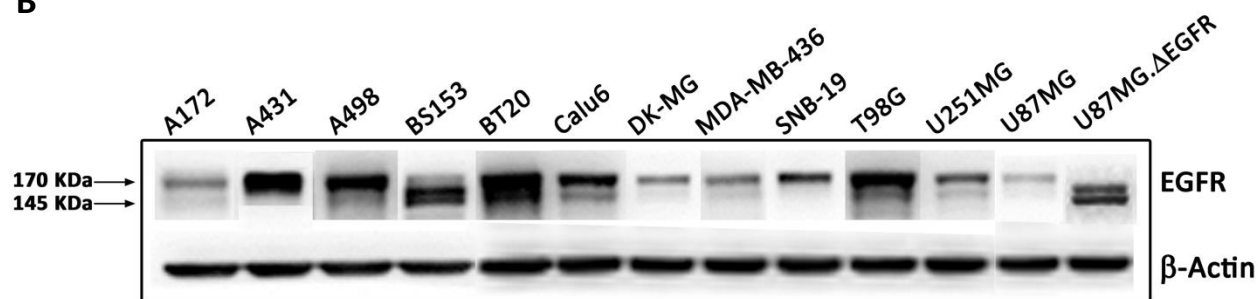
Figure 15: A, Sensitivity of 13 EGFR-expressing cell lines to shikonin and erlotinib. Cells were treated with varying concentrations of shikonin and erlotinib for 72 h. Cell viability was measured by resazurin assay and representative cell viability curves are shown. Results shown are mean values and standard deviation of at least two independent experiments with each 6 parallel measurements. B, The basal expression levels of EGFR in all the tested cell lines. β-actin was used as loading control.

Consequently, the two cell lines were used for Loewe additivity model analysis. DK-MG and A431 cells were treated with varying concentrations of shikonin either in the absence or presence of indicated concentrations of erltinib for 72 h. The cell viability was then determined by resazurin assay and five dose-response curves and the corresponding IC_{50} values for both cell line were shown in Figure 16A and B. We found that the IC_{50} values of shikonin in A431 cells decreased with the presence of increasing erlotinib concentrations to less than 0.05 μM, 30-fold less than the IC_{50} of shikonin alone. However, in case of DK-MG cells, the IC_{50} values of shikonin in combination with erlotinib were only reduced by less than half of the IC_{50} of shikonin alone. The dose-normalized IC_{50} isobolograms for both cell lines were made by plotting of the combination treatment IC_{50} values of shikonin against erlotinib and clearly illustrated a synergistic inhibition in A431 cells but only additive effect in DK-MG cells (Figure 16C and D). The basal expression level of EGFR in all the tested cell lines were displayed in Figure 15B.

A

C

B

D
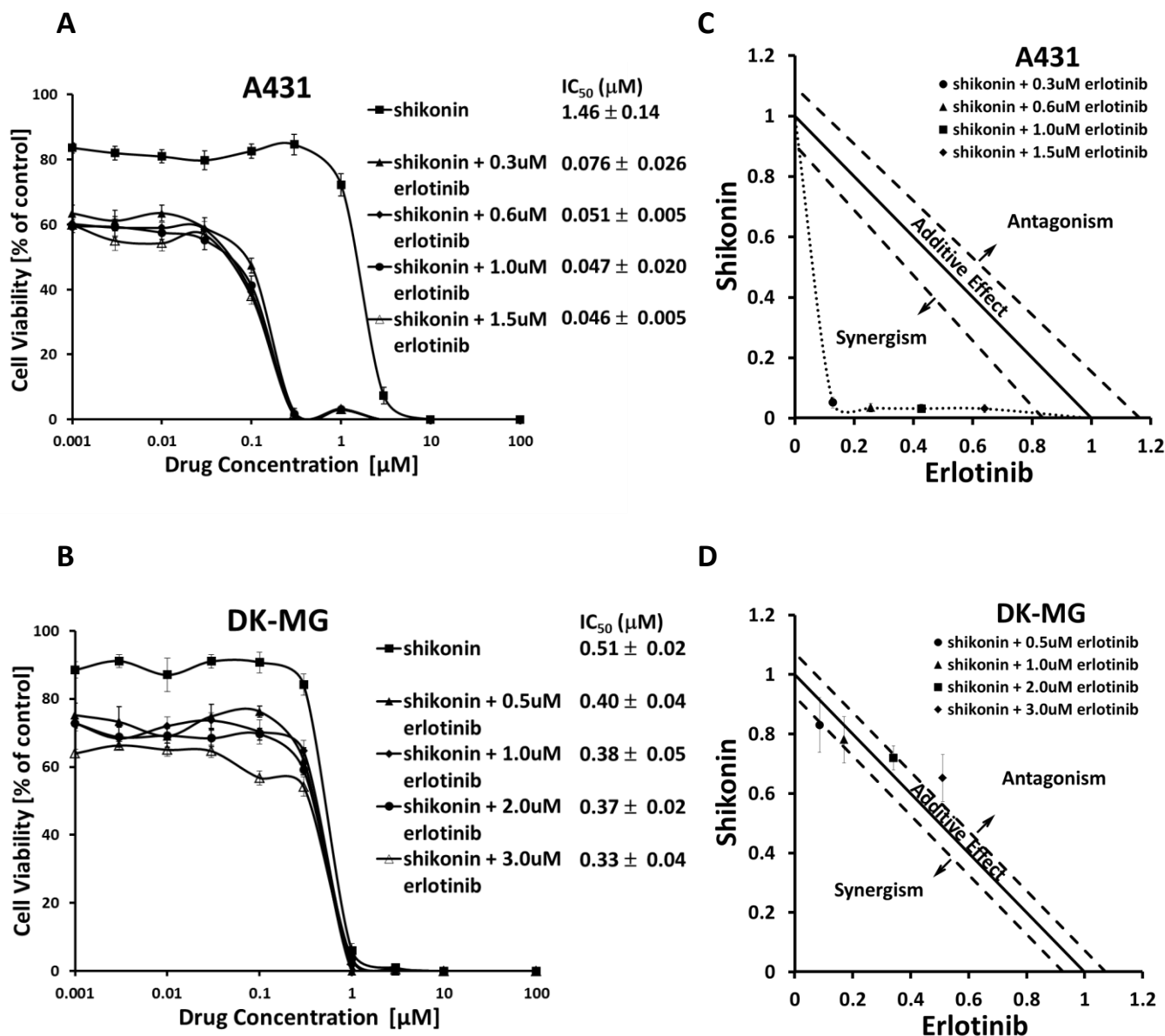
Figure 16: A and B, Effect of varying concentrations of shikonin on the proliferation of A431 and DK-MG cells in the absence or presence of indicated concentrations of erltinib. C and D, The dose-normalized isobolograms calculated from A and B for A431 and DK-MG cells. The doses of erlotinib and shikonin normalized with the dose of their IC_{50} to unity on both x and y axis. All points represent the drug combination that yield 50% cell inhibition. Synergism is indicated if the point falls on the lower left part of the graph. All the results shown are mean values and standard deviation of at least three independent experiments with each 6 parallel measurements.

3.1.3   Inhibitory effects on EGFR signaling pathway

The cell growth suppression of a panel of 13 EGFR-expressing cell lines by shikonin and increased cytotoxicity of shikonin towards U87MG.ΔEGFR, BS153, A431 cells in combination with erlotinib prompted us to examine the possible mechanisms responsible for shikonin-induced apoptosis and cellular targets that may be critical for the response to this combination treatment. We supposed that EGFR itself and its down-stream pathways were potential targets, therefore, the effect of shikonin and erlotinib on the phosphorylation of EGFR and the influence of shikonin on the EGFR down-stream signaling molecular were determined by Western blotting.
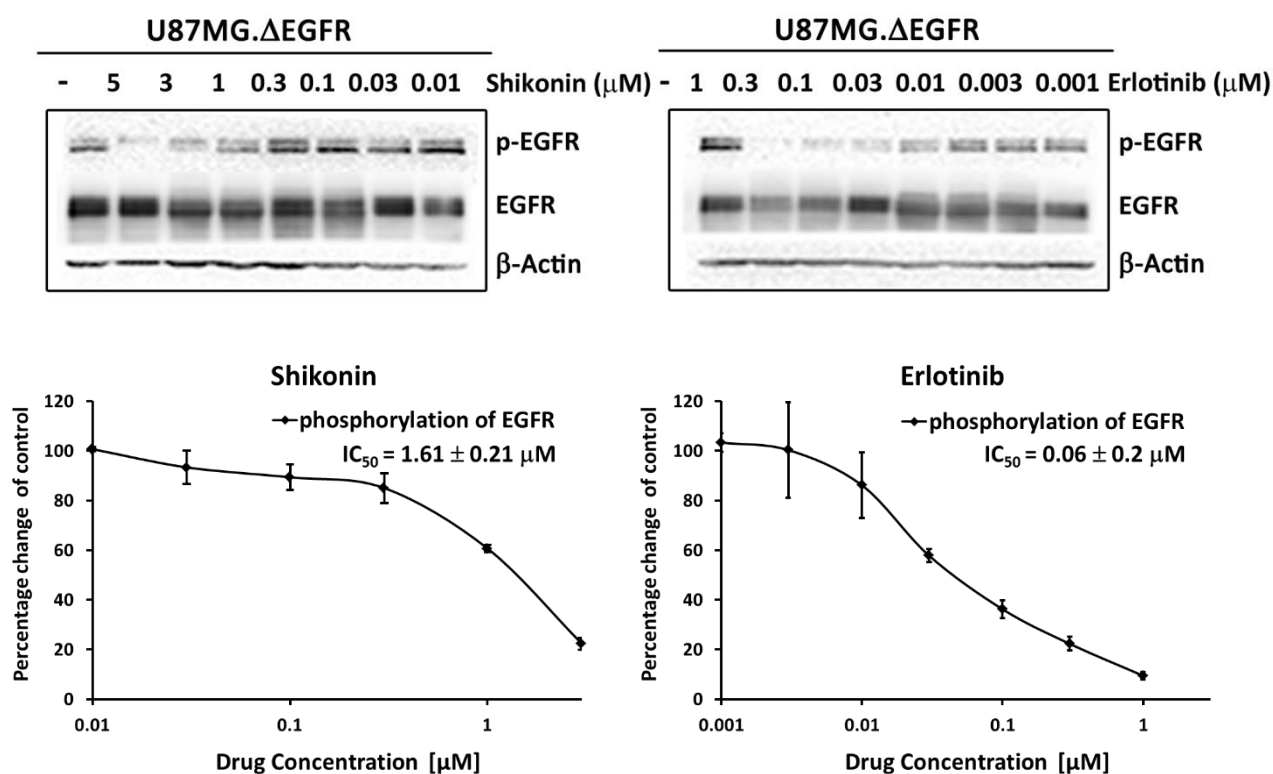
Figure 17: Effects of erlotinib and shikonin on the phosphorylation of ΔEGFR on U87MG.ΔEGFR cells as determined by Western blot. Analysis of band density of phosphorylation of ΔEGFR normalized to total EGFR levels. β-actin was used as loading control. Representative results and dose–response curves of three independent experiments are shown.

Both shikonin and erlotinib dose-dependently inhibited the phosphorylation of ΔEGFR without influencing the expression of total EGFR. The IC_{50} values for shikonin and erlotinib were 1.6 µM and 0.06 µM, respectively (Figure 17). The IC_{50} here was defined as the concentration needed for a 50% reduction in the phosphorylation of ΔEGFR calculated based on the dose-response curve. Compared to the untreated control, 3 µM shikonin treatment not only led to clear reduction of ΔEGFR phosphorylation in U87MG.ΔEGFR cells, but also to a corresponding decrease of the phosphorylation of EGFR downstream proteins, including the apoptosis-promoting proteins AKT (Ser473), P44/42 MAPK (Thr202/Thr204) and PLCγ1 (Tyr783) (Figure 18).
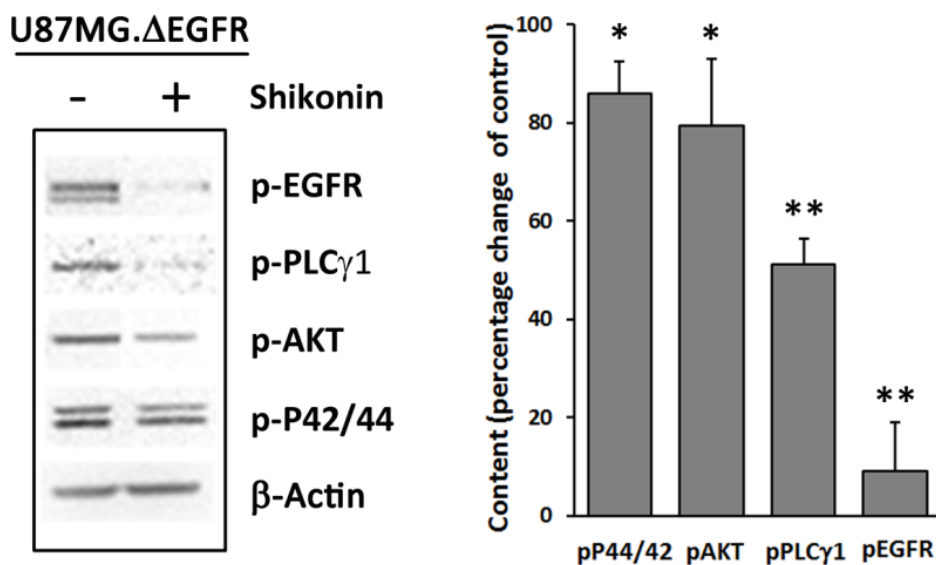
Figure 18: Western blot analysis of effect of shikonin on the phosphorylation of ΔEGFR, Akt, P44/42 and PLCγ1. Representative bands normalized to β-actin and the digitalized graph of the average and error bars of three independent experiments are shown. Statistical analysis was performed by two-tailed Student's *t*-test. *: $P < 0.05$ compared to control group; **: $P < 0.01$ compared to control group.

3.1.4   Inhibition of ΔEGFR phosphorylation by combination treatments

Based on these findings, especially considering the relationship between expression levels of EGFR and the combined effect produced by shikonin plus erlotinib in different cell lines, we

hypothesized that the synergy of erlotinib with shikonin and its derivatives displayed in inhibiting U87MG.ΔEGFR cell growth could be attributed at least in part to the ability to synergistically inhibit ΔEGFR phosphorylation. We therefore performed Bliss and Loewe analyses of Western blots to characterize drug interactions between erlotinib and shikonin and its derivatives in inhibition of ΔEGFR phosphorylation.

3.1.4.1 Assessment by Bliss independence model

U87MG.ΔEGFR cells were treated with indicated concentrations of erlotinib, shikonin or derivatives either alone or in combination for 24 h. U87MG.ΔEGFR cells were treated with erlotinib, shikonin or derivatives either alone or in combination. Fractional inhibitions of ΔEGFR phosphorylation by each compound alone and each combination were calculated from folds of control based on band density analyses of Western blots (Figure 19A). Compared to cells treated with erlotinib, shikonin or its derivatives alone, we observed a significant decrease in ΔEGFR phosphorylation in cells treated with the combination of erlotinib and shikonin or its derivatives (Figure 19B). Bliss analyses revealed values of shikonin and derivatives above 0 (Figure 19C).
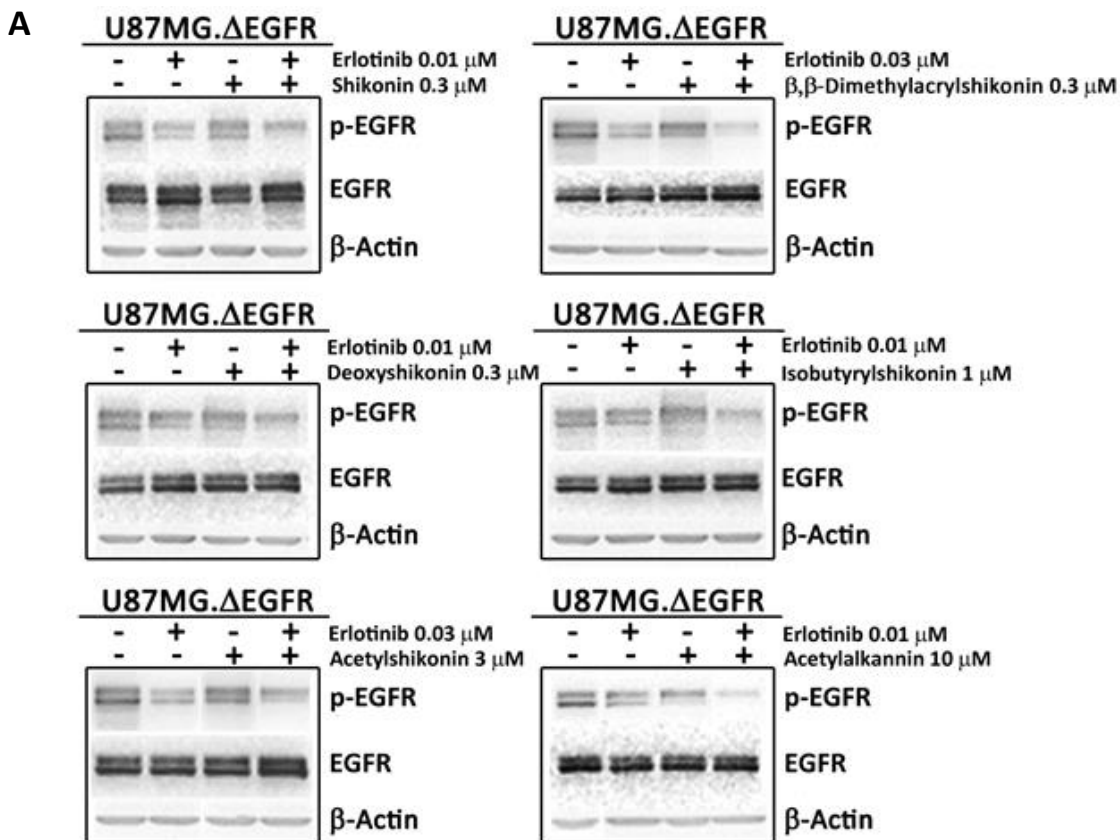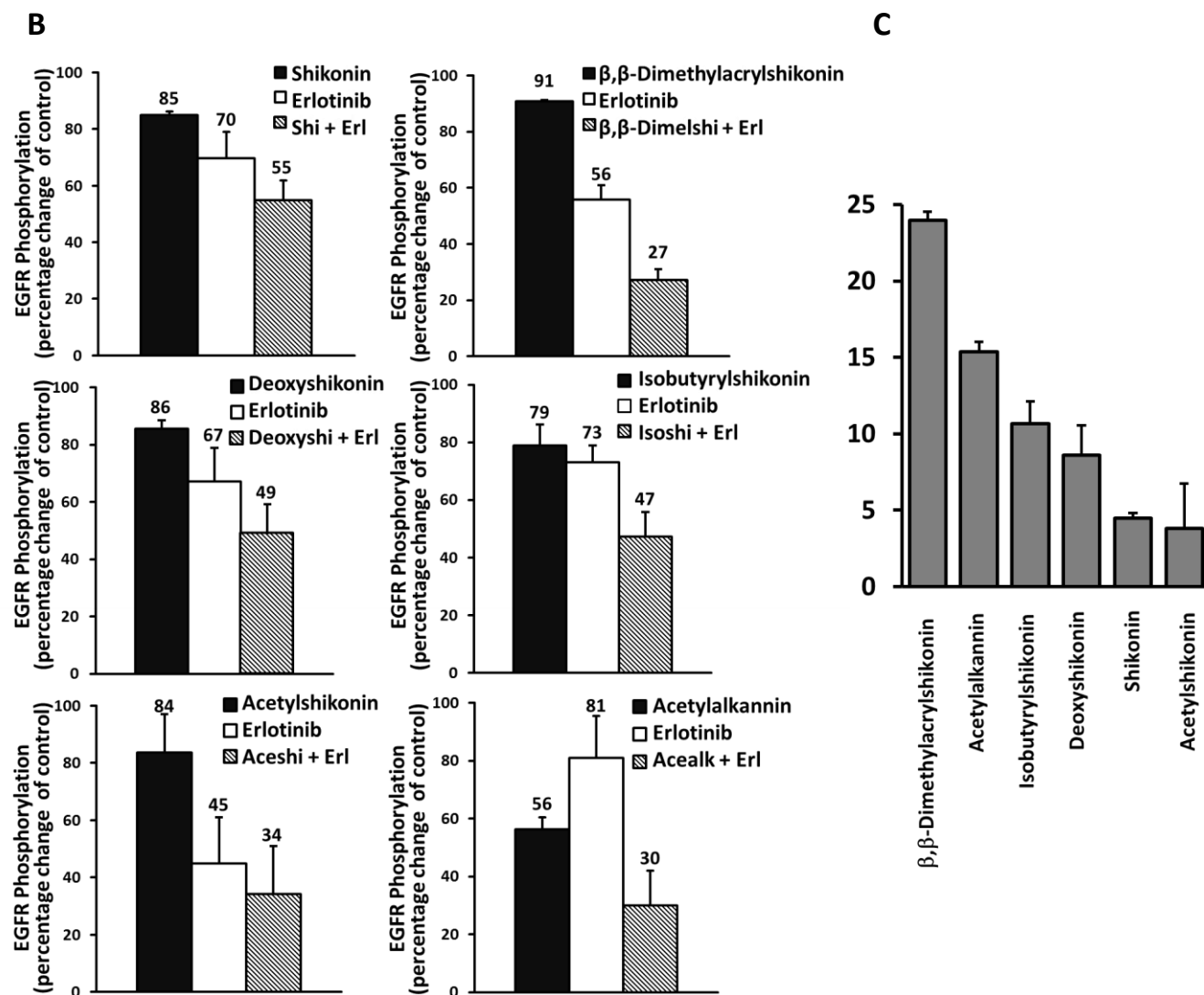
Figure 19: Combination of erlotinib with shikonin and its derivatives shows synergy in inhibiting ΔEGFR phosphorylation. A, Western blot for phosphorylation of ΔEGFR in U87MG.ΔEGFR cells after treatment with erlotinib combined with shikonin and derivatives. Analysis of band density of phosphorylation of ΔEGFR normalized to total β-actin levels. B, The digitalized graphs of the average and of A. C, Sensitivity of ΔEGFR phosphorylation to the combination of erlotinib with shikonin and its derivatives. Synergy, as noted by a positive Bliss value, was observed in all tested compounds.

3.1.4.2 Assessment by Loewe additivity model

Since both erlotinib and shikonin inhibited ΔEGFR phosphorylation in a dose-dependent manner, we applied Loewe additivity model to confirm the synergy of erlotinib with shikonin in

inhibiting ΔEGFR phosphorylation. U87MG.ΔEGFR cells were treated with varying concentrations of erlotinib in the presence of 20, 40, 60 and 80% of the IC_{50} concentration of shikonin for 24 h. The typical results of at least two independent experiments are shown in **Figure 20A**. Based on the analyses of band density, we calculated the content of ΔEGFR phosphorylation and obtained four dose-response curves for the four different combinations of erlotinib and shikonin (data not shown) and the corresponding IC_{50} values. Compared to erlotinib treatment alone ($IC_{50} = 0.06$ μM), the addition of shikonin led to a more pronounced inhibition of ΔEGFR phosphorylation. The IC_{50} values were reduced by 2-fold to more than 50-fold. The increase in ΔEGFR phosphorylation inhibition rose with serially increasing shikonin concentrations, indicating that the increasing IC_{50} fractions of shikonin enhanced the inhibitory activity of erlotinib on ΔEGFR phosphorylation. A dose-normalized IC_{50} isobologram generated by plotting of the combination treatment IC_{50} values of erlotinib against shikonin illustrated a synergistic inhibition of ΔEGFR phosphorylation (Figure 20B).

A

U87MG.ΔEGFR

- 1 0.3 0.1 0.03 0.01 0.003 0.001 Erlotinib (μM)

20% IC_{50} of shikonin
$IC_{50} = 0.011 \pm 0.002$ μM

40% IC_{50} of shikonin
$IC_{50} = 0.005 \pm 0.001$ μM

60% IC_{50} of shikonin
$IC_{50} = 0.003 \pm 0.0001$ μM

80% IC_{50} of shikonin
$IC_{50} < 0.001$ μM

p-EGFR

EGFR

β-Actin

B

Figure 20: A, Western blot for phosphorylation of ΔEGFR in U87MG.ΔEGFR cells after treatment with indicated concentrations of erlotinib combined with 20%-40%-60%-80% IC_{50} of shikonin. Representative bands and IC_{50} values of erlotinib combined with 20%-40%-60%-80% IC_{50} of shikonin in U87MG.ΔEGFR cells of at least two independent experiments are shown. **B**, The dose-normalized isobologram for erlotinib and shikonin with normalization of dose with IC_{50} to unity on both x and y axis. All points represent the drug combination that yield 50% reduction of ΔEGFR phosphorylation. Synergism is indicated if the point falls on the lower left part of the graph. Analysis of band density of phosphorylation of ΔEGFR normalized to total EGFR levels. β-actin was used as loading control.

3.1.5   Molecular docking analysis

In order to explore probable interaction models of shikonin and its derivatives and EGFR active sites, we performed *in silico* molecular docking of shikonin and its five derivatives that showed

synergism with erlotinib into EGFR kinase domain. The blind docking results showed us two binding sites for shikonin and its derivatives. One was in the catalytic site, the same binding site of the known inhibitor erlotinib. Shikonin and its derivatives bound to this pocket with the binding energy ranged from -7.85 kcal/mol to -8.81 kcal/mol which were comparable to that of erlotinib (-8.22 kcal/mol). The other binding site was on the distal surface of the carboxy-terminal lobe (C lobe) where Mig6 bound to and also was the asymmetric kinase domain dimer interface [111]. The binding energy of shikonin and its derivatives to this site was from -5.36 kcal/mol to -6.06 kcal/mol which was higher than that to erlotinib-binding site, indicating this may be a minor binding domain. Docking positions of shikonin and its derivatives and the standard inhibitors into the two different binding pockets of EGFR kinase domain were depicted in Figure 21.
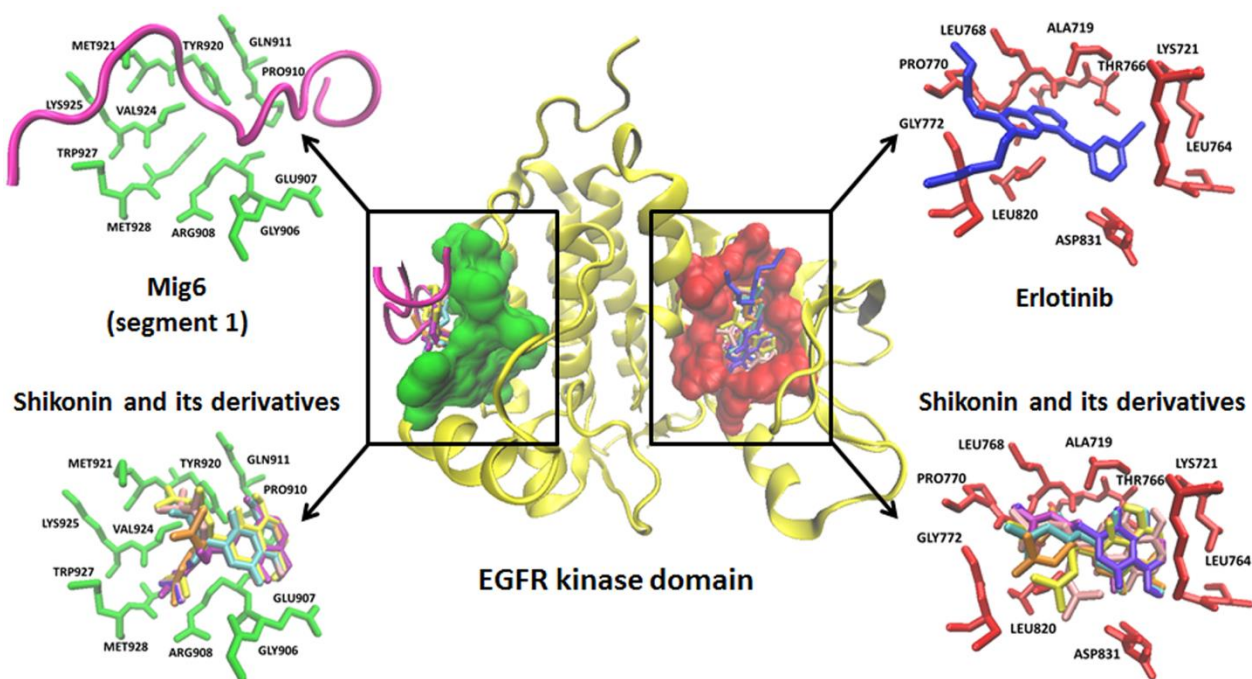
Figure 21: Dockings of shikonin and its derivatives at the EGFR kinase domain (PDB code: 1M17). In the middle, the protein was represented in yellow newcartoon format with surfaces of two different interaction sites: Erlotinib-binding pocket, red; Mig6-binding interface, green. On the left, the interacting amino acids with the control peptide Mig6 (mauve, newcartoon) and shikonin derivatives (different colors, licorice) were represented. On the right, we show the interacting amino acids with the control molecule Erlotinib (blue, licorice) and shikonin derivatives (different colors, licorice).

3.1.6 Summary: Inhibition of EGFR signaling and synergism with erlotinib in glioblastoma cells

In the previous part of this work, the effects of erlotinib in combination with shikonin and 14 shikonin derivatives in parental U87MG and transfected U87MG.ΔEGFR glioblastoma cells were investigated. Most of the shikonin derivatives revealed strong cytotoxicity towards both cell lines which were resistant to erlotinib. Shikonin together with five other derivatives, namely deoxyshikonin, isobutyrylshikonin, acetylshikonin, β,β-dimethylacrylshikonin, and acetylalkannin showed synergistic cytotoxicity towards U87MG.ΔEGFR in combination with erlotinib. Moreover, the combined cytotoxic effect of shikonin and erlotinib was further confirmed with another three EGFR-expressing cell lines, BS153, A431 and DK-MG. They exerted synergistic effect in A431 and BS153 cells which overexpressed EGFR/ΔEGFR. In the effort to clarify mechanisms underlying the response of cells to combination treatment, western blotting analysis was performed. It showed that shikonin not only dose-dependently inhibited EGFR phosphorylation and decreased phosphorylation of EGFR downstream molecules, including AKT, P44/42MAPK and PLCγ1, but also together with erlotinib synergistically inhibited ΔEGFR phosphorylation in U87MG.ΔEGFR cells as determined by Loewe additivity and Bliss independence drug interaction models. *In silico* molecular docking analysis illustrated the interaction models of shikonin and its derivatives in EGFR tyrosine kinases domain. Two active sites including erlotinib-binding pocket and Mig6-binding interface could be occupied by shikonin and its derivatives, indicating the molecular basis for the synergism between shikonin and erlotinib.

3.2   Inhibition of MYC and deregulation of ERK/JNK/MAPK and AKT signaling as a novel mechanism in leukemia cells

The previous chapter elucidated that shikonin and its derivatives exerted their strong cytotoxic effect against glioblastoma cells by inhibiting EGFR signaling pathway and synergistically worked with EGFR TKI erlotinib. However, the initial cytotoxicity screen of shikonin towards a panel of various tumor cell lines (carried out in our laboratory by Dr. Benjamin Wiench) found that leukemia cell lines were more sensitive to shikonin compared to solid tumor cell lines including breast cancer cell lines (MCF7, SK-BR-3 and MDA-MB-231), colorectal cancer cell lines (SW-1116, HCT-116 and SW680), pancreas cancer cell lins (Capan1 and SUIT-2) and kidney cancer cell line (786-O) [112]. Moreover, the IC_{50} values in glioblastoma cell lines tested in this study were also higher than those in leukemia cells, further confirming the particularly effect of shikonin towards leukemia cells. Since EGFR expression was not detected in leukemia cells and shikonin was known as a multi-targeted compound, there should be other mechanisms for leukemia cells in response to shikonin treatment. Hence, the second part of the thesis aimed at identifying new mechanisms of shikonin and its derivatives in hematological malignances. Experiments were first performed on U937 histocytic leukemia cells and subsequently verified on other four leukemia cell lines.[2]

3.2.1 Cytotoxicity towards U937 leukemia cells

In the previous report, the sensitivities of a panel of 15 different cell lines to shikonin were analyzed and the U937 histiocytic leukemia cell line turned out to be the most sensitive one [112]. Thereby, this cell line was used for screening the cytotoxicity of shikonin and 14 shikonin derivatives.

---

[2] The results presented in this section have been submitted to a peer-reviewed scientific journal:

Zhao Q, Assimopoulou A, Klauck S, Damianakos H, Chinou I, Kretschmer N, Rios J, Papageorgiou V, Bauer R and Efferth T. Inhibition of c-MYC with involvement of ERK/JNK/MAPK and AKT pathways as a novel mechanism for shikonin and its derivatives in killing leukemia cells. Submitted at *Oncotarget*.

All text passages, tables and figures of this publication that are used in a modified form in this dissertation were prepared or written by myself.
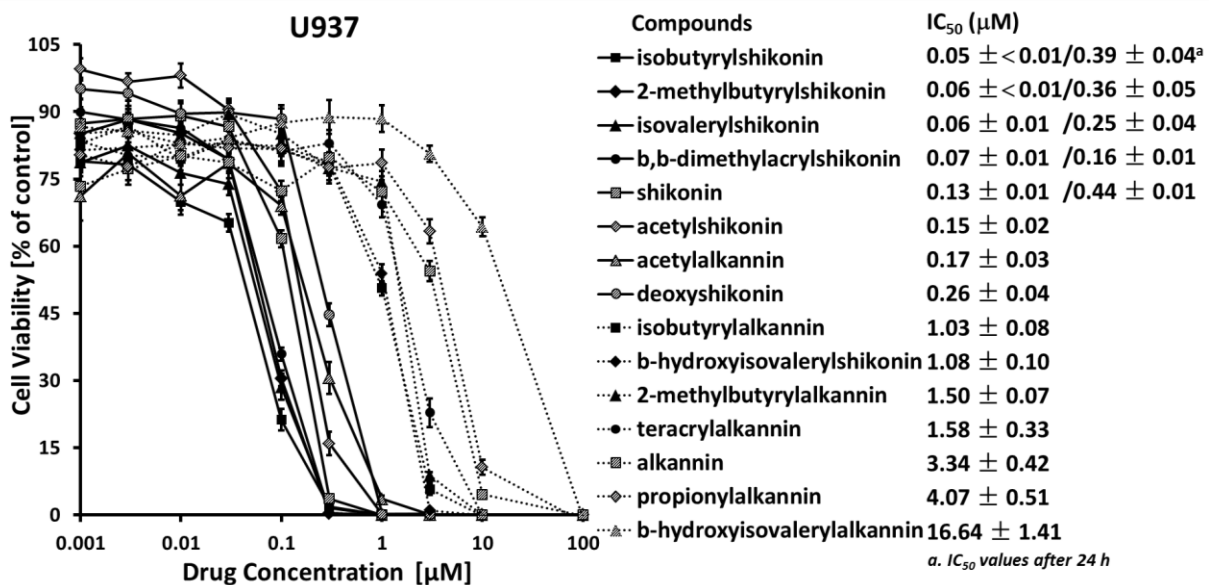
Figure 22: Cytotoxicity of shikonin and derivatives towards U937 leukemia cells. Cells were treated with varying concentrations of shikonin or 14 derivatives and cell viability was measured by resazurin assay after 24 h or 72 h. Representative dose-response curves and IC$_{50}$ values (mean ± SEM) of 72 h treatment for shikonin and 14 derivatives are shown. The IC$_{50}$ values for shikonin and four derivatives after 24 h are also diaplayed in parallel. Results are mean values and standard deviation of three independent experiments with each 6 parallel measurements.

The dose-response curves and IC$_{50}$ values of 72 h treatment with varying concentrations of shikonin and derivatives are summarized in Figure 22. Four compounds, *i.e.* isobutyrylshikonin, 2-methylbutyrylshikonin, isovalerylshikonin and β,β-dimethylacrylshikonin, showed stronger effects than shikonin itself. Therefore, these derivatives were further analyzed together with shikonin for their molecular mechanism against leukemia cells. The IC$_{50}$ values for shikonin and these four derivatives after 24 h were also measured by resazurin assay. The other derivatives were less toxic than shikonin towards U937 cells. Furthermore, it was interesting that shikonin and its homochiral derivatives were more active than their enantiomers, *e.g.*, the IC$_{50}$ values of isobutyrylshikonin (0.05 μM), 2-methylbutyrylshikonin (0.06 μM) and β-hydroxyisovalerylshikonin (1.08 μM) were much less than those of their corresponding enantiomers, isobutyrylalkannin (1.03 μM), 2-methylbutyrylalkannin (1.50 μM) and β-hydroxyisovalerylalkannin (16.64 μM).

3.2.2 Assessment of cell death mode by flow cytometry

To further investigate death modes caused by shikonin and derivatives in U937 cells, we performed flow cytometry with annexin V and PI double staining in U937 cells treated with and without shikonin and four derivatives in the presence or absence of the specific necroptosis inhibitor Nec-1 and the caspase apoptosis-specific inhibitor z-VAD-fmk. As shown in Figure 23,
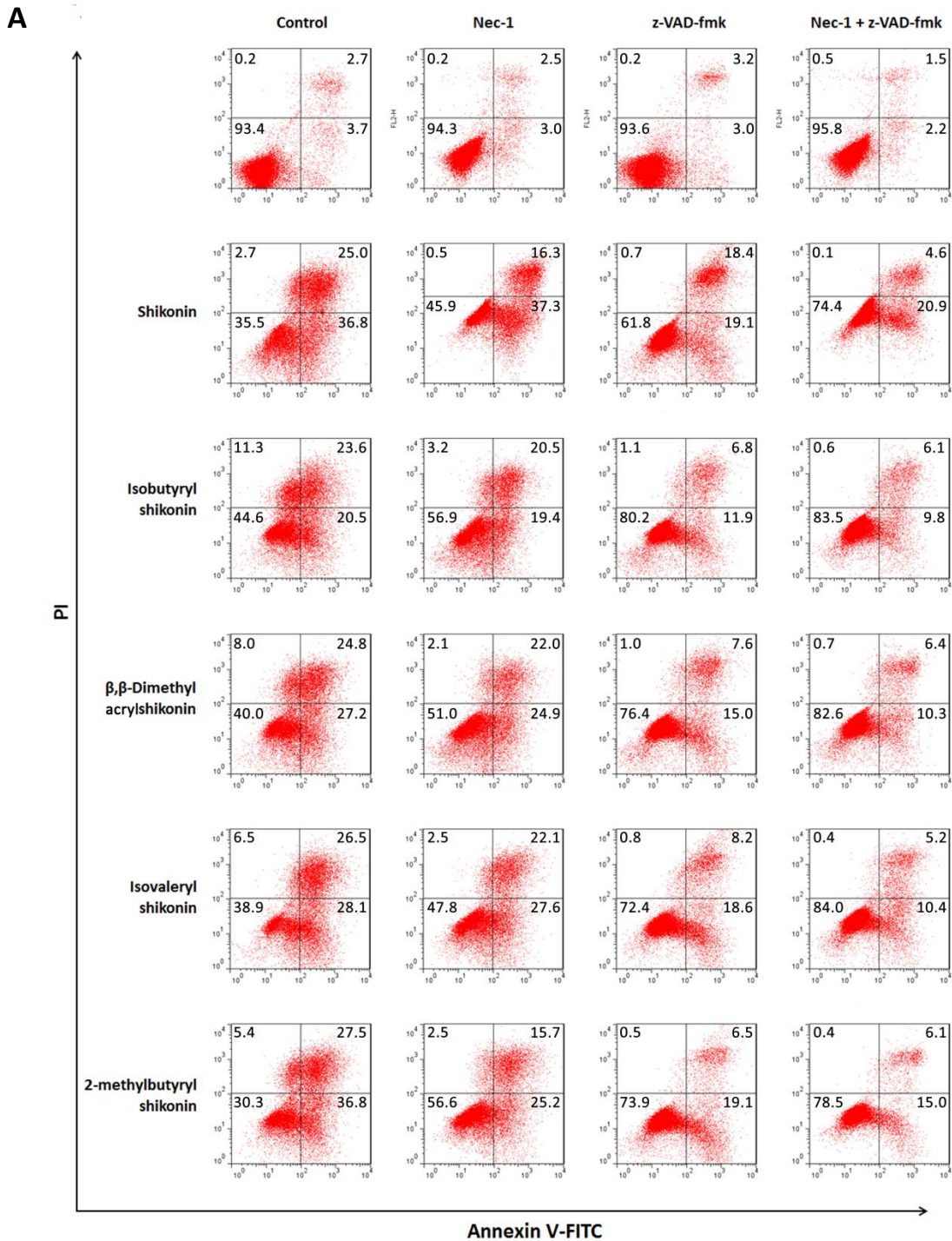
B
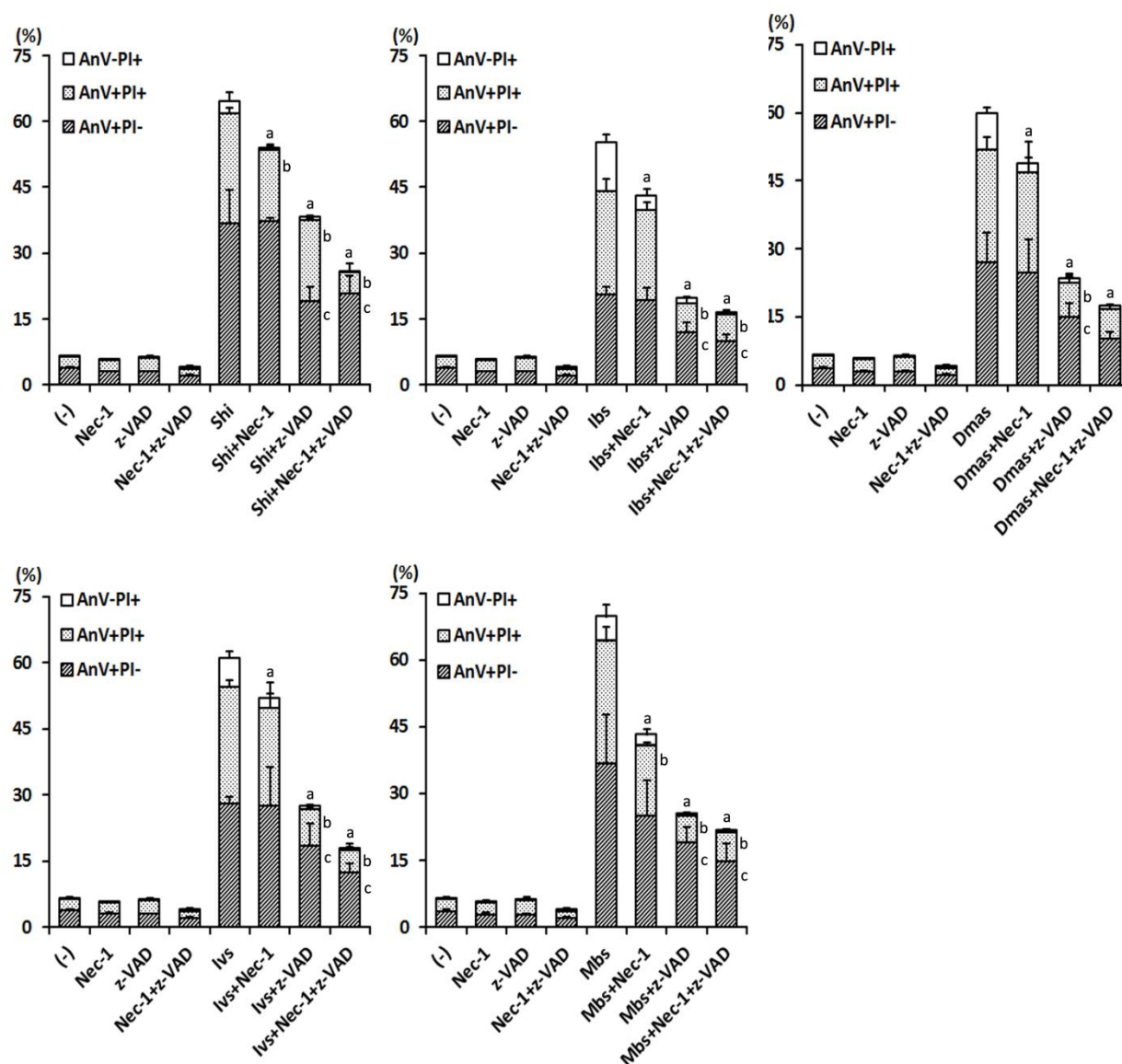
Figure 23: Modes of cell death induced by shikonin and its derivatives in U937 cells. A, Representative dot plots of flow cytometry analysis after treatment of U937 cells with 50 μM necrostatin-1 (Nec-1) or z-VAD-fmk (z-VAD) 1 h prior to co-incubation with IC_{50} concentrations of shikonin or its derivatives for 24 h. A dual staining with annexin V-FITC/PI was performed. The values indicate the percentage of cells in each region. B, The digitalized graghs of means ± SEM of three independent experiments one is shown in Fig. 23A. [a], $p < 0.05$ *vs.* shikonin or its derivatives AnV-PI+; [b], $p < 0.05$ *vs.* shikonin or its derivatives AnV+PI+; [c], $p < 0.05$ *vs.* shikonin or its derivatives AnV+PI-, calculated by two-tailed Student's t test. AnV-PI+, annexin V−/PI+ (late necrosis); AnV+PI+, annexin V+/PI+ (late apoptosis or early necrosis); AnV+PI-, annexin V+/PI− (early apoptosis). Shi, shikonin; Ibs, isobutyrylshikonin; Dmas, β,β-dimethylacrylshikonin; Ivs, isovalerylshikonin; Mbs, 2-methylbutyrylshikonin.

pretreatment with Nec-1 reduced necrosis (annexin V-/PI+) and partly late apoptosis (annexin V+/PI+), but not early apoptosis (annexin V+/PI-). By contrast, z-VAD-fmk attenuated early and late apoptosis and resulted in more cell viability than Nec-1, indicating that low concentrations of shikonin or its four derivatives mainly induced cell death by caspase-dependent apoptosis. However, the most effective inhibition of cell death by shikonin and its derivatives was achieved by the combination of Nec-1 and z-VAD-fmk, suggesting that necroptosis, as additional mode of death also contributes to cell death.

3.2.3 Gene expression profiling

Gene expression analyses were performed to get deeper insights into the cytotoxic activity of shikonins. U937 cells were treated 24 h with IC_{50} values of shikonin, isobutyrylshikonin, 2-methylbutyrylshikonin, isovalerylshikonin, β,β-dimethylacrylshikonin or DMSO solvent control, respectively. Then, total RNA was isolated for transcriptome-wide microarray analysis.

The numbers of deregulated genes upon treatment with shikonin compounds were visualized as Venn diagram (**Figure 24**). Remarkably, about 18% of the genes were present in the datasets of all five compounds. If four of five compounds were taken into account, 265 genes are commonly differentially expressed between treated and untreated cells.
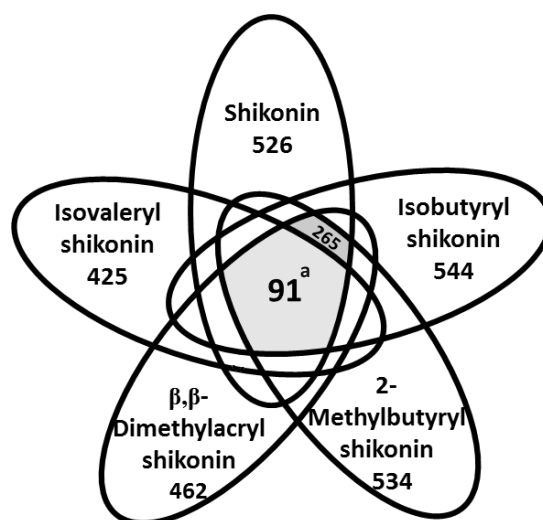
Figure 24: Venn diagrams: Numbers of genes deregulated after 24 h. Only molecules with fold changes $\geq \pm 1.65$ are presented in the diagram. [a], $p < 0.0001$, indicating the probability of 91 genes occurred by chance, calculated by Monte Carlo simulation method.

A ranking list of deregulated genes is shown in Table 2. Remarkably, *MYC* was the most commonly down-regulated gene among all five compounds. Six commonly deregulated genes including *MYC* were quantified by real-time RT-PCR to technically validate the microarray results. The correlation coefficients (R-values) between mRNA expression values determined by microarray hybridization and real-time RT-PCR were in the range of 0.80 to 0.93 for each compound (Pearson correlation test). Importantly, this indicated a high degree of concordance between the data obtained from the two different methods (Table 3).

Table 2: Top up- and down regulated molecules in U937 cells upon treatment with shikonin and its derivatives for 24 h.

	Shikonin		Isobutyrylshikonin		β,β-Dimethylacrylshikonin		Isovalerylshikonin		2-Methylbutyrylshikonin	
	Gene	Fold change	Gene	Fold change	Gene	Fold change	Gene	Fold change	Gene	Fold change
Top up-regulated genes	RNU11	18,5	LY96	12,4	IER3	10,6	RMRP	74,0	LY96	11,2
	IER3	9,6	IER3	10,5	RNU11	10,6	RNU11	73,3	IER3	9,5
	LY96	9,0	JUN	7,1	LY96	9,8	RNU4ATAC	44,5	CCL3L1/CCL3L3	4,7
	HMOX1	8,3	CCL3L1/CCL3L3	6,0	HMOX1	6,3	HIST1H4A	44,2	JUN	4,7
	HIST1H4A	5,9	HMOX1	5,8	EMP1	5,5	mir-320	41,4	EMP1	4,6
	mir-320	5,8	MLLT11	5,7	HIST1H4A	5,5	RNU12	35,4	VIM	4,6
	JUN	5,8	EMP1	5,2	JUN	5,1	HIST1H2BB	30,2	MLLT11	4,4
	ALB	5,6	GABARAPL1	5,2	CCL3L1/CCL3L3	4,6	VTRNA1-1	22,5	GABARAPL1	4,3
	GABARAPL1	5,4	RNU11	5,0	UPP1	4,6	HIST1H2AG	22,2	HMOX1	4,1
	RNU12	5,2	CYP1A1	4,7	CYP1A1	4,2	ALB	22,0	ANXA1	3,8
Top down-regulated genes	MYC	-5,4	MYC	-10,3	MYC	-10,4	MYC	-9,9	MYC	-8,3
	MYB	-4,5	MS4A3	-7,0	MS4A3	-6,8	PAFAH1B3	-8,5	MS4A3	-8,3
	LRP3	-4,2	MYB	-5,7	CCND2	-5,2	LRP3	-6,8	CTSG	-4,9
	PPIA	-3,9	CTSG	-5,2	MYB	-5,2	PPIA	-6,7	MT1G	-4,4
	MS4A3	-3,6	CCND2	-4,8	CTSG	-4,5	MYB	-6,0	CCND2	-4,4
	DTD1	-3,5	MT1G	-4,5	RPL29	-4,3	NIP7	-5,9	RPL29	-4,3
	IFITM2	-3,5	IFITM2	-4,2	RNASE3	-3,8	DTD1	-5,9	MYB	-3,9
	WASH1	-3,5	RPL29	-4,2	IFITM2	-3,8	CDCA7	-5,4	NOP16	-3,3
	PAFAH1B3	-3,4	ELANE	-3,8	RRS1	-3,4	DUT	-5,4	RPL36A	-3,3
	CCND2	-3,3	LRP3	-3,6	RPS15	-3,3	MS4A3	-5,3	RRS1	-3,3

Table 3: Comparison of microarray gene expression profiling and real-time RT-PCR for six selected genes. The correlation coefficient (R-value) between mRNA expression values determined by microarray hybridization and real-time RT-PCR were caculated with Pearson correlation test.

Genes	Fold change									
	Shikonin		Isobutyrylshikonin		β,β-Dimethylacrylshikonin		Isovalerylshikonin		2-Methylbutyrylshikonin	
	Microarray	RT-PCR	Microarray	RT-PCR	Microarray	RT-PCR	Microarray	RT-PCR	Microarray	RT-PCR
JUN	5.8	30.67	7.1	160.45	5.1	19.37	7.7	37.24	4.7	32.05
GABARAPL1	5.4	78.16	5.2	78.14	4.1	56.77	4.5	96.57	4.3	112.43
LY96	9.0	69.84	12.4	161.44	9.8	49.32	4.7	93.54	11.2	103.92
IFITM2	-3.5	-1.05	-4.2	-1.31	-3.8	-1.59	-5.1	-1.27	-3.2	-1.32
MYC	-5.4	-2.37	-10.3	-2.30	-10.4	-5.97	-9.9	-5.26	-8.3	-2.20
MS4AS	-3.6	-1.72	-7.0	-2.62	-6.8	-10.03	-5.3	-4.63	-8.3	-1.24
R-value	0.9011		0.9386		0.8662		0.7954		0.8480	

All data obtained by microarray analyses were subjected to Ingenuity Pathway Analysis (IPA). The deregulated genes were correlated with several molecular and cellular functions, including cell death and survival, cellular growth and proliferation, cellular development, cellular movement, gene expression, cell cycle, cell-to-cell signaling and interaction, etc. Figure 25A and B displays the top cellular functions and pathways affected by shikonin and derivatives in U937 cells.

A
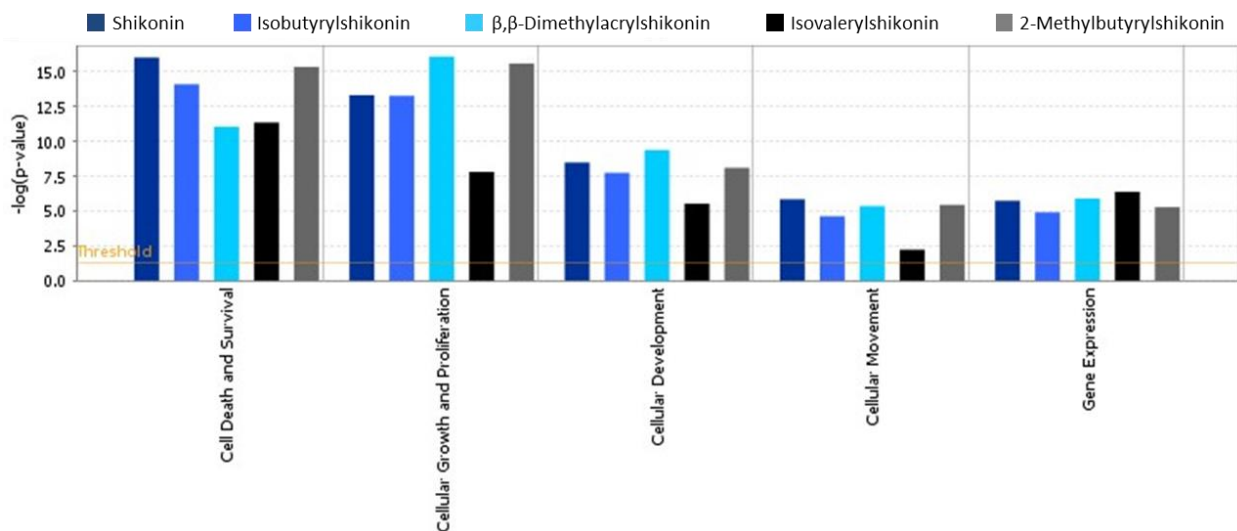
B
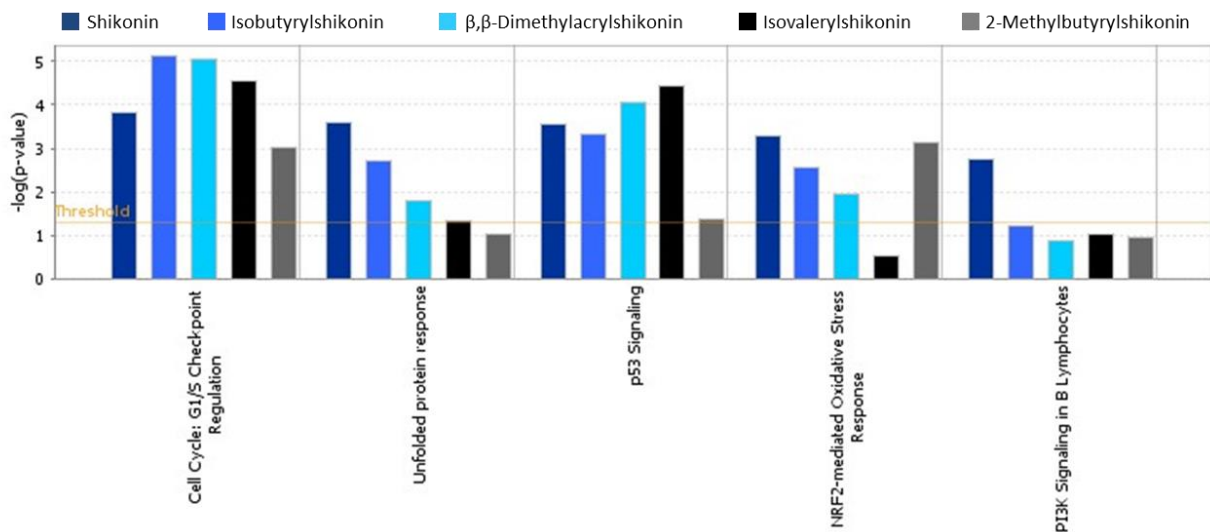
Figure 25: Pathway analyses: Top cellular functions (A) and canonical pathways (B) affected by shikonin and its derivatives examined by mRNA microarray hybridization. P-values were calculated using right-tailed Fisher's exact test.

Furthermore, an upstream regulator analysis was performed with IPA to identify transcriptional regulators, kinases, or enzymes that may be responsible for gene expression changes in U937 cells after treatment. Table 4 shows the upstream regulators predicted by IPA to be activated or inhibited by shikonin or derivatives. The most likely activated and inhibited upstream regulators for each compound were underlined. MYC was found to be a commonly inhibited transcription regulator by shikonin and derivatives. Figure 26 shows the deregulated genes controlled by MYC.

Table 4: Upstream regulators presumably affected by shikonin and its derivatives after 24 h in U937 cells. The most likely activated and inhibited upstream regulators for each compound were underlined.

Shikonin		Isobutyrylshikonin		β,β-Dimethylacrylshikonin		Isovalerylshikonin		2-Methylbutyrylshikonin	
Activated	Inhibited	Activated	Inhibited	Activated	Inhibited	Activated	Inhibited	Activated	Inhibited
TP53	MYC	PDGF BB	MYC	PDGF BB	MYC	FOXO3	MYC	PDGF BB	MYC
ATF4	BRD4	ATF4	BRD4	CEBPA	BRD4	NANOG	BRD4	TNF	BRD4
ATF2	MAX	FOXO3	Mek	TREM1	Hdac	SMAD4		TCR	Mek
CDKN2A	TRIB3	ELANE	MGEA5	FOXO3	Mek	RUVBL1		TGM2	mir-146
FOXL2	MNT	TREM1		TREM1	MGEA5	PAF1		EGF	miR-155-5p
CEBPB	Mek	CEBPB		TP53		HIF1A		PF4	TAB1
PGR		CDKN2A		TGM2		PPRC1		TREM1	MGEA5
IGF1		FOXL2		CDKN2A				CCL5	
PPRC1		TP53		CEBPB				KRAS	
FOXO1		TGM2		FOXO1				Fcer1	
		ERK1/2		GLI1				TGFB1	
		IGF1		SELPLG				IKBKB	
		FOXO1		NEDD9				NFkB	
		NFkB		EP300				IRF3	
		EP300		Jnk				CEBPB	
		SELPLG		Cg				Jnk	
		PPRC1						SELPLG	
		Jnk						IGF1	
		CXCL12						CAMP	
		NEDD9							
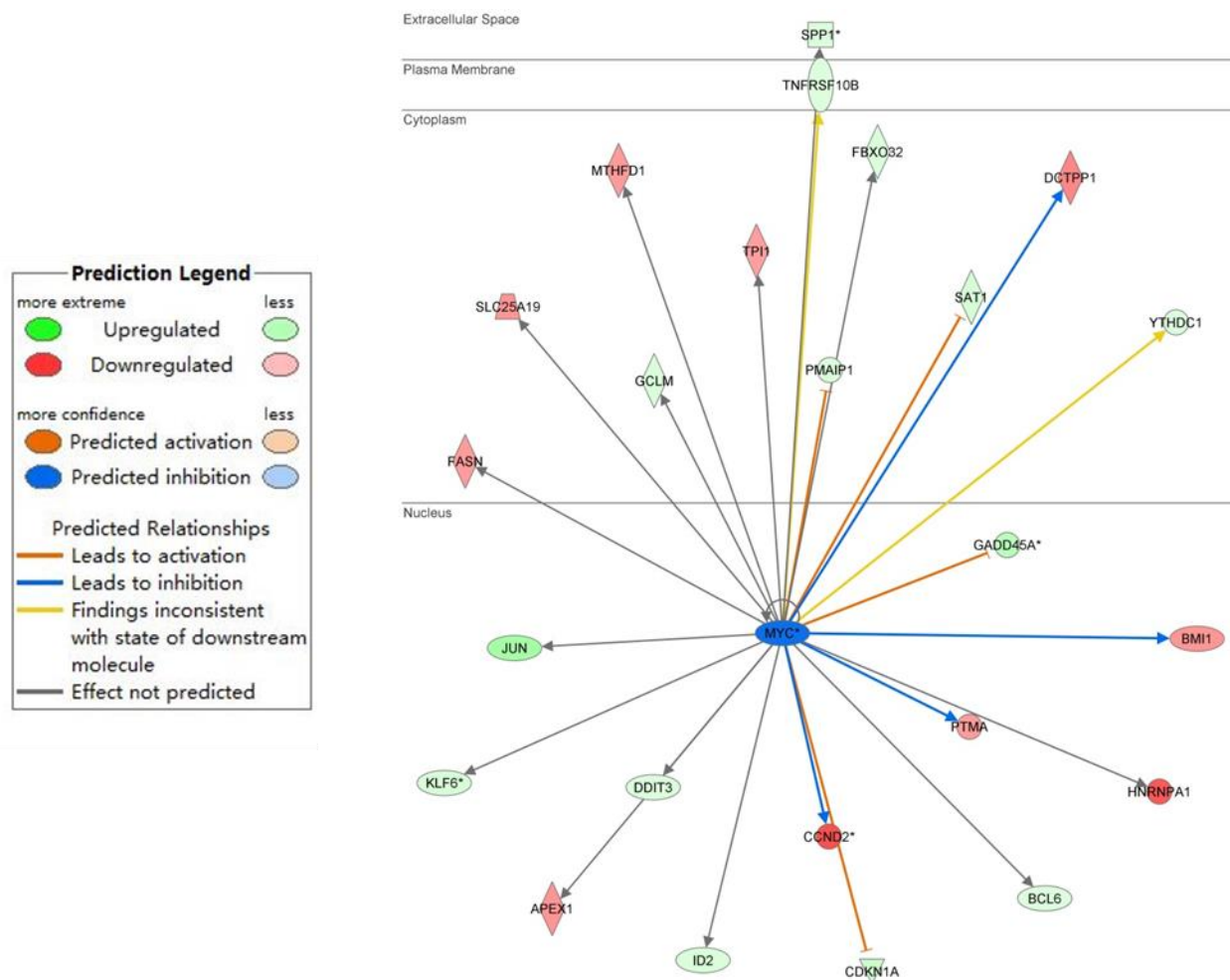
Figure 26: Deregulated genes under the influence of MYC as common upstream regulator inhibited by shikonin and its derivatives.

3.2.4 Inhibition of c-MYC expression

The microarray analysis indicated that *MYC* was not only the most commonly down-regulated gene, but also the common upstream regulator affected by shikonin and its four derivatives. Moreover, cell cycle G1/S check point regulation, which is mainly regulated by MYC [88], was also the top canonical pathway affected by all shikonins. Therefore, we supposed that MYC itself may be a potential target of this type of compounds. To analyze this hypothesis, we performed Western blotting to prove whether shikonin and its derivatives affect c-MYC expression. Two known c-MYC inhibitors, 10074-G5 and 10058-F4 were used as control drugs.

As shown in Figure 27A, B, shikonin and all four derivatives indeed revealed a strong inhibition of c-MYC expression in U937 cells at 1 µM and 0.3 µM. This effect was greater than that of 10058-F4 and comparable to that of 10074-G5, however at much lower concentrations than the control compounds.

A

B
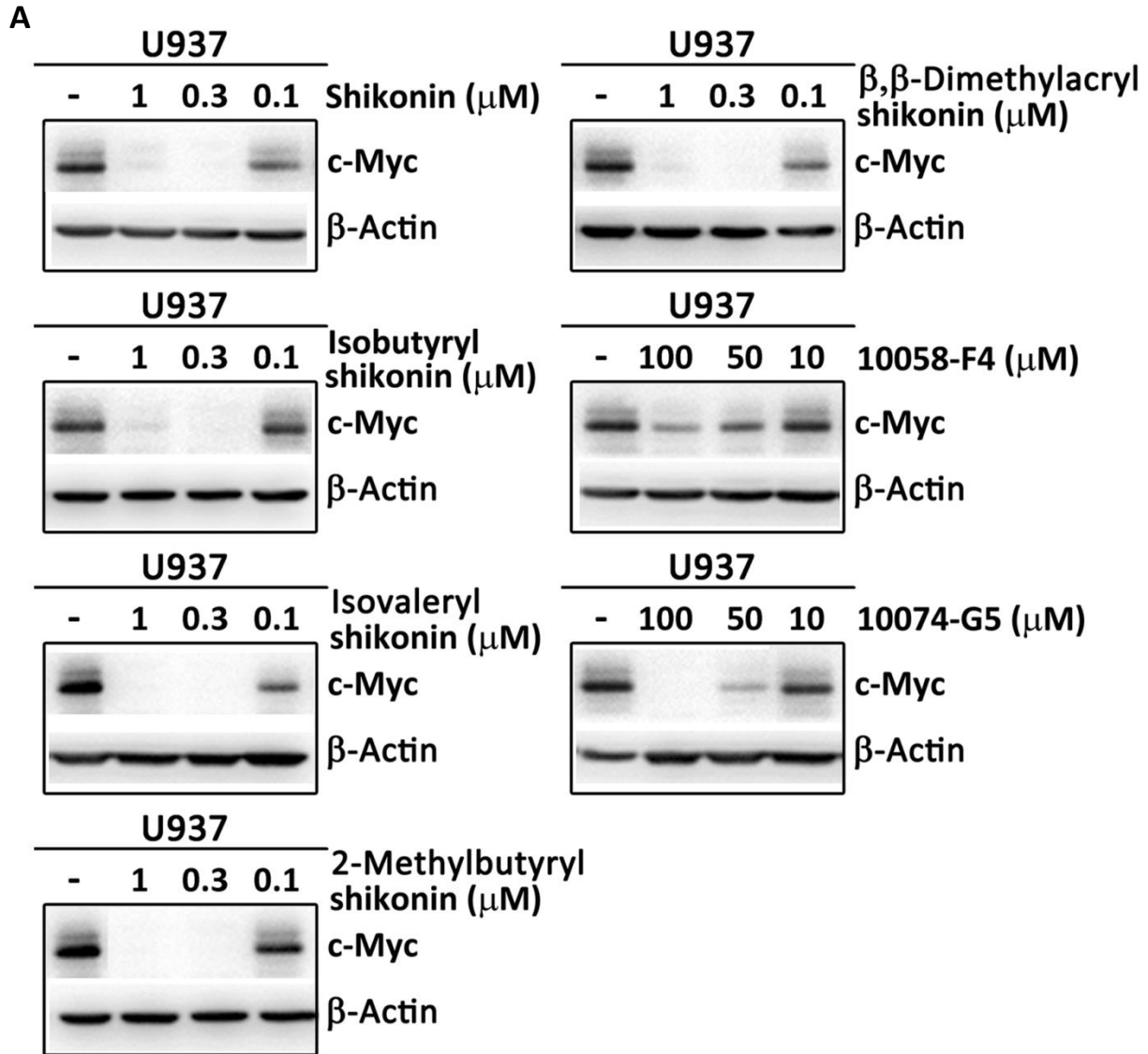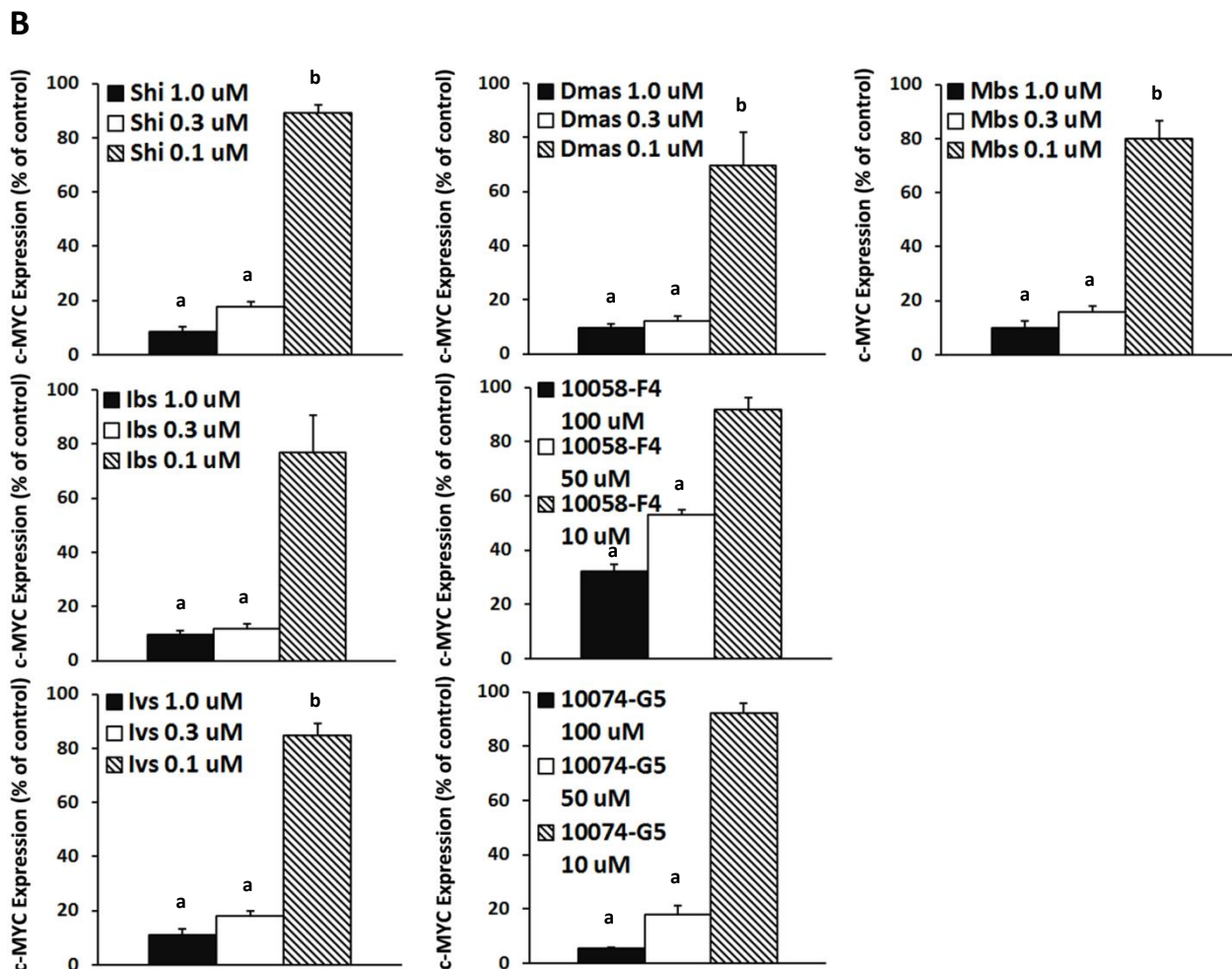
Figure 27: Inhibition of c-MYC protein expression by shikonin, its derivatives, 10058-F4 and 10074-G5 in U937 cells. **A**, Western blot analysis of c-MYC expression after 24 h treatment with these compounds. β-Actin was used as loading control. **B**, Digitalized graphs of c-MYC protein levels as quantified by FluorChem Q. Data were normalized to β-actin expression and represented as means ± SEM of three independent experiments. [a], $p < 0.01$ *vs.* control; [b], $p < 0.05$ *vs.* control, calculated by two-tailed Student's t test. Shi, shikonin; Ibs, isobutyrylshikonin; Dmas, β,β-dimethylacrylshikonin; Ivs, isovalerylshikonin; Mbs, 2-methylbutyrylshikonin.

3.2.5 Inhibition of c-MYC DNA-binding activity

Next, we attempted to determine, whether the inhibition of c-MYC expression in U937 cells by shikonin and its derivatives was associated with decreased transcriptional activity and DNA binding activity of c-MYC. For this purpose, we used a specific ELISA-based DNA-binding

assay. In Figure 28, the DNA binding activity of c-MYC in nuclear extracts of U937 cells was suppressed to different extents by treatment of 0.3 µM shikonin and derivatives or 50 µM of the two control inhibitors. These results were in concordance with the Western blot analysis, since 10058-F4 caused the weakest inhibition, while shikonin and derivatives showed strong inhibition, which was similar to 10074-G5. This clearly suggests that shikonin and its derivatives possess MYC inhibitory activities.
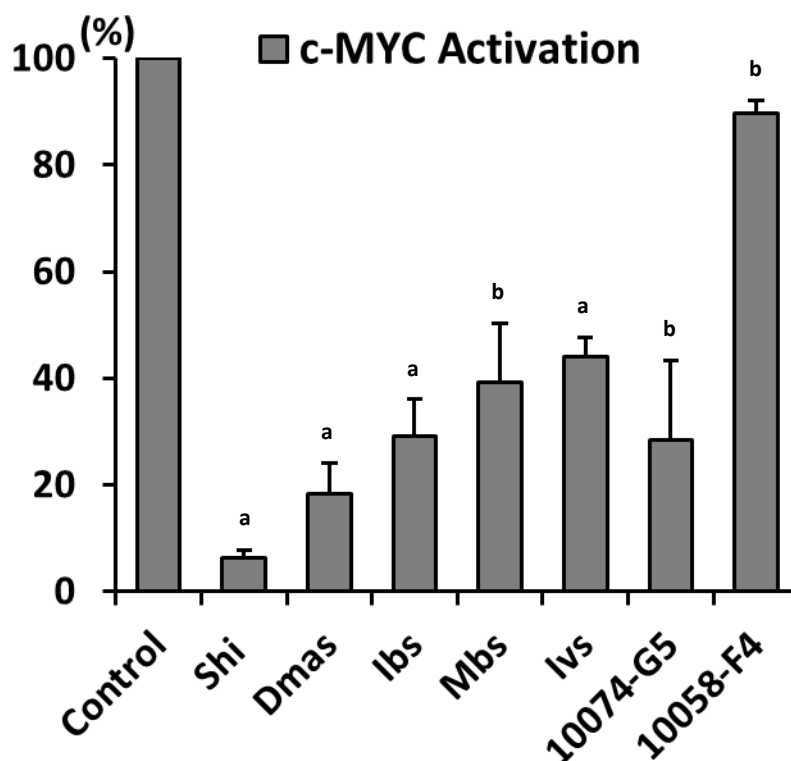
Figure 28: Determination of DNA binding activity of c-MYC by Trans-AM ELISA-based kit. Nuclear extracts were obtained after treatment of U937 cells with 0.3 µM shikonin and its derivatives or 50 µM 10058-F4 and 10074-G5 for 24 h. Protein/oligonucleotide binding activity was measured by colorimetric analysis with 10 µg of nuclear extracts. The absorbance at 450 nm was recorded by an ELISA plate reader. Results are presented as percentage with respect to the untreated control and represented as mean values ± SEM of three independent experiments. [a], $p < 0.01$ *vs.* control; [b], $p < 0.05$ *vs.* control, calculated by two-tailed Student's t test. Shi, shikonin; Ibs, isobutyrylshikonin; Dmas, β,β-dimethylacrylshikonin; Ivs, isovalerylshikonin; Mbs, 2-methylbutyrylshikonin.

3.2.6 Involvement of AKT and ERK1/2, JNK MAPK signaling in c-MYC downregulation

It is known that c-MYC is regulated by multiple signaling pathways, including MAPK and AKT signal transduction cascades [101, 113-115]. Therefore, we further employed Western blot analysis to evaluate, whether the MAPK and AKT signal transduction pathways were involved in shikonin-induced c-MYC down-regulation (Figure 29). The results showed that shikonin inhibited phospho-ERK1/2 and activated phospho-SAPK/JNK without influencing total ERK1/2 and SAPK/JNK expression. However, both phospho-AKT and total AKT expression were reduced by shikonin. No appreciable changes were detected in phospho-p38 or total p38. Comparable results were also found for the other shikonin derivatives.
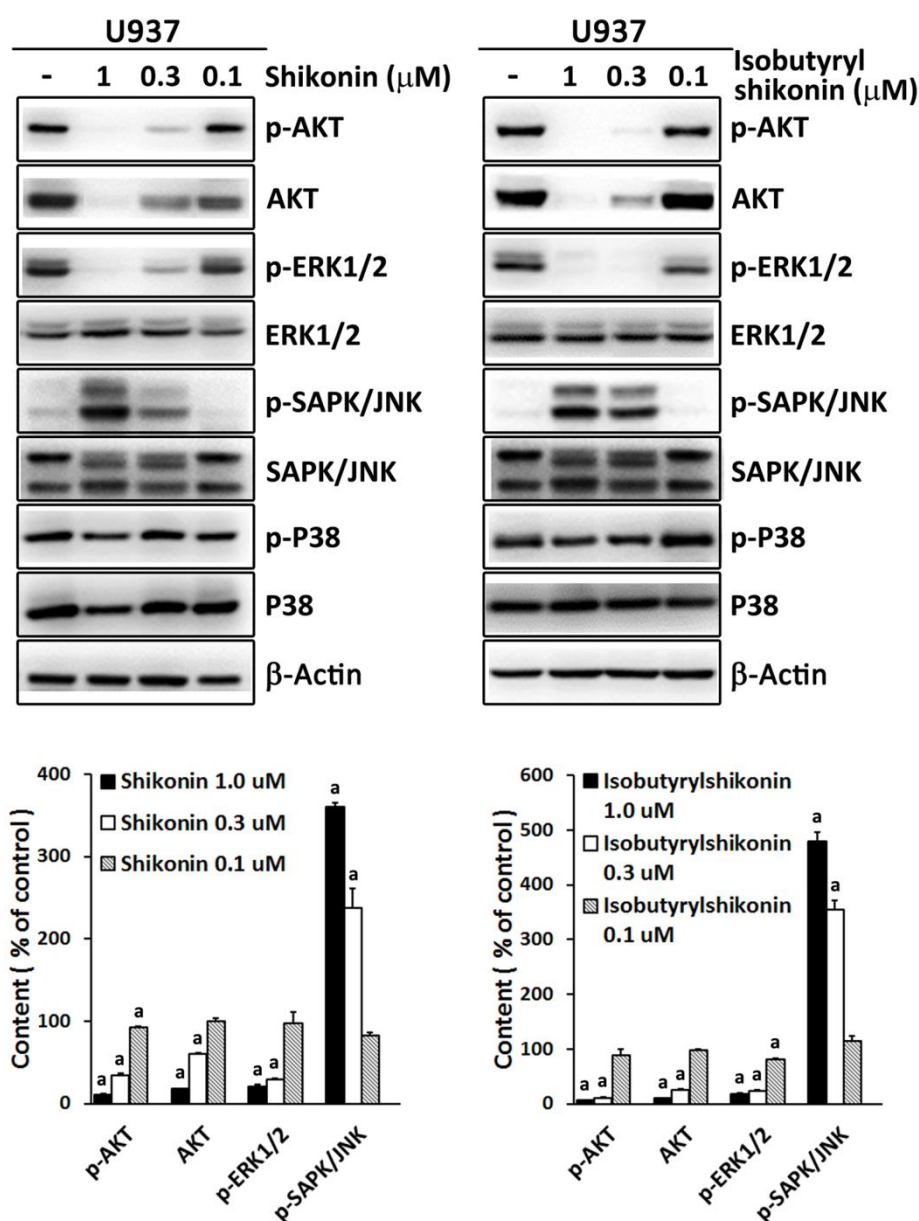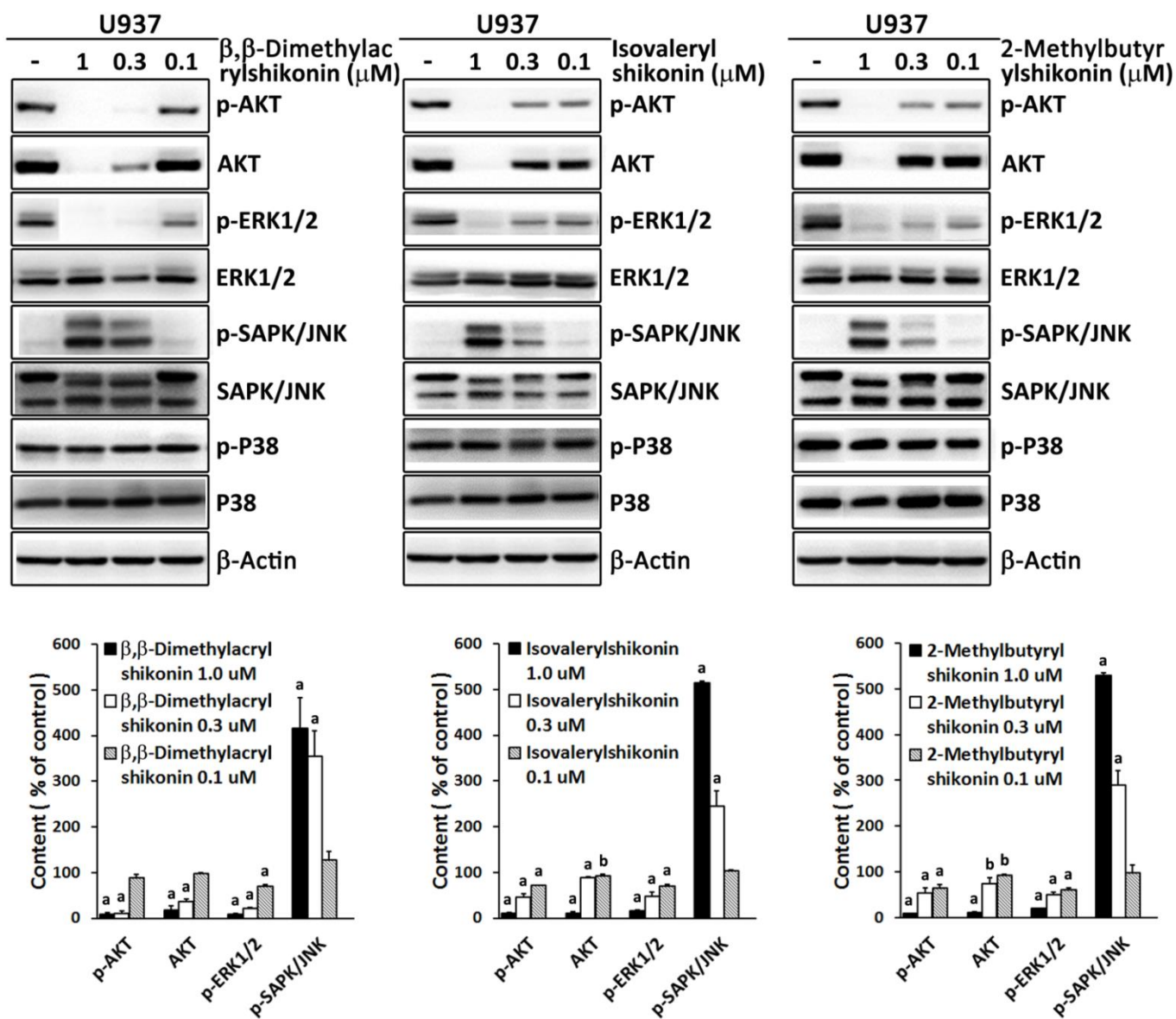
Figure 29: Effect of shikonin and its derivatives on AKT/MAPK signaling in U937 cells as determined by Western blotting. Band density of phosphorylation of AKT, ERK1/2, SAPK/JNK and P38 was normalized to their corresponding total protein levels. β-actin was used as loading control. Below the Western blots, the corresponding digitalized graphs of affected proteins levels for each compound are shown. Data are represented as mean values ± SEM of three independent experiments. [a], $p < 0.01$ *vs.* control; [b], $p < 0.05$ *vs.* control, calculated by two-tailed Student's t test.

Then, we examined which signaling pathway may play a critical role in regulation of c-MYC. A specific AKT activator (SC79) and a specific JNK inhibitor (SP600125) were independently used in combination with shikonin and the expression of c-MYC was measured (Figure 30). Western blotting analysis showed neither SC79 nor SP600125 appreciably reversed shikonin-induced c-MYC reduction, though they partly attenuated shikonin's effect on phospho-AKT and phospho-SAPK/JNK, indicating that the down-regulation of c-MYC probably resulted from the joint contributions of AKT and ERK1/2, SAPK/JNK MAPK signaling cascades and the direct binding of shikonin to c-MYC.
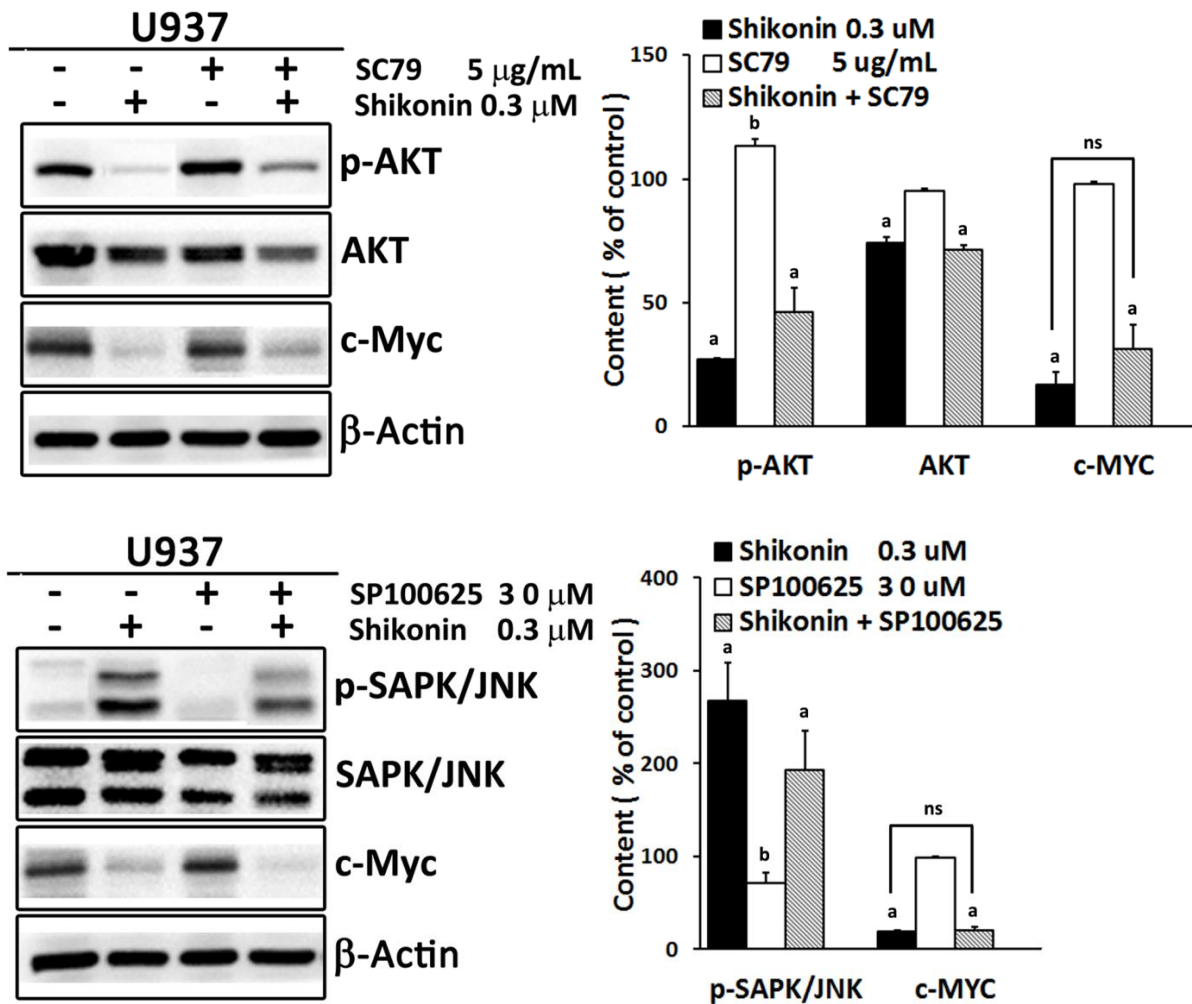
Figure 30: Western blot analysis of the indicated proteins in U937 cells treated with 0.3 μM shikonin in the absence or presence of 5 μg/mL SC79 or the absence or presence of 30 μM SP600125 for 24 h. Digitalized graphs of affected proteins levels are shown aside. Data are represented as mean values ± SEM of three independent experiments. [a], $p < 0.01$ *vs.* control; [b], $p < 0.05$ *vs.* control; [ns], no significance, calculated by two-tailed Student's t test.

3.2.7 Validation in other leukemia cell lines

In addition to U937 cells, we investigated four other different leukemia cell lines (CEM/ADR5000, CCRF-CEM, Molt4 and Jurkat) to prove, whether or not inhibition of c-MYC expression is a general mechanism for shikonin in killing leukemia cells. We first tested the sensitivities of four cell lines to shikonin. The IC_{50} values after 24 h for CEM/ADR5000, CCRF-CEM, Molt4 and Jurkat cells were 0.29 ± 0.03 µM, 1.68 ± 0.23 µM, 0.24 ± 0.03 µM and 0.97 ± 0.14 µM, respectively. Then, the cells were treated with 0.3 or 1 µM shikonin for 24 h depended on their different sensitivities, followed by whole cell lysate extraction for Western blot analyses. The effect of shikonin on c-MYC expression as well as AKT and MAPK signaling cascades were measured.

A
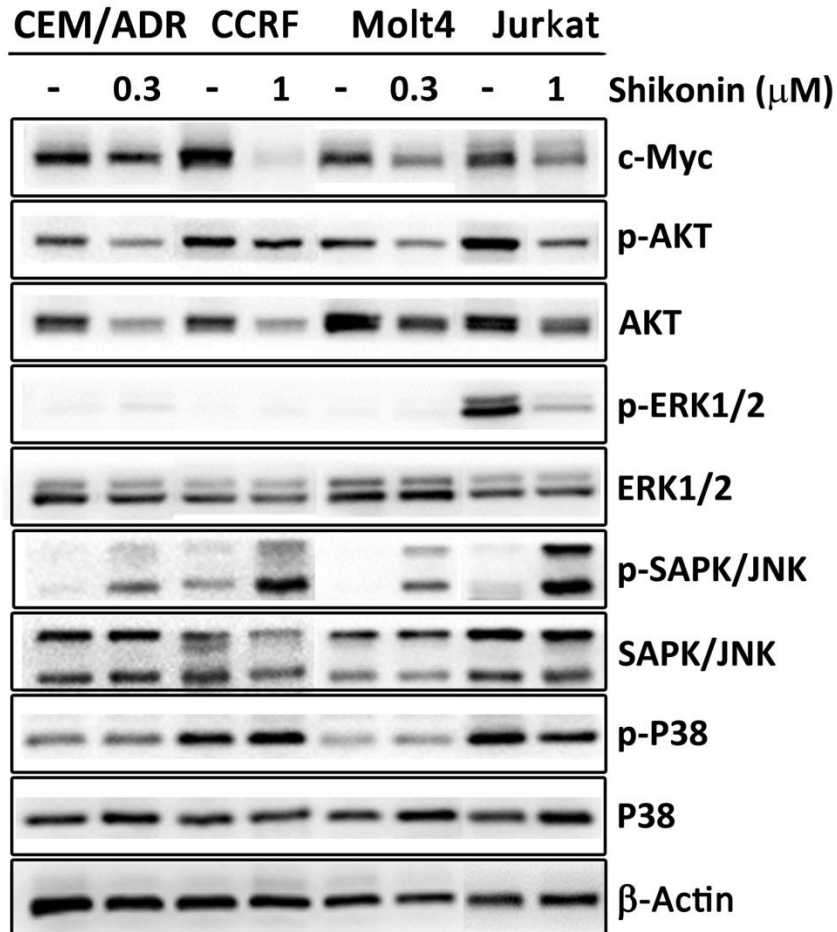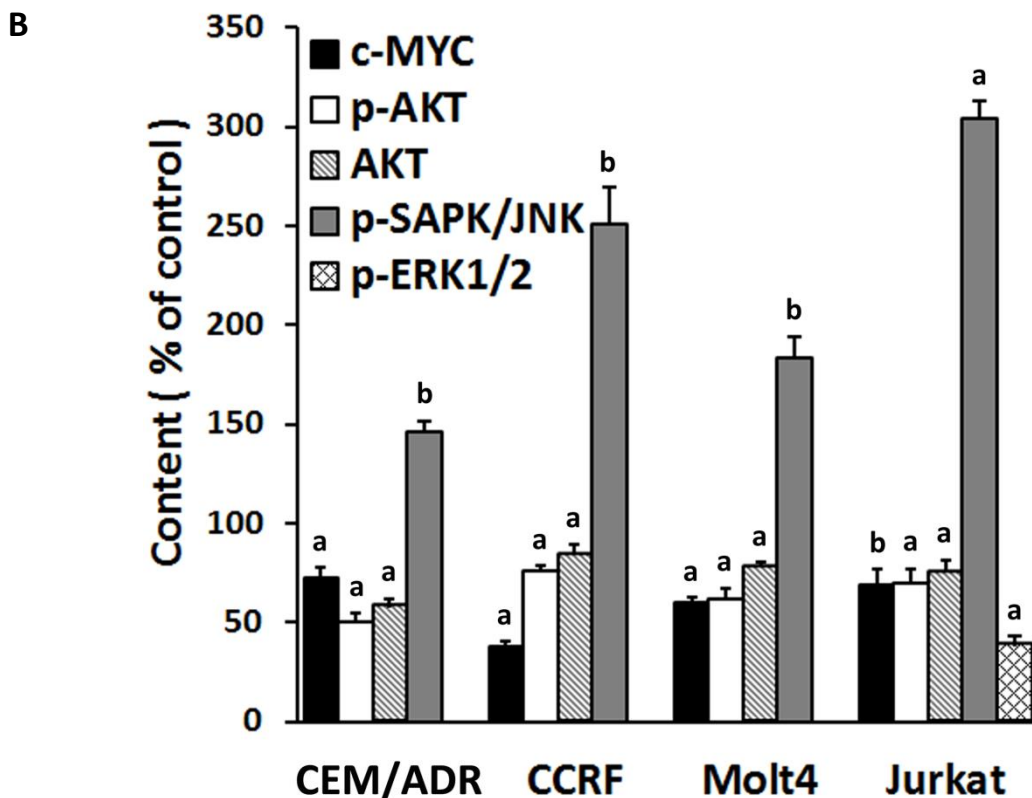
Figure 31: **A,** Effect of shikonin on c-MYC expression and AKT/MAPK signaling in four different leukemia cell lines as determined by Western blotting. CEM/ADR5000, CCRF-CEM, Molt4 and Jurkat cells were treated with 0.3 or 1 µM shikonin depending on their sensitivities to shikonin treatment for 24 h and the whole cell lysates were subjected to Western blotting. Band density of phosphorylation of AKT, ERK1/2, SAPK/JNK and P38 was normalized to their corresponding total protein levels. Others were normalized to β-actin, which was also used as loading control. B, The digitalized graphs of affected protein levels were quantified by FluorChem Q for each cell line. Data are represented as mean values ± SEM of three independent experiments. [a], $p < 0.01$ *vs.* control; [b], $p < 0.05$ *vs.* control, calculated by two-tailed Student's t test. CEM/ADR, CEM/ADR5000; CCRF, CCRF-CEM.

As displayed in Figure 31, shikonin suppressed c-MYC expression to a different extent in all tested cell lines. Meanwhile, reduction of phospho-AKT and total AKT, activation of phospho-SAPK/JNK were also found in all four cell lines upon shikonin treatment. Phospho-ERK1/2 was only activated in Jurkat cells and was inhibited by shikonin. There were still no significant changes in phospo-p38 and total p38 in all cell lines. All these results were comparable to those of U937 cells, suggesting that AKT, ERK1/2, SAPK/JNK/MAPK signaling cascades involved c-MYC inhibition play a general role in shikonin-caused leukemia cell death.

3.2.8   Molecular docking on MYC-MAX complex

To further investigate the possible interaction of shikonin and derivatives with c-MYC, molecular *in silico* docking studies were performed. There exist at least two binding sites in the basic helix-loop-helix (bHLH) leucine zipper domain of the MYC-MAX complex [99]. Our blind docking results showed that shikonin preferentially bound to the same site as the control drug 10058-F4, while the other derivatives docked to the domain, where the other control drug 10074-G5 bound. Both binding sites were in close proximity to the DNA binding region of MYC and MAX. Shikonin and derivatives formed hydrogen bonds with residues at the DNA binding regions of MYC, *i.e*. Arg925, Lys939. The lowest binding energies of shikonin and its derivatives were similar and in a range from -6.65 ± 0.11 kcal/mol to -6.85 ± 0.01 kcal/mol. These values were also comparable with those of the control inhibitors, indicating the feasibility for shikonin and its derivatives directly targeting the c-MYC complex and inducing MYC-related gene expression changes. Docking modes and the binding energies for shikonin and its derivatives and the control inhibitors on the MYC-MAX complex are summarized in Figure 32.

Figure 32: (next page) Docking modes and binding energies of shikonin, its derivatives, 10058-F4 and 10074-G5 on MYC/MAX complex (PDB code: 1NKP). The proteins were represented in yellow (MYC) and brown (MAX) in New Cartoon format, while the chemical molecules were represented in different colors. Shikonin preferentially bound to the same pharmacophore as the control drug 10058-F4, while the other derivatives docked to the same domain as the second control drug 10074-G5. Both binding sites were in close proximity to the DNA binding region of MYC/MAX complex.
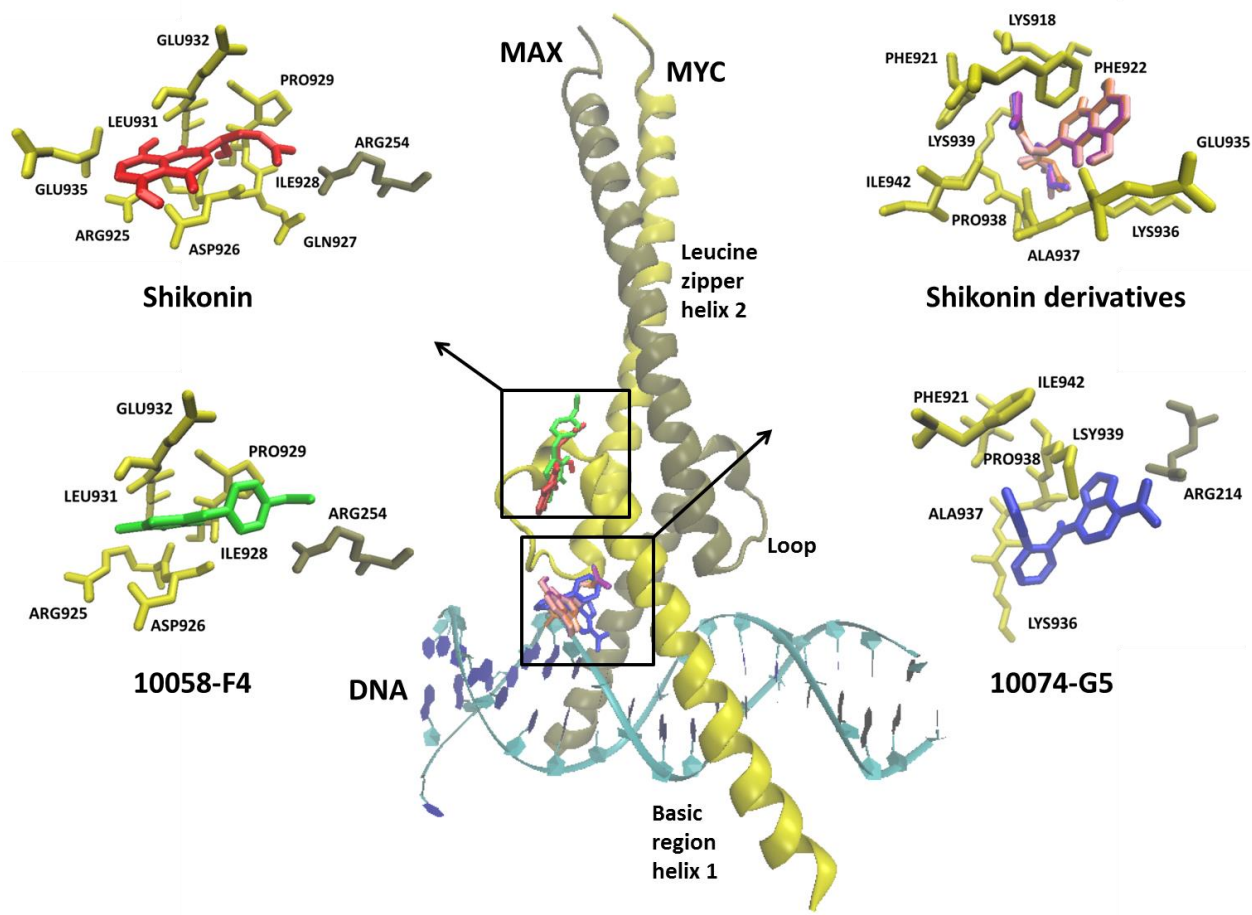
Compounds	Lowest binding energy (kcal/mol)	pKi (µM)	Interacting amino acids (residues in H-Bond highlighted)
Shikonin	-6.74±0.02	11.43±0.34	on MAX: ARG254 on MYC: **ARG925** ASP926 GLN927 ILE928 PRO929 **LEU931** GLU932 GLU935
Isobutyrylshikonin	-6.85±0.01	9.63±0.07	on MYC: **LYS918** PHE921 PHE922 GLU935 LYS936 ALA937 PRO938 **LYS939** ILE942
Isovalerylshikonin	-6.77±0.01	10.99±0.22	on MYC: **LYS918** PHE921 PHE922 GLU935 LYS936 ALA937 PRO938 **LYS939** ILE942
2-Methylbutyryl shikonin	-6.65±0.11	13.81±2.67	on MYC: **LYS918** PHE921 PHE922 GLU935 LYS936 ALA937 PRO938 **LYS939** ILE942
β,β-Dimethylacryl shikonin	-6.77±0.02	10.85±0.27	on MYC: **LYS918** PHE921 PHE922 GLU935 LYS936 ALA937 PRO938 **LYS939** ILE942
10058-F4	-4.92±0.03	246.35±4.13	on MAX: ARG254 on MYC: **ARG925** ASP926 ILE928 PRO929 LEU931 GLU932
10074-G5	-8.11±0.03	1.14±0.06	on MAX: **ARG214** on MYC: PHE921 LYS936 ALA937 PRO938 **LYS939** ILE942

3.2.9   Summary: Inhibition of MYC and deregulation of ERK/JNK/MAPK and AKT signaling as a novel mechanism in leukemia cells

In this section of the work, we investigated the cytotoxicity of shikonin and 14 derivatives on U937 leukemia cells. Four derivatives namely isobutyrylshikonin, 2-methylbutyrylshikonin, isovalerylshikonin and β,β-dimethylacrylshikonin were more active than shikonin. AnnexinV-PI double staining analysis revealed that IC_{50} concentrations of shikonin and its derivatives mainly induced apoptosis. mRNA microarray hybridization was used to analyze gene expression changes in U937 cells after treatment with shikonin and its derivatives. Cell cycle G1/S check point regulation and the transcription factor c-MYC, which plays a vital role in cell cycle regulation and proliferation, were identified as the most commonly down-regulated mechanisms upon treatment with shikonins. Western blotting and DNA-binding assays confirmed the strong inhibitory effect of shikonin and its derivatives on c-MYC expression and transcriptional activity. Reduction of c-MYC expression was closely associated with deregulated ERK, JNK MAPK and AKT activity, indicating the involvement of these signaling molecules in shikonin-triggered c-MYC inactivation. Molecular docking studies revealed that shikonin and its derivatives bind to the same DNA-binding domain of c-MYC, as the known c-MYC inhibitors 10058-F4 and 10074-G5. Together with the results obtained from DNA binding assay, this finding indicates that shikonins bind and inhibit c-MYC. Additionally, the effect of shikonins on U937 cells were confirmed in other leukemia cell lines (Jurkat, Molt4, CCRF-CEM, and multidrug-resistant CEM/ADR5000), where the shikonins also inhibited c-MYC expression and phosphorylation of AKT, ERK1/2, SAPK/JNK and P38. In summary, our results indicate that inhibiting c-MYC and related pathways represents a novel mechanism of shikonin and its derivatives to explain their anti-leukemic activity.

4   Discussion

4.1   Inhibition of EGFR signaling and synergism with erlotinib in glioblastoma cells

4.1.1   Structure activity relationship of shikonin and derivatives

The cytotoxicity of shikonin and 14 derivatives were investigated on two glioblastoma cell lines. Most of shikonin derivatives exhibited strong cytotoxicity, especially towards EGFR-mutated erlotinib-resistant U87MG.ΔEGFR transfectants. Although a body of studies found that shikonin and its derivatives revealed anticancer activity *in vitro* and *in vivo* [43], information on structural-functional relationships is limited yet. Taking the cytotoxic results and chemical structures of the tested compounds (Figure 33) into consideration, it was intriguing to observe that shikonin and its homochiral derivatives were more active than their enantiomers towards glioblastoma cell lines.
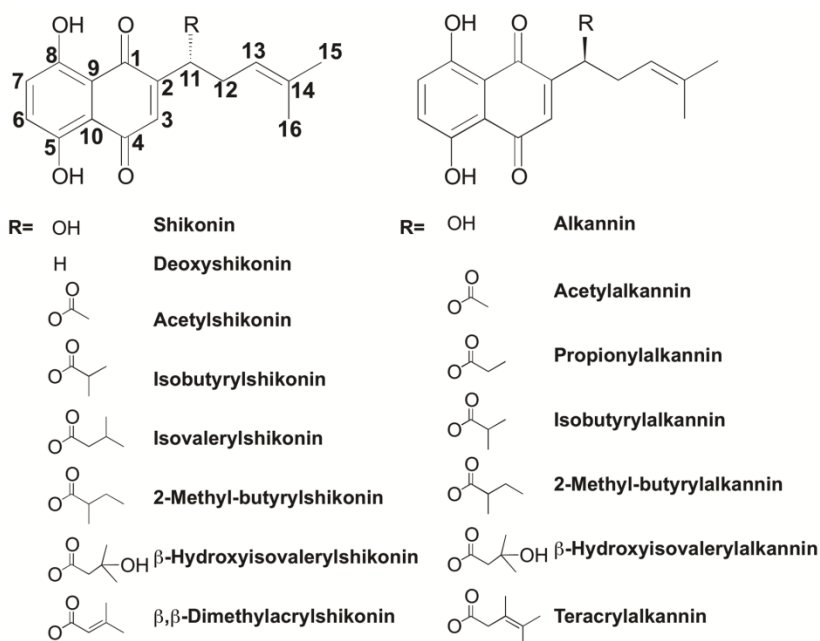
Figure 33: The chemical structures of shikonin and its derivatives studied in the thesis.

For example, shikonin could inhibit proliferation of U87MG and U87MG.ΔEGFR cells at concentrations below 5 µM. β-Hydroxyisovalerylshikonin was effective against U87MG and

U87MG.ΔEGFR cells with IC$_{50}$ values of 21.6 μM and 14.7 μM respectively, whereas their enantiomers, alkannin and β-hydroxyisovalerylalkannin, were inactive (IC$_{50}$ > 100 μM). Comparable data were found for 2-methylbutyrylshikonin and 2-methylbutyrylalkannin as well as isobutyrylshikonin and isobutyrylalkannin, indicating that differences in the stereochemistry at C-11 may influence the activity. A previous study reported that the activities of isobutylshikonin and isobutylalkanin and those of acetylshikonin and acetylalkannin were almost identical towards both human HCT116 colorectal cancer cells with low P-glycoprotein expression and human HepG2 hepatoma cells with high P-glycoprotein expression [116]. This implies that the configuration of C-11 may affect the cytotoxicity of this class of molecules depending on the type of tumor cells and mechanism of action. On the other hand, the cytotoxicity also seems to be correlated with the R group of C-11. Early studies suggested for acylshikonins in general that an acyl group with shorter chain lengths (containing 2-6 carbon atoms) exert stronger inhibitory effects than those with longer chain lengths (containing 7-20 carbon atoms) against DNA topoisomerase-I or telomerase enzymes and among short-side-chain acylshikonins, analogues with larger R group or olefinic double bonds in acyl chains showed better cytotoxicity [117, 118]. Our results are consistent with these previous reports based on the fact that acetylshikonin, with the smallest R group, displayed less activity than the other acylshikonins. β,β-dimethylacrylshikonin, which contains an olefinic double bond in the R group showed marked enhancement of cytotoxicity against both U87MG and U87MG.ΔEGFR cells compared to isovaltrylshikonin with saturated acyl chain. However, this structure-activity relationship does not seem to be applicable to acylalkannins.

4.1.2 Shikonin, erlotinb efficacy and EGFR expression

It was reported in recent studies that shikonin induced apoptosis through multiple pathways, such as generation of reactive oxygen species, depletion of glutathione, disruption of mitochondrial transmembrane potential, as well as upregulation of p53 [53, 57]. Furthermore, necroptosis is also activated by shikonin mediated by RIP-1 pathway and oxidative stress in human glioma cell lines, including U87MG cells [119]. In this study, shikonin inhibited cell growth of a panel of 13 EGFR-expressing cancer cell lines with IC$_{50}$ values much lower than that of erlotinib, which is a specific inhibitor of EGFR. Therefore, we postulated that the strong

cytotoxicity of shikonin may be related to EGFR. Previous studies indicated that shikonin modulated cell proliferation by inhibiting EGFR phosphorylation and regulated the EGFR signaling cascade [120]. Our results confirmed this assumption, because shikonin dose-dependently inhibited ΔEGFR phosphorylation with an IC_{50} value of 1.6 μM and decreased the phosphorylation of EGFR downstream molecules such as AKT, P44/42 MAPK and PLCγ1 to different degrees in U87MG.ΔEGFR cells. But it is notable that the sensitivity of these cell lines to shikonin and erlotinib did not depend on the expression level of EGFR/ΔEGFR. For example, A431 cells expressed high EGFR and were sensitive to erlotinib, but other cell lines that also expressed high level EGFR/ΔEGFR, such as U87MG.ΔEGFR, BS153, T98G and Calu-6 (Figure 15) were resistant to erlotinib. Instead, DK-MG cells which expressed relatively lower EGFR were more sensitive to erlotinib. The situation was also similar in sensitivity to shikonin, suggesting that high levels of EGFR are not required to render cells sensitive to erlotinib or shikonin, which also implied the existence and contribution of other mechanisms. This agrees with several previous investigations, which have reported that the efficacy of first line generation inhibitors such as erlotinib and gefitinib is independent from EGFR overexpression [121-124].

4.1.3 Effect of combination treatments

Based on the results that shikonin exhibited strong inhibitory effect on cell growth and EGFR signaling, we assume that the shikonins may act synergistically with other EGFR-targeting small molecules, *e.g.* erlotinib. The markedly enhanced cytotoxicity towards U87MG.ΔEGFR, BS153 and A431 cells achieved by the combination of shikonin and erlotinib proved our hypothesis. Moreover, synergistic interactions were also observed with five other shikonin analogues in U87MG.ΔEGFR cells, implying a general scientific significance. To the best of our knowledge, this is the first report for shikonin and its analogues to interact synergistically with another established antitumor drug, suggesting a role of shikonins as sensitizer for otherwise drug-resistant tumors.

Moreover, when considering the combination effect and EGFR expression level of the tested cell lines, it is not hard to find that the synergistic effect was only achieved in inhibiting

U87MG.ΔEGFR, BS153 and A431 cell lines with high expression of EGFR/ΔEGFR. In DK-MG and U87MG cells, which expressed very few EGFR molecules, the combination of shikonin and erlortinib only showed additive even antagonistic effect, indicating that although the sensitivity of these cell lines to erlotinib and shikonin was not associated with EGFR expression, the synergism between two compounds may be EGFR specificity.

4.1.4 Molecular basis for the synergistic effect of erlotinib and shikonin

Erlotinib, as an EGFR TK inhibitor approved by FDA for non-small cell lung cancer (NSCLC) since 2004, has been frequently investigated concerning combination treatment with other natural or synthetic compounds for various types of cancer [125]. Several cellular and molecular mechanisms have been ascribed to be responsible for synergistic effects, such as enhanced inhibition of EGFR activation [126], modulation of Akt phosphorylation [108, 127], suppression of RAC1 activation [126], induction of cell cycle arrest [127], and so on, depending on different tumor types and different combined agents. Our study demonstrated that shikonin synergistically acted with erlotinib by inhibition of phosphorylation of ΔEGFR in U87MG. ΔEGFR cells by using both Loewe additivity and Bliss independence drug interaction models. Furthermore, all of the five shikonin analogues which showed synergistic cytotoxicity of U87MG.ΔEGFR cells in combination with erlotinib also achieved a synergistic reduction of ΔEGFR phosphorylation by combination with erlotinib. Therefore, we believe that the enhanced inhibition of ΔEGFR phosphorylation accounts as a main mechanism of synergy in U87MG.ΔEGFR cells for the erlotinib and shikonin or shikonin derivatives combination.

Besides, activation of the PI3K/AKT/mTOR pathway and failure in inhibition of at least one phosphorylated downstream signaling molecule was reported to lead to resistance to EGFR-targeted therapy [128, 129]. Therefore, the deregulation of the PI3K-Akt-mTOR signaling cascade by shikonin [130, 131] and the complementary inhibitory effect of shikonin in the phosphorylation of several EGFR downstream molecules, might be another contributor to synergy of erlotinib-shikonin combination. Additionally, the inhibitory activity of shikonin and its derivatives against the telomerase enzyme [118], reduction of which has been recently demonstrated in association with the increasing sensitivity of malignant glioma cells to

temozolomide [132], the standard chemotherapeutic drug for brain cancer, and the common inhibition of SRC family kinases by shikonin and erlotinib may also play a role in the erlotinib-shikonin combination effect on U87MG.ΔEGFR, BS153 and A431 cells, which need further investigation.

Erlotinib ablates phosphorylation of EGFR by competing for the ATP-binding site in the tyrosine kinase domain of EGFR. The hypothesis for the synergistic inhibition of ΔEGFR phosphorylation by the combination of shikonins and erlotinib was that shikonins might target regions outside the ATP-binding site of the receptor, since it has been reported that a shikonin derivative, β-hydroxyisovalerylshikonin could strongly inhibit EGFR kinase activity in a non-ATP-competitive way, suggesting both this and the parent compound may bind to the peptide-binding site [133, 134]. Meanwhile, our own molecular docking studies also showed the feasibility for shikonins binding to different pharmacophores at EGFR than erlotinib (Figure 21). It is worth performing further experiments to verify the assumption.

Synthetic small molecules, such as erlotinib, are designed with high selectivity towards a single target, *e.g.* EGFR. This high selectivity might favor the rapid development of drug resistance due to the selection and outgrowth of point-mutated tumor subpopulations, which are then resistant to this small molecule [135]. In contrast, during evolution of life, plants developed multi-targeted chemical compounds. The advantage of multi-targeted compounds is that point-mutations in a single target may not result in resistance, since affecting the other targets may still lead to substantial tumor killing. Naphthoquinones such as shikonin and its derivatives are a class of natural products illustrating this typical feature. If shikonins would find their way into the clinic, it can be expected that they would be used as a part of combination drug therapies rather than as monotherapy. Hence, the synergism with erlotinib and possibly other drugs is a beneficial feature making the shikonins attractive candidates for the improvement of cancer therapy.

4.2 Inhibition of MYC and deregulation of ERK/JNK/MAPK and AKT signaling as a novel mechanism in leukemia cells

As discussed in the previous chapter, targeting of EGFR signaling and synergizing with erlotinib on EGFR phosphorylation are the cellular mechanisms of shikonin and combination treatment, which are primarily responsible for the induction of glioblastoma cell death. However, the particular activity of shikonin against leukemia cells, which did not express EGFR, indicated the existence of other mechanisms for shikonin in these cells. By means of microarray-based gene expression profiling, we were able to identify that *c-MYC* was commonly deregulated in U937 cells upon treatment with shikonin and its derivatives. Their effect on c-MYC was validated via Western blot analysis, DNA-binding activity assays and *in silico* molecular docking. Meanwhile AKT, and ERK1/2, JNK/MAPK signaling pathways were also heavily influenced by shikonins treatment. Finally, the effect of shikonins on U937 cells was further confirmed in other leukemia cell lines.

4.2.1 Cytotoxicity towards leukemia cells and c-MYC

As a first step, we tested the cytotoxicity of shikonin and 14 derivatives towards U937 leukemia cells, the most sensitive cell line to shikonin in the initial cytotoxicity screen. The results showed they had marked cytotoxicity towards U937 leukemia cells Especially, the four derivatives−isobutyrylshikonin, 2-methylbutyrylshikonin, isovalerylshikonin and β,β-dimethyl-acrylshikonin−that were more effective than the lead compound shikonin. Moreover, it was intriguing to observe that shikonin and its homochiral derivatives were more active than their enantiomers. For example, the IC_{50} value for shikonin was 25 folds lower than that of alkannin. Similarly, isobutyrylshikonin, 2-methylbutyrylshikonin and β-hydroxyisovaleryl-shikonin also showed lower IC_{50} values than their corresponding enantiomers, isobutyryl-alkannin, 2-methylbutyrylalkannin and β-hydroxyisovalerylalkannin, indicating that differences in the stereochemistry at C-11 may influence the activity. This structure-activity relationship was consistent with what we found in glioblastoma cell lines. Another interesting point is that leukemia cell lines were more sensitive than solid tumor cell lines [112]. A plethora of studies, including clinical research, reported that leukemia is generally very sensitive to anticancer reagents that either block the cell cycle process or cause apoptosis [136-139]. Therefore, we

proposed that the particular activities of shikonin and its derivatives against leukemia cells may be correlated with their strong effect to induce cell cycle disruption and apoptosis. Previous studies reported that shikonin caused an arrest of U937 cells in the G1 and S phase and decreased expression of cell cycle-related proteins, such as cyclin D, CDK and PCNA [112, 140]. However, the mechanism of this effect remains unknown as of yet. By means of microarray-based gene expression analysis, we noticed that the transcription factor MYC, which plays a very critical role in cell cycle control, was the commonly deregulated molecule by shikonin and its derivatives. MYC can influence cell cycle progression through several parallel mechanisms, such as transcription of target genes including CDKs, cyclins and E2F that encode many important positive cell cycle regulators, hyperactivating cyclin/Cdk complexes through the induction of CDK-activating kinase (CAK) and CDC25 phosphatases as well as impairment of cell cycle inhibitors such as p21 and p27 [141]. Inhibition of MYC expression, down-regulation or inactivation of MYC in cycling cells results in cell cycle arrest and impairs cell cycle progression in various cell lines, including human lymphoid and myeloid cells [141-143]. Cellular pathways analysis by IPA also provided supporting information that G1/S checkpoint regulation was the most disturbed pathway upon treatment with shikonin and its derivatives. This further indicated that cell cycle arrest in U937 cells resulted from deregulation of MYC and shikonin and its derivatives may be potential MYC inhibitors. To prove this hypothesis, we examined the effect on c-MYC expression and its transcriptional activity by Western blotting and a specific ELISA-based DNA-binding assay. Shikonin and its derivatives exerted remarkable inhibition on c-MYC expression and its DNA-binding activity, which was much better than the known MYC inhibitor 10058-F4 and comparable to 10074-G5. Moreover, the effective concentrations for c-MYC inhibition were much lower than those of both control drugs. To the best of our knowledge, this is the first report for shikonin to kill cancer cells by targeting c-MYC, suggesting a novel role of shikonins as antitumor agents.

Except for *MYC*, another two cancer-related molecules *MYB* and *MS4A3* were also significantly down-regulated by all five shikonin derivatives. *MYB* is a proto-oncogene which is overexpressed in most human myeloid and acute lymphoid leukemias [144]. It actively contributes to leukemogenesis by promoting proliferation, suppressing apoptosis and blocking differentiation [145]. *MS4A3* (also known as *HTm4*) encodes a member of membrane-spanning 4-domains subfamily, which acts as an important cell cycle regulator in various cancers,

especially in hematological malignancies [146, 147]. Therefore, it was very likely that the dysregulation of *MYB* and *MS4A3* also contribute to shikonin and its derivatives induced cell cycle arrest and cell death in U937 cells. It is worth performing further experiments to clarify the potential effect of shikonin on them.

4.2.2 Cell death modes and c-MYC

On the other hand, we clarified the death mode of U937 cells by annexin V-PI double staining in the presence or absence of the specific necroptosis inhibitor Nec-1 and the caspase inhibitor z-VAD-fmk. IC$_{50}$ concentrations of shikonin and derivatives mainly induced cell death by caspase-dependent apoptosis, as evidenced by a remarkable decrease in annexin V+/PI- and annexin V+/PI+ cells in presence of z-VAD-fmk. This was in agreement with previous reports that low concentrations of shikonin induced caspase-dependent apoptosis in mitochondriae in leukemia cells [148]. However, in addition to apoptosis, we found that necroptosis seemed to be also induced by shikonin and derivatives, as Nec-1 could partly rescued cell from death. This means that necroptosis, which was induced mostly by high dose of shikonin or its derivatives [58, 61, 148], perhaps could also be triggered by low concentrations of shikonins as a secondary death mechanism. Additional experiments such as electron microscopy analysis will help to further confirm this effect. The role of c-MYC in apoptosis is intricate, depended on the specific cell type and the physiological status of the cell. Both reduction and overexpression of c-MYC can lead to apoptosis [149, 150]. However, in hematopoietic cells, apoptosis is closely correlated with reduction of c-MYC expression. For example, apoptosis of CEM lymphoblastoid cells induced by oxysterol 25-hydroxycholesterol was preceded by $\geq$ 90% reduction in c-MYC levels [151]. Treatment of K562 erythroleukemia cells with the protein phosphatase inhibitors okadaic acid or calyculin A caused down-regulation of c-MYC and MAX expression and led to apoptosis [152]. The myeloid HL-60 leukemia cell line also underwent apoptosis by treatments that reduce c-MYC expression [153]. In addition, the small molecule c-MYC inhibitor 10058-F4 inhibited proliferation and induced apoptosis through the mitochondrial pathway of apoptosis in several acute myelocytic leukemia cell lines [154]. Therefore, we believe that apoptosis induced by shikonin and its derivatives in U937 cells is also associated with inhibition of c-MYC expression.

4.2.3   Role of ERK/JNK/MAPK and AKT pathways in c-MYC regulation

In an attempt to explore, how shikonin and its derivatives inhibit c-MYC expression and activity, we examined the effect of shikonins on signaling pathways that may regulate c-MYC expression. It has been showed that shikonin or its derivatives inhibit cancer cells via AKT/mTOR and MAPK signaling cascades [43, 130, 155-157]. Our results are consistent with these previous findings, as shikonin and derivatives demonstrated significant effects on ERK1/2, SAPK/JNK MAPK kinases pathways and AKT pathways. These pathways play an important role in the control of c-MYC protein stability, accumulation and subsequent transcriptional activity. c-MYC protein stability is strongly influenced by phosphorylation of two adjacent N-terminal sites, threonine 58 (Thr58) and serine 62 (Ser62), which display opposing roles. Phosphorylation of Ser62 that is mediated by ERK pathway kinase activity stabilizes c-MYC, while phosphorylation of Thr58 by GSK-3 promotes c-MYC degradation [89]. GSK-3 activity is usually inhibited through PI3K/AKT. Only if AKT activity declines, GSK-3 has the capacity to phosphorylate Thr58 and to induce the degradation of c-MYC [158]. Meanwhile, JNK also contributes to c-MYC stability by increasing its ubiquitin-dependent degradation via a δ-like domain [159]. In addition to the influence on c-MYC protein stability, the PI3K/AKT and MAPK pathways also take part in the regulation of c-MYC-mediated transcription by phosphorylating and promoting MAD1 degradation. MAD1 suppresses c-MYC transcriptional activity by competing with c-MYC for heterodimerization with its partner MAX [113]. Thus, inhibition of the ERK/PI3K/AKT pathway, or activation of JNK signaling may lead to down-regulation of c-MYC. Our results showed that reduction of c-MYC expression by shikonins and its derivatives was closely correlated with inhibition of phosphorylation of ERK1/2 and AKT and activation of phosphorylation of SAPK/JNK. This further confirms the role of these pathways for c-MYC regulation. However, neither the inhibition of AKT nor the activation of SAPK/JNK alone appreciably reversed shikonin-induced c-MYC suppression. This indicates a comprehensive effect of ERK1/2, JNK MAPK and AKT signaling for down-regulation of c-MYC and a direct interaction of shikonin with c-MYC.

Our molecular docking studies demonstrated the binding of shikonin and its derivatives to the DNA-binding domain of c-MYC in a similar manner as the known c-MYC inhibitors 10074-G5 and 10058-F4. Additionally, c-MYC deregulation may in turn also act on AKT activity. Recent studies reported that reduced c-MYC levels led to decreased AKT activity *in vitro* and *in vivo*

[160, 161]. Thus, AKT down-regulation upon shikonin treatment may be further reinforced as negative feedback of c-MYC down-regulation. Co-targeting of AKT and c-MYC has been recently shown to be a synergistic treatment strategy for leukemia therapy [162, 163], since shikonin and its derivatives strongly deregulate the AKT signaling pathway and directly inhibit c-MYC activity. Therefore, they represent promising candidates for leukemia treatment.

Moreover, the mechanism of shikonin in U937 cells also applies for other acute leukemia cell lines, including the multidrug-resistant cell line CEM/ADR5000. This indicates that inhibition of c-MYC with involvement of the ERK/JNK/MAPK and AKT pathways represents a general mechanism for shikonin and its derivatives in killing leukemia cells. Notably, multidrug-resistant CEM/ADR5000 cells were even more sensitive to shikonin than the wild-type cell line CCRF-CEM, as evidenced by the lower IC_{50} value. The phenomenon of hypersensitivity of multidrug-resistant cells has been termed collateral sensitivity [164]. Considering the important role of c-MYC in drug-resistant leukemia, we assume that shikonin's collateral sensitivity in CEM/ADR5000 cells may be also c-MYC-related. This opens avenues for shikonin and its derivatives for combination therapies to treat otherwise drug-resistant tumors.

In a word, the novel mechanisms for shikonin and its derivatives reported in the present study make these compounds attractive candidates for the treatment of hematological malignancies.

5 Summary and conclusion

In this study, the molecular mechanisms that underlie the anti-cancer effects of shikonin and its derivatives were investigated in two different tumor cell types – solid tumor cells taking glioblastoma cell lines as examples and hematological tumor cells, specifically leukemia cells. EGFR and c-MYC were identified as the common molecular targets of shikonin and its derivatives in glioblastoma and leukemia cells respectively.

In U87MG and transfected U87MG.ΔEGFR glioblastoma cells, most of the shikonin derivatives showed strong cytotoxicity, especially towards EGFR-mutated erlotinib-resistant U87MG.ΔEGFR cells. Combination treatment with shikonin and erlotinib produced synergistic cell growth inhibitory effect in EGFR/ΔEGFR overexpression cell lines including U87MG.ΔEGFR, BS153 and A431 cells, but only additive even antagonistic effect in DK-MG and U87MG cells, which expressed very few EGFR. This implied us that their synergy effect seems to rely at least in part on EGFR. Western blotting analysis displayed that shikonin itself dose-dependently inhibited ΔEGFR phosphorylation as erlotinib and decreased phosphorylation of EGFR downstream molecules, including AKT, P44/42MAPK and PLCγ1. When treated by shikonin or its derivatives in combination with erlotinib, the phosphorylation of ΔEGFR reduced much more than any one treated alone, proving that the enhanced inhibition of ΔEGFR phosphorylation accounts as a main mechanism of synergy in U87MG.ΔEGFR cells for the erlotinib and shikonin or shikonin derivatives combination. Since overexpression and mutation of EGFR has been a major cause for development of drug resistance to EGFR inhibitos, the synergism of shikonin and its derivatives with erlotinib towards EGFR/ΔEGFR overexpression cells is a beneficial feature making the shikonins attractive candidates for the improvement of cancer therapy.

Compared to solid tumor cells, *e.g.* glioblastoma cells, leukemia cells seem to exhibit higher sensitivity to shikonin treatment. As cell viability assays revealed, the IC_{50} value for each of shikonin and 14 derivatives in U937 leukemia cells was much lower than their corresponding IC_{50} value in glioblastoma cells. Since expression of EGFR was not the case in leukemia cells, there should be other cellular mechanisms responsible for the particular effectivity of shikonin towards leukemia cells. IC_{50} concentrations of shikonin and its derivatives induced both

apoptosis and necroptosis in U937 cells. mRNA microarray assay showed that the transcription factor c-MYC was the common molecular intensely down-regulated by shikonin and its derivatives. c-MYC plays a vital role in cell cycle regulation and apoptosis by transcription and activation of downstream target genes. The effect of shikonin and its derivatives on c-MYC was functionally validated by Western blotting analysis and DNA-binding assays, which demonstrated a markedly decreased expression and transcriptional activity of c-MYC after shikonins treatment. The mechanisms of shikonin-triggered c-MYC inactivation may integrate the deregulation of ERK, JNK MAPK and AKT activity, which are important upstream signaling pathways for c-MYC control, and the direct binding of shikonins to c-MYC–MAX dimerization thereby disrupting the transcriptional activity of c-MYC. It has reported that leukemia is generally very sensitive to anticancer reagents that either block the cell cycle process or cause apoptosis. Seeing as the critical role of c-MYC in cell cycle control and apoptosis and the close association between c-MYC deregulation and hematological malignancies, inhibiting c-MYC and related pathways represents a novel mechanism of shikonin and its derivatives to explain their anti-leukemic activity and strengthen their potential for the treatment of hematological malignancies.

6 Material and Methods

6.1 Chemicals and equipment

Shikonin and 14 derivatives

Shikonin and its 14 derivatives were kindly provided by ███████████████ (Department of Pharmacognosy, University of Graz, Graz, Austria) and ███████████████ (Faculty of Pharmacy, University of Athens, Athens, Greece). They were isolated and purified from *Arnebia euchroma* and *Onosma paniculata* as described [165, 166]. The chemical structures are shown in Figure 6B. Stock solutions (50 mM) were prepared in DMSO, stored at −20 °C and diluted to the final concentration in fresh media before each experiment. Freeze/thaw-cycles of dissolved shikonin and its derivatives were avoided.

Chemotherapeutics

Erlotinib and z-VAD-fmk were purchased from SelleckChem (Munich, Germany). SC79, 10058-F4 and 10074-G5 were purchased from Sigma-Aldrich (Taufkirchen, Germany). SP100625 and necrostatin-1 (Nec-1) were purchased from Enzo Life Sciences (Lörrach, Germany).

Doxorubicin was provided by the University Medical Center of the Johannes Gutenberg University (Mainz, Germany) and dissolved in DPBS at a concentration of 10 mM. It was stored in the dark at 4 °C for a maximum of 4 weeks.

Cell culture media, reagents and disposable material

Table 5: Cell culture media, reagents and disposable material

Product	Supplier
6-well cell culture microplate, clear, Nunclon®	Thermo Scientific, Germany
12-well cell culture microplate, clear, Nunclon®	Thermo Scientific, Germany
96-well, flat bottom cell culture microplate, clear, Nunclon®	Thermo Scientific, Germany
96-well, flat bottom cell culture microplate, white, Nunclon®	Thermo Scientific, Germany
Cell culture flasks (25 cm^2), Nunclon®	Thermo Scientific, Germany

Cell culture flasks (75 cm^2), Nunclon®	Thermo Scientific, Germany
Cell scraper	Greiner Bio-One, Germany
Centrifuge tube (15 ml)	Sarstedt, Germany
Centrifuge tube (50 ml)	Sarstedt, Germany
Cover Glass 24 × 32 mm	VWR International, Austria
DMEM, High Glucose, GlutaMAXTM, Pyruvate	Life Technologies, Germany
DPBS, no calcium, no magnesium	Life Technologies, Germany
FACS tubes	BD Biosciences, USA; Sarstedt, Germany
FACS tubes with cell strainer cap	BD Biosciences, USA
Fetal Bovine Serum (FBS)	Life Technologies, Germany
G418 disulfate salt	Sigma-Aldrich, Germany
L-Glutamine	PAA Laboratories, Germany
Micro tubes (1.5 mL, 2.0 mL)	Sarstedt, Germany
PCR plate sealing foils	Axon Labortechnik, Germany
PCR plates (384-well)	Axon Labortechnik, Germany
Penicillin (10000 U/mL)/Streptomycin (10000 μg/mL)	Life Technologies, Germany
Phytohemagglutinin M form	Life Technologies, Germany
Pipette tip (10, 200 and 1250 μL)	Sarstedt, Germany
Pipette with tip (5 and 10 mL)	Greiner BIO-ONE, Germany
Roti® PVDF blot membrane (0.45 μm)	Roth, Germany
RPMI 1640	Life Technologies, Germany
Trypsin-EDTA 0.25% (1×), phenol red	Life Technologies, Germany

Chemicals, dyes, antibodies, enzymes and kits

Table 6: Chemicals, dyes, antibodies, enzymes and kits

Product	Supplier
30% acrylamide/bis solution 29:1	Bio-Rad, Germany
5 × Hot Start Taq EvaGreen qPCR Mix (no ROX)	Axon Labortechnik, Germany
Akt (pan) (C67E7) Rabbit mAb	Cell Signalling, Germany
Ammonium persulfate (APS)	Sigma-Aldrich, Germany
Annexin V-FITC Apoptosis Kit	BioVision, Germany
Biotin-16-UTP	Roche, Germany
Bovine serum albumin (BSA)	Sigma-Aldrich, MO, USA
Bromophenol Blue	Merck, Germany
c-Myc (D84C12) Rabbit mAb	Cell Signalling, Germany
Complete Mini Protease Inhibitor	Roche, Germany

Dimethyl sulfoxide (DMSO)	Sigma-Aldrich, Germany
Doxorubicin	JGU Medical Center, Germany
EGF Receptor (D38B1) XP® Rabbit mAb	Cell Signalling, Germany
Ethanol (EtOH)	Sigma-Aldrich, Germany
Glycerol	AppliChem, Germany
Glycine	AppliChem, Germany
HRP-linked anti-mouse IgG	Cell Signaling, Germany
HRP-linked anti-rabbit IgG	Cell Signaling, Germany
Hydrochloric Acid 37% (HCl)	AppliChem, Germany
Illumina® TotalPrep™ RNA Amplification Kit	Life Technologies, Germany
InviTrap® Spin Universal RNA Mini kit	STRATEC Biomedical, Germany
LuminataTM Classico Western HRP substrate	Merck Millipore, Germany
MagicMark™ XP Western Standard	Life Technologies, CA, USA
MAPK Antibody Sampler Kit	Cell Signalling, Germany
MessageAmp II aRNA Amplification kit	Ambion, TX, USA
Methanol	J. T. Baker, NJ, USA
M-PER® Mammalian Protein Extraction Reagent	Thermo Scientific, IL, USA
NE-PER® Nuclear and Cytoplasmic Extraction Reagents	Thermo Scientific, IL, USA
Phospho-Akt (Ser473) (D9E) XP® Rabbit mAb	Cell Signalling, Germany
Phospho-EGF Receptor Pathway Antibody Sampler Kit	Cell Signalling, Germany
Phospho-MAPK Antibody Sampler Kit	Cell Signalling, Germany
PhosSTOP Phosphatase Inhibitor Cocktail Tablets	Roche, Germany
QIAamp® DNA Mini Kits	Qiagen, Germany
Resazurin	Sigma-Aldrich, Germany
RevertAid H Minus First Strand cDNA Synthesis Kit	Thermo Scientific, Germany
RevertAid H Minus First Strand cDNA Synthesis Kit	Thermo Scientific, Germany
Sodium bicarbonate	Sigma-Aldrich, Germany
Sodium chloride (NaCl)	Grüssing, Germany
Sodium dodecyl sulfate (SDS)	J. T. Baker, NJ, USA
Sodium hydroxide (NaOH)	Sigma-Aldrich, Germany
Tetramethylethylenediamine (TEMED)	AppliChem, Germany
TotalPrep™ RNA Amplification Kit	Life Technologies, Germany
TransAM® c-Myc Transcription Factor ELISA Kits	Active Motif, Belgium
Tris (hydroxymethyl) aminomethane (Tris)	AppliChem, Germany
Trypsin (modified, sequencing grade)	Promega, WI, USA
Tween20	Sigma-Aldrich, Germany
Ultravision Quanto Detection System HRP	Thermo Scientific, Germany
Water, nuclease-free	Thermo Scientific, Germany

β-Actin (13E5) rabbit mAb	Cell Signalling, Germany
β-Mercaptoethanol	AppliChem, Germany

Technical equipment and software

Table 7: Technical equipment and software

Device	Supplier
Adobe Photoshop CS5 v 12.0.0.2	Adobe Systems, USA
Agilent 2100 Bioanalyzer	Agilent Technologies GmbH, Germany
Alpha Innotech FluorChem Q system	Biozym, Germany
AutoDock 4.2 software	Molecular Graphics Laboratory, CA, USA
AutoDockTools 1.5.6rc3 software	Molecular Graphics Laboratory, CA, USA
AutoGrid 4.2 software	Molecular Graphics Laboratory, CA, USA
BD Calibur Flow Cytometer	Becton-Dickinson Biosciences, CA, USA
BD CellQuest™ software	Becton-Dickinson Biosciences, CA, USA
BeadStudio software	Illumina Inc., CA, USA
C1000™ Thermal Cycler	Bio-Rad, Germany
Centrifuge 5424	Eppendorf, Germany
CFX384™ Real-Time PCR Detection System	Bio-Rad, Germany
ChemSketch	ACD, Canada
Chipster software	CSC, Finland
Coulter Counter Z1	Beckman Coulter, Germany
ENVAIR eco air V 0.8m vertical laminar flow workbench	ENVAIR, Germany
Eppendorf 8-channel electric pipette	Eppendrof, Germany
FlowJo software	FlowJo LLC, OR, USA
FluorChem® Q imaging system	Alpha Innotech, CA, USA
Forma Steri-Cult 3310 CO_2-Incubator	Thermo Scientific, Germany
Heraeus Cytospin	Thermo Scientific, Germany
Heraeus Fresco 21 microcentrifuge	Thermo Scientific, Germany
Heraeus Labofuge 400 R centrifuge	Thermo Scientific, Germany
ImageJ 1.4.6	NIH, MD, USA
Illumina Human HT-12 v4 BeadChip array	Illumina Inc., CA, USA
Illumina BeadStation array scanner	Illumina Inc., CA, USA
Infinite M2000 Pro™ plate reader	Tecan, Germany
Ingenuity Pathway Analysis (IPA)	Ingenuity Systems Inc., CA, USA
Maxisafe 2020 laminar flow hood	Thermo Scientific, Germany
Microsoft Office	Microsoft Corporation, WA, USA

Milli-Q ultrapure water purification system	Millipore, Germany
Mini-PROTEAN® Tetra Cell	Bio-Rad, Germany
MODELLER 9.11	University of California, CA, USA
Molecular Operating Environment (MOE) 2012.10	Chemical Computing Group Inc., Canada
NanoDrop 1000 Spectrophotometer	PEQLAB, Germany
Neubauer counting chamber	Marienfeld, Germany
Optika XDS-2 trinocular inverted microscope	Optika, Italy
Precisa BJ2200C balance	Precisa Gravimetrics AG, Switzerland
PyMOL 1.3	Schroedinger LLC, USA
REAX 2000 vortexer	Heidolph, Germany
Safe 2020 Biological Safety Cabinets	Thermo Scientific, Germany
Sartorius R 160 P balance	Sartorius, Germany
Sonorex RK 102 H Ultrasonic Cleaning Unit	Babdelin, Germany
Spectrafuge™ Mini Centrifuge	Labnet, Germany
SUB Aqua 26 waterbath	Grant Scientific, Germany
Thermomixer comfort	Eppendorf, Germany
TopMix vortexer	Fisher Scientific, Germany
VMD 1.9 software	University of Illinois at Urbana Champaign, IL, USA

6.2 Cell culture

All cell lines were maintained in a humidified environment at 37 °C with 5% CO_2. Passaging was performed twice per week. Adherent cells were detached by treatment with 0.25% trypsin/EDTA solution (Life Technologies). All experiments were performed on cells in the logarithmic growth phase. Cell counting was carried out by the use of Coulter Counter Z1 (Beckman Coulter) or a Neubauer counting chamber (Marienfeld).

6.2.1 Glioblastoma cell lines

U87MG and its mutant U87MG.ΔEGFR, which over-expresses constitutively active EGFR with a genomic deletion of exons 2-7 were kindly provided by ▮▮▮▮▮▮▮▮ (Ludwig Institute for Cancer Research, San Diego, CA, USA).

DK-MG and SNB-19 cells were kindly provided by ████████████████████ (Department of Radiation Oncology, University Hospital, Würzburg, Germany).

BS153 cells were obtained from ██████████████ (Department of Neurosurgery, University Medical Center Hamburg-Eppendorf, Hamburg, Germany) and originally generated by Adrian Merlo [167].

A172, T98G and U251MG cells were obtained from the German Cancer Research Center (DKFZ, Heidelberg, Germany). The original source of these cell lines is the American Type Culture Collection (ATCC, USA).

All glioblastoma cell lines were cultivated in complete DMEM culture medium with GlutaMAX (Invitrogen) supplemented with 10% fetal bovine serum, L-glutamine (2 mM), and 1% of a 10,000 U/mL penicillin G and 10 mg/mL streptomycin. To maintain the expression of ΔEGFR, U87MG.ΔEGFR was cultured in the medium containing 400 µg/mL G418.

6.2.2 Leukemia cell lines

Acute myeloid leukemia (AML) cells U937, acute lymphocytic leukemia (ALL) cell lines Molt4 and Jurkat were obtained from the German Cancer Research Center (DKFZ, Heidelberg, Germany). The original source of the cell lines is the American Type Culture Collection (ATCC, USA).

ALL cell lines CCRF-CEM and its derived CEM/ADR5000 cell lines were generously provided by ██████████████ (Department of Pediatrics, University of Jena, Jena, Germany).

All leukemia cell lines were cultivated in complete RPMI 1640 medium with 2 mM L-glutamine (Invitrogen) supplemented with 10% fetal bovine serum and 1% of a stock solution of 10,000 U/mL penicillin G and 10 mg/mL streptomycin. CEM/ADR5000 cells were continuously treated with 5000 ng/mL doxorubicin to maintain the multidrug-resistance phenotype.

6.2.3 Other tumor cell lines

The skin carcinoma cell line A431, the kidney carcinoma cell line A498, the lung carcinoma cell line Calu-6 and the breast carcinoma cell lines BT-20 as well as MDA-MB-436 were obtained from the German Cancer Research Center (DKFZ, Heidelberg, Germany). The original source of these cell lines is the American Type Culture Collection (ATCC, USA).

All these cell lines were cultivated in complete DMEM culture medium with GlutaMAX (Invitrogen, Germany) supplemented with 10% fetal bovine serum, L-glutamine (2 mM), and 1% of a 10,000 U/mL penicillin G and 10 mg/mL streptomycin.

6.3 Cell line authentication

6.3.1 DNA isolation

1 to 5×10^6 cells for each of used solid tumor cell lines were harvested and genomic DNA was extracted using QIAamp® DNA Mini Kits (QIAGEN) according to the manufacturer's protocol. The DNA concentrations were determined by NanoDrop 1000 spectrophotometer (PEQLAB) and adjusted to $15 - 30$ ng/µL.

6.3.2 SNP-profiling

Identification of all cell lines was performed using Single Nucleotide Polymorphism (SNP)-profiling by Multiplexion (Heidelberg, Germany) as described recently [168]. Complete genotype information is compared to reference database, which currently comprises > 800 distinct STR-Profiling authenticated human reference cell lines. The SNP profiles matched known profiles or were unique.

6.4 Cytotoxicity assay

Cell viability was evaluated by the resazurin assay. This test is based on the reduction of the indicator dye, resazurin, to the highly fluorescent resorufin by viable cells. Nonviable cells

rapidly lose the metabolic capacity to reduce resazurin and, thus, do not produce a fluorescent signal [169].

In brief, adherent cells were harvested with 0.25% trypsin/EDTA (Invitrogen) and diluted to a final concentration 5×10^4 cells/mL. One hundred micro-liters of the cell suspension were sowed into the wells of a 96-well culture plate one day before treatment. For suspension cells, 2×10^4 cells were directly sowed prior to the assay in a 96-well culture plate in a total volume of 100 μL for each well. Marginal wells were filled with 200 μL of pure medium in order to minimize effects of evaporation. Besides, wells filled with medium served as the negative control to determine background fluorescence that may be present. Then cells were treated with different concentrations of the compound of interest alone or combined.

After 24 or 72 h, 20 μL resazurin (Sigma-Aldrich) 0.01% w/v in ddH$_2$O was added to each well and the plates were incubated at 37 °C for 4 h. Fluorescence was measured on an Infinite M2000 Proplate reader (Tecan) using an excitation wavelength of 544 nm and an emission wavelength of 590 nm. Each assay was done at least two times, with six replicates each. The cytotoxic effect of the treatment was determined as percentage of viability and compared to untreated cells. The toxicity of compounds was determined by means of the formula:

$$\text{Cell Viability (\% of control)} = \frac{\text{absorption from sample well - absorption from medium}}{\text{absorption from solvent treated cells - absorption from medium}} \times 100$$

The calculated cell viability (y-axis) was plotted against the log drug concentration (x-axis) using Microsoft Excel. The obtained curve was used to determine the IC$_{50}$ value, which represented the concentration of the test compound or the tested combination required to inhibit 50% of cell proliferation.

6.5 Assessment of combination effect

The effect of a combined treatment can be classified as additivity, in which the response of a drug combination is just what is expected from the dose-response relationships of drugs; synergism, in which the response is greater than expected; and antagonism, in which the response is less than expected [170]. Two most commonly used reference models to evaluate drug combination efficacy are the Bliss independence and Loewe additivity models. They

handle the same question from two different perspectives: the Bliss independence model focuses on treatment effect enhancement while the Loewe additivity model focuses on dose reduction [171].

6.5.1 Bliss independence model

The Bliss independence model was used to evaluate the combined effect of shikonin and derivatives with erlotinib. A theoretical curve was calculated for combined inhibition using the equation $E_{bliss} = E_A + E_B - E_A \times E_B$, where E_A and E_B were the fractional inhibitions obtained by drug A alone and drug B alone at specific concentrations. Here, E_{bliss} was the fractional inhibition that would be expected if the combination of the two drugs was exactly additive. If the experimentally measured fractional inhibition (E_{expt}) was greater than E_{bliss}, the combination was said to be synergistic. If E_{expt} was less than E_{bliss}, the combination was said to be antagonistic. For dose-response curves, the Bliss additivity value was calculated for varying doses of drug A when combined with a constant dose of drug B. This allowed an assessment of whether drug B affected the potency of drug A or shifted its intrinsic activity [108].

6.5.2 Loewe additivity model

The Loewe additivity model was used to confirm the drug interaction between erlotinib and shikonin in inhibiting cell growth and ΔEGFR phosphorylation [172, 173]. In this model, the combination index (CI) was defined as $CI = d1/D1 + d2/D2$, where D1 and D2 were the doses of drug 1 and drug 2 that produced an response Y (*e.g.* 50% inhibition of ΔEGFR phosphorylation) when used alone, d1 and d2 were the doses of drug 1 and drug 2 in combination, which can generate the same response Y. If the CI is equal, less than, or greater than 1, the combination dose (d1, d2) is termed as additive, synergistic or antagonistic, respectively. The drug interaction was illustrated geometrically by isobologram.

6.6 mRNA microarray gene expression profiling

6.6.1 RNA isolation

U937 cells were treated with shikonin, isobutyrylshikonin, β,β-dimethylacrylshikonin, isovalerylshikonin and 2-methylbutyrylshikonin, at IC$_{50}$ concentrations or DMSO as solvent control for 24 h, before total RNA was isolated using InviTrap spin Universal RNA Mini kit (STRATEC Molecular) according to the manufacture's instruction. RNA concentrations were determined using the nanodrop spectrophoto meter (Thermo Fisher).

6.6.2 Probe labeling and hybridization

Microarray hybridizations were performed in duplicates for treated samples and for control samples by the Genomics and Proteomics Core Facility at the German Cancer Research Center (DKFZ, Heidelberg, Germany).

Briefly, 1 μg total RNA was used for complementary DNA (cDNA) synthesis, followed by an amplification/labeling step (*in vitro* transcription) to synthesize biotin-labeled cRNA according to the MessageAmp II aRNA Amplification kit (Ambion). Biotin-labeled cRNA samples for hybridization on Illumina Human HT-12 BeadChip arrays were prepared according to Illumina's recommended sample labeling procedure based on the modified Eberwine protocol [174]. The cRNA was column purified according to TotalPrep™ RNA Amplification Kit (Life Technologies) and eluted in 60-80 μL water. Hybridization was performed according to the manufacture's instructions.

6.6.3 Scanning and data processing

Microarray scanning was done by the Genomics and Proteomics Core Facility at the German Cancer Research Center using an Illumina® BeadStation array scanner (Illumina), setting adjusted to a scaling factor of 1 and PMT settings at 430. Data was extracted for each individually, and outliers were removed, if the median absolute deviation (MAD) exceeded 2.5. Then, mean average signals and standard deviations were calculated for each probe. Data analysis was done by using the quantile normalization algorithm without background subtraction, and differentially regulated genes were defined by calculating the standard

deviation differences of a given probe in a one-by-one comparison of samples or groups.

6.6.4 Data analysis

Chipster analysis

The expression data sets obtained were further filtered with Chipster software, which is an analysis platform for high-throughput data. It includes the steps that filtering of genes by two times standard deviation and a subsequent assessment of significance using empirical Bayes t-test ($p < 0.05$) with Bonferroni correction.

Ingenuity pathway analysis

Filtered genes were fed into Ingenuity Pathway Analysis software (IPA; Ingenuity Systems Inc.), which allows to integrate the experimental data to known biological and chemical interactions, mechanisms and functions. It relies on the Ingenuity Knowledge Base, a frequently updated giant database of biological interactions and functional annotations gathered from literatures. Only molecules with an expression fold changes $\geq \pm 1.65$ were used for IPA analysis. Core Analyses using the Core Analysis tool were performed for all datasets to determine cellular networks and functions associated with deregulated mRNA that affected by each drug treatment. The results of the core analyses were further studied using the comparison analysis tool, offering the possibility to compare datasets of samples treated by different compounds.

6.7 Real-time RT PCR

Real-time RT-PCR was performed with the same samples used for microarray experiments. Total RNA samples were converted to cDNA with random hexamer primers by RevertAid H Minus First Strand cDNA Synthesis Kit (Thermo Scientific). Primers for real-time RT-PCR were designed by Primer Blast (http://www.ncbi.nlm.nih.gov/tools/primer-blast/) and selected according to their amplification specificities based on the sequence data from the NCBI RefSeq Human mRNA data base (http://www.ncbi.nlm.nih.gov/refseq/). The obtained primers were then input into Oligo Property Scans (MOPS) (https://ecom.mwgdna.com/services

/webgist/mops.tcl) for their usability. Oligonucleotides were synthesized by Eurofins MWG Operon and primer sequences are shown in Table 8. The efficiency of all primer pairs used for real-time PCR expression was better than 90%. Quantification of cDNA was performed on CFX384 Real-Time PCR Detection System (Bio-Rad) using a Hot Start Taq EvaGreen qPCR Mix (Axon). RT-PCR was performed with an initial denaturation at 95 °C for 10 min followed by 40 cycles including strand separation at 95 °C for 15 s, annealing at 57.4 °C for 40 s and extension at 72 °C for 1 min. After PCR product amplification, melting curves were computed. Expression levels were normalized to the transcription level of the housekeeping gene *RPS13*. All samples were run in duplicates and the experiment was repeated once.

Table 8: Primer sequences used for real-time RT-PCR

Target gene	Primer sequences
JUN	FW: 5'-GCCAACTCATGCTAACGCAG-3'
	REV: 5'-CTCTCCGTCGCAACTTGTCA-3'
GABARAP1	FW: 5'-GAAATGAGTGGTTGGAAGCCC-3'
	REV: 5'-TTCACCTTCTGTCTCCTTGCG-3'
LY96	FW: 5'-ACACCTACTGTGGGAGAGAT-3'
	REV: 5'-CGTCATCAGATCCTCGGCAA-3'
MYC	FW: 5'-AGAGTTTCATCTGCGACCCG-3'
	REV: 5'-GAAGCCGCTCCACATACAGT-3'
IFITM2	FW: 5'-CATCCCGGTAACCCGATCAC-3'
	REV: 5'-CCCAGCATAGCCACTTCCTG-3'
MS4A3	FW: 5'-GACAAGGTGGACTTGGGAGG-3'
	REV: 5'- CTGAACTACAGAACTTGGAGGCT-3'
RPS13	FW: 5'-GGTTGAAGTTGACATCTGACGA-3'
	REV: 5'-CTTGTGCAACACATGTGAAT-3'

6.8 Annexin V and PI double staining by flow cytometry

The U937 cell death mode induced by shikonin and its derivatives was analyzed by annexin V-PI double staining. Annexin V is an intracellular protein that calcium-dependently binds to phosphatidylserine (PS), which translocates from the intracellular leaflet of the plasma membrane to the external leaflet during early apoptosis. Propidium iodide (PI) is excluded by

living or early apoptotic cells with intact membranes and stains late apoptotic and necrotic cells with red fluorescence due to DNA intercalation. Therefore, cells with annexin V (-) and PI (-) are considered to be alive, while cells with annexin V (+) and PI (-) are in early apoptosis. Cells in late apoptosis or necrosis are both annexin V and PI positive.

Briefly, 5×10^5 U937 cells were were seeded into the wells of a 12-well culture plate (Thermo Scientific) and treated 50 μM necrostatin-1 (Nec-1; Enzo Life Sciences) or 50 μM z-VAD-fmk (Selleckchem) 1 h prior to co-incubation with IC_{50} concentrations of shikonin or its derivatives for 24 h. Following incubation, cells were collected and incubated with annexin V and PI staining solution (BioVision) according to the manufacturer's protocol. Subsequently, cells were transferred to a FACS tube (BD Biosciences) and measured with FACS Calibur analyzer (Becton-Dickinson Biosciences). For each sample, 2×10^4 cells were counted. The annexin V-FITC signal was measured with 488 nm excitation and detected using a 530/30 nm band pass filter. The PI signal was analyzed with 561 nm excitation and detected using a 610/20 nm band pass filter. All parameters were plotted on a logarithmic scale. Cytographs were analyzed using FlowJo software (Tree star).

6.9 DNA binding activity of c-MYC transcription factor

The c-MYC DNA binding activity assays were performed using TransAM enzyme-linked Immunosor Bent assay (ELISA)-based kits (Active Motif) according to the manufacturer's protocol. Briefly, 1×10^6 U937 cells were seeded into the wells of a 6-well culture plate (Thermo Scientific) and treated with indicated concentrations of control, shikonin, derivatives, 10074-G5 or 10058-F4. After 24 h, cells were harvested and nuclear proteins were extracted using NE-PER® Nuclear and Cytoplasmic Extraction Reagents (Thermo Scientific) supplemented with 1% Halt™ Protease Inhibitor Cocktail (Thermo Scientific). The concentrations of extracted nuclear protein were determined by NanoDrop 1000 spectrophotometer. 10 μg of nuclear extracts from control, shikonin, derivatives, 10074-G5 or 10058-F4-treated cells were separately incubated in a 96-well plate immobilized with an oligonucleotide containing the c-MYC consensus binding site (5'-CACGTG-3'). The active forms of transcription factors from extracts, which specifically bound to this oligonucleotide, were detected by a primary antibody against c-MYC in an ELISA-like format. The absorbance

of the sensitive colorimetric reaction mediated by a secondary HRP-conjugated antibody was measured on the Infinite M2000 Proplate reader (Tecan) at 450 nm with a reference wavelength of 655 nm.

6.10 Analysis of protein expression by Western blotting

6.10.1 Sample preparation

For adherent cells, 50×10^4 cells were sowed into the wells of a 6-well culture plate (Thermo Scientific) one day before treatment. For suspension cells, they were directly sowed prior to treatment. The cells were washed twice with PBS after treated with the indicated concentrations of the compound of interest alone or combined for 24 h and lysed in lysis buffer (M-PER Mammalian Protein Extraction Reagent, Thermo Scientific, plus protease inhibitor, Roche) containing phosphatase inhibitor (Roche). After shaking 30 min at 4 °C, the lysate was centrifuged at $14,000 \times$ g for 15 min and the supernatant was quantified by NanoDrop 1000 spectrophotometer.

6.10.2 SDS-PAGE and blotting

Equal amounts of protein extracts were separated on 10% SDS-PAGE and electroblotted onto a PVDF membrane using the Mini-PROTEAN® Tetra Cell system (Bio-Rad). In short, 30 µg protein were mixed with 4 µL 6 × sample loading buffer and H_2O to a final volume of 24 µL. Prior to electrophoresis, samples were boiled at 95°C for 10 min. 3 µL of Magic Mark Western Blot Standard protein ladder (Life Technologies) was loaded asides and run in parallel to estimate molecular weights of the protein. Samples were run through the stacking gel under 50 V and the voltage was increased up to 100 V and maintained till the end of electrophoresis. Then the separating samples were transferred to a Roti® PVDF blot membrane (Roth) by wet sandwich method at a 250 mA current for 2.5 h.

6.10.3 Antibody incubation and detection

After blotting, the membrane was first rinsed with TBST and then blocked with 5% (w/v) bovine serum albumin in TBST for 1 h at room temperature. The blocked membrane was subsequently incubated overnight at 4 °C with specific primary antibodies (Cell Signaling) that diluted 1:1000 in blocking solution. After washing for three times with TBST for 10 min, the membrane was incubated for 1 h at room temperature with HRP-conjugated secondary antibody (Cell Signaling) (1:2000 in blocking solution). After the membrane had been washed with TBST (3×10 min), the immunoreactivity was revealed by use of a Luminata Classico Western HRP Substrate (Millipore Corporation), and the densities of the protein bands were quantified by FluorChem Q software (Biozym Scientific Company). β-Actin was used as loading control.

6.10.4 Gel and Buffer recipes

The gels and buffers used in the experiments were prepared according to the following recipes:

Table 9: Preparation of SDS-PAGE

Stacking gel (4%)		Running gel (10%)	
H_2O	3.075 mL	H_2O	3.075 mL
0.5 M Tris-HCl (pH 6.8)	1.25 mL	1.5 M Tris-HCl (pH 8.8)	1.875 mL
20% SDS (w/v)	0.025 mL	20% SDS (w/v)	0.0375 mL
30% acrylamide/bis Solution, 29:1	0.67 mL	30% acrylamide/bis Solution, 29:1	2.475 mL
10% APS (w/v)	0.025 mL	10% APS (w/v)	0.0375 mL
TEMED	0.005 mL	TEMED	0.005 mL

Table 10: Buffers for SDS-PAGE

$6 \times$ sample loading buffer		Running buffer	
SDS	1.2 g	Tris-HCl	25 mM
Bromophenol Blue	0.006 g	Glycin	200 mM
Glycerol	4.7 mL	SDS (w/v)	0.1%
1 M Tris-HCl (pH 6.8)	0.6 mL	in H_2O	
H_2O	2.7 mL		
ß-Mercaptoethanol (v/v)	5%		

Table 11: Transfer buffer and washing buffer

Transfer buffer (Towbin buffer)		Tris-buffered saline Tween 20 (TBS-T)	
Tris	25 mM	Tris-HCl (pH 7.5)	20 mM
Glycine	192 mM	NaCl	500 mM
Methanol	20%	Tween 20 (w/v)	0.1%
in H_2O		in H_2O	

6.11 Molecular docking

The X-ray crystallography based structures of EGFR kinase (PDB code: 1M17) and MYC/MAX complex (PDB code: 1NKP) were obtained from RCSB Protein Data Bank (http://www.rcsb.org/pdb/home/home.do) and used as docking templates throughout the docking calculations. All bound waters and ligands were eliminated from the protein and the polar hydrogen was added to the protein. The 2D structures of shikonin and its derivatives were energy-minimised and converted to 3D structures compatible for docking operation using an open source program named Corina of the company Molecular Networks. The known inhibitors for EGFR, erlotinib and Mig6 (mitogen-induced gene 6, picked from the crystal structure of the complex between the EGFR kinase domain and aMig6 peptide, PDB code: 2RFD) were selected as standard to compare their binding modes with shikonin and its derivatives to EGFR kinase. Two known MYC inhibitors, 10074-G5 and 10058-F4, were used as control drugs to compare their binding modes and affinities with shikonin and its derivatives to MYC.

Molecular docking was then carried out with Autodock program (AutoDock 4.2, The Scripps Research Institute, La Jolla, CA, USA) following a protocol previously reported by us [175]. In brief, all the macromolecular and ligands were first converted to the PDBQT format files with AutodockTools 1.5.6rc3, the graphical user interface for Autodock 4.2 software (Molecular Graphics Laboratory). A grid box where the docking took place was then constructed in a way that it covered the binding sites of the target protein. Docking parameters were set to 100 runs and 2,500,000 energy evaluations for each cycle. The results were written in dlg files, which were later used to analyze the binding energies and the interacting amino acids for each ligand. VMD (Visual Molecular Dynamics) was used as visualization tool to further get a deeper

insight on the binding modes obtained from docking.

6.12 Statistical analysis

Results are represented as mean $\pm$ SEM. P-values were calculated by Student's t-test or right-tailed Fisher's exact test (IPA data). Differences were considered as significant at $P < 0.05$.

7 References

[1] Stewart BW, Wild C, International Agency for Research on Cancer, World Health Organization. World cancer report 2014.

[2] Ferlay J, Soerjomataram I, Dikshit R, Eser S, Mathers C, Rebelo M, et al. Cancer incidence and mortality worldwide: Sources, methods and major patterns in GLOBOCAN 2012.

[3] Vardiman JW, Thiele J, Arber DA, Brunning RD, Borowitz MJ, Porwit A, et al. The 2008 revision of the World Health Organization (WHO) classification of myeloid neoplasms and acute leukemia: rationale and important changes. Blood. 2009;114:937-51.

[4] Weiss RA. Multistage carcinogenesis. Br J Cancer. 2004;91:1981-2.

[5] Kufe DW, Pollock RE, Weichselbaum RR, Bast RC, Gansler TS, Holland JF, et al. Multistage Carcinogenesis. 2003.

[6] Cooper GM. The development and causes of cancer. 2000.

[7] Balis FM. The Goal of Cancer Treatment. The oncologist. 1998;3:V.

[8] DeVita VT, Jr., Chu E. A history of cancer chemotherapy. Cancer Res. 2008;68:8643-53.

[9] Malhotra V, Perry MC. Classical chemotherapy: mechanisms, toxicities and the therapeutic window. Cancer biology & therapy. 2003;2:S2-4.

[10] Lind MJ. Principles of cytotoxic chemotherapy. Medicine. 2011;39:711-6.

[11] Lotfi-Jam K, Carey M, Jefford M, Schofield P, Charleson C, Aranda S. Nonpharmacologic Strategies for Managing Common Chemotherapy Adverse Effects: A Systematic Review. Journal of Clinical Oncology. 2008;26:5618-29.

[12] Hanahan D, Weinberg RA. Hallmarks of cancer: the next generation. Cell. 2011;144:646-74.

[13] Gerber DE. Targeted therapies: a new generation of cancer treatments. American family physician. 2008;77:311-9.

[14] Vita M, Henriksson M. The Myc oncoprotein as a therapeutic target for human cancer. Seminars in cancer biology. 2006;16:318-30.

[15] Prochownik EV, Vogt PK. Therapeutic Targeting of Myc. Genes & cancer. 2010;1:650-9.

[16] Courtney KD, Corcoran RB, Engelman JA. The PI3K Pathway As Drug Target in Human Cancer. Journal of Clinical Oncology. 2010;28:1075-83.

[17] Vyas S, Chang P. New PARP targets for cancer therapy. Nature reviews Cancer. 2014;14:502-9.

[18] Link W, Madureira PA, Hill R. Identifying New Targets for Personalised Cancer Therapy. eLS: John Wiley & Sons, Ltd; 2001.

[19] Garraway LA, Janne PA. Circumventing cancer drug resistance in the era of personalized medicine. Cancer discovery. 2012;2:214-26.

[20] Lippert TH, Ruoff HJ, Volm M. Current status of methods to assess cancer drug resistance. International journal of medical sciences. 2011;8:245-53.

[21] Holohan C, Van Schaeybroeck S, Longley DB, Johnston PG. Cancer drug resistance: an evolving paradigm. Nature reviews Cancer. 2013;13:714-26.

[22] Lackner MR, Wilson TR, Settleman J. Mechanisms of acquired resistance to targeted cancer therapies. Future oncology. 2012;8:999-1014.

[23] Hammerman PS, Janne PA, Johnson BE. Resistance to Epidermal Growth Factor Receptor Tyrosine Kinase Inhibitors in Non-Small Cell Lung Cancer. Clinical cancer research : an official journal of the American Association for Cancer Research. 2009;15:7502-9.

[24] Pao W, Miller VA, Politi KA, Riely GJ, Somwar R, Zakowski MF, et al. Acquired resistance of lung adenocarcinomas to gefitinib or erlotinib is associated with a second

mutation in the EGFR kinase domain. PLoS medicine. 2005;2:225-35.

[25] Engelman JA, Zejnullahu K, Mitsudomi T, Song Y, Hyland C, Park JO, et al. MET amplification leads to gefitinib resistance in lung cancer by activating ERBB3 signaling. Science. 2007;316:1039-43.

[26] Szakacs G, Paterson JK, Ludwig JA, Booth-Genthe C, Gottesman MM. Targeting multidrug resistance in cancer. Nature reviews Drug discovery. 2006;5:219-34.

[27] Lin JH, Yamazaki M. Role of P-glycoprotein in pharmacokinetics: clinical implications. Clinical pharmacokinetics. 2003;42:59-98.

[28] Luqmani YA. Mechanisms of drug resistance in cancer chemotherapy. Medical principles and practice : international journal of the Kuwait University, Health Science Centre. 2005;14 Suppl 1:35-48.

[29] Thomas H, Coley HM. Overcoming multidrug resistance in cancer: an update on the clinical strategy of inhibiting p-glycoprotein. Cancer control : journal of the Moffitt Cancer Center. 2003;10:159-65.

[30] Al-Lazikani B, Banerji U, Workman P. Combinatorial drug therapy for cancer in the post-genomic era. Nat Biotechnol. 2012;30:679-91.

[31] Komarova NL, Boland CR. Cancer: calculated treatment. Nature. 2013;499:291-2.

[32] Bock C, Lengauer T. Managing drug resistance in cancer: lessons from HIV therapy. Nature reviews Cancer. 2012;12:494-501.

[33] Pinto AC, Moreira JN, Simões S. Combination chemotherapy in cancer: principles, evaluation and drug delivery strategies: INTECH Open Access Publisher; 2011.

[34] Trusheim MR, Berndt ER, Douglas FL. Stratified medicine: strategic and economic implications of combining drugs and clinical biomarkers. Nature reviews Drug discovery. 2007;6:287-93.

[35] Ouyang L, Luo Y, Tian M, Zhang SY, Lu R, Wang JH, et al. Plant natural products: from traditional compounds to new emerging drugs in cancer therapy. Cell proliferation. 2014;47:506-15.

[36] Buchanan BB, Gruissem W, Jones RL. Biochemistry & molecular biology of plants: American Society of Plant Physiologists Rockville, MD; 2000.

[37] Demain AL, Vaishnav P. Natural products for cancer chemotherapy. Microbial biotechnology. 2011;4:687-99.

[38] Feitelson MA, Arzumanyan A, Kulathinal RJ, Blain SW, Holcombe RF, Mahajna J, et al. Sustained proliferation in cancer: Mechanisms and novel therapeutic targets. Seminars in cancer biology: Elsevier; 2015.

[39] Mann J. Natural products in cancer chemotherapy: past, present and future. Nature reviews Cancer. 2002;2:143-8.

[40] Ovadje P, Roma A, Steckle M, Nicoletti L, Arnason JT, Pandey S. Advances in the research and development of natural health products as main stream cancer therapeutics. Evidence-based complementary and alternative medicine : eCAM. 2015;2015:751348.

[41] Agbarya A, Ruimi N, Epelbaum R, Ben-Arye E, Mahajna J. Natural products as potential cancer therapy enhancers: A preclinical update. SAGE Open Medicine. 2014;2.

[42] Pfisterer PH, Wolber G, Efferth T, Rollinger JM, Stuppner H. Natural products in structure-assisted design of molecular cancer therapeutics. Current pharmaceutical design. 2010;16:1718-41.

[43] Andujar I, Rios JL, Giner RM, Recio MC. Pharmacological properties of shikonin - a review of literature since 2002. Planta medica. 2013;79:1685-97.

[44] Papageorgiou VP, Assimopoulou AN, Couladouros EA, Hepworth D, Nicolaou KC. The Chemistry and Biology of Alkannin, Shikonin, and Related Naphthazarin Natural

Products. Angewandte Chemie International Edition. 1999;38:270-301.

[45] Chen X, Yang L, Oppenheim JJ, Howard MZ. Cellular pharmacology studies of shikonin derivatives. Phytotherapy research : PTR. 2002;16:199-209.

[46] Majima R, Kuroda C. The coloring matter of Lithospermum erythrorhizon. Acta Phytochem. 1922;1:43-65.

[47] Sankawa U, Otsuka H, Kataoka Y, Iitaka Y, Hoshi A, Kuretani K. Antitumor activity of shikonin, alkannin and their derivatives. II. X-ray analysis of cyclo-alkannin leucoacetate, tautomerism of alkannin and cyclo-alkannin and antitumor activity of alkannin derivatives. Chemical & pharmaceutical bulletin. 1981;29:116-22.

[48] Sankawa U, Ebizuka Y, Miyazaki T, Isomura Y, Otsuka H. Antitumor activity of shikonin and its derivatives. Chemical & pharmaceutical bulletin. 1977;25:2392-5.

[49] Duan D, Zhang B, Yao J, Liu Y, Fang J. Shikonin targets cytosolic thioredoxin reductase to induce ROS-mediated apoptosis in human promyelocytic leukemia HL-60 cells. Free Radical Biology and Medicine. 2014;70:182-93.

[50] Hashimoto S, Xu M, Masuda Y, Aiuchi T, Nakajo S, Cao J, et al. ß-Hydroxyisovalerylshikonin Inhibits the Cell Growth of Various Cancer Cell Lines and Induces Apoptosis in Leukemia HL–60 Cells through a Mechanism Different from Those of Fas and Etoposide. Journal of biochemistry. 1999;125:17-23.

[51] Zhang Y, Qian RQ, Li PP. Shikonin, an ingredient of Lithospermum erythrorhizon, down-regulates the expression of steroid sulfatase genes in breast cancer cells. Cancer Lett. 2009;284:47-54.

[52] Yao Y, Zhou Q. A novel antiestrogen agent Shikonin inhibits estrogen-dependent gene transcription in human breast cancer cells. Breast cancer research and treatment. 2010;121:233-40.

[53] Chen CH, Lin ML, Ong PL, Yang JT. Novel multiple apoptotic mechanism of shikonin in human glioma cells. Annals of surgical oncology. 2012;19:3097-106.

[54] Zhao Q, Kretschmer N, Bauer R, Efferth T. Shikonin and its derivatives inhibit the epidermal growth factor receptor signaling and synergistically kill glioblastoma cells in combination with erlotinib. International journal of cancer Journal international du cancer. 2015;137:1446-56.

[55] Yeh CC, Kuo HM, Li TM, Lin JP, Yu FS, Lu HF, et al. Shikonin-induced apoptosis involves caspase-3 activity in a human bladder cancer cell line (T24). In vivo. 2007;21:1011-9.

[56] Hashimoto S, Xu Y, Masuda Y, Aiuchi T, Nakajo S, Uehara Y, et al. Beta-hydroxyisovalerylshikonin is a novel and potent inhibitor of protein tyrosine kinases. Jpn J Cancer Res. 2002;93:944-51.

[57] Andujar I, Recio MC, Giner RM, Rios JL. Traditional chinese medicine remedy to jury: the pharmacological basis for the use of shikonin as an anticancer therapy. Current medicinal chemistry. 2013;20:2892-8.

[58] Xuan Y, Hu X. Naturally-occurring shikonin analogues--a class of necroptotic inducers that circumvent cancer drug resistance. Cancer Lett. 2009;274:233-42.

[59] Fu Z, Deng B, Liao Y, Shan L, Yin F, Wang Z, et al. The anti-tumor effect of shikonin on osteosarcoma by inducing RIP1 and RIP3 dependent necroptosis. BMC cancer. 2013;13:580.

[60] Zhang FL, Wang P, Liu YH, Liu LB, Liu XB, Li Z, et al. Topoisomerase I inhibitors, shikonin and topotecan, inhibit growth and induce apoptosis of glioma cells and glioma stem cells. Plos One. 2013;8:e81815.

[61] Wada N, Kawano Y, Fujiwara S, Kikukawa Y, Okuno Y, Tasaki M, et al. Shikonin, dually

functions as a proteasome inhibitor and a necroptosis inducer in multiple myeloma cells. International journal of oncology. 2015;46:963-72.

[62] Guo XP, Zhang XY, Zhang SD. [Clinical trial on the effects of shikonin mixture on later stage lung cancer]. Zhong xi yi jie he za zhi = Chinese journal of modern developments in traditional medicine / Zhongguo Zhong xi yi jie he yan jiu hui. 1991;11:598-9, 80.

[63] Roskoski R, Jr. The ErbB/HER family of protein-tyrosine kinases and cancer. Pharmacological research : the official journal of the Italian Pharmacological Society. 2014;79:34-74.

[64] Urruticoechea A, Alemany R, Balart J, Villanueva A, Vinals F, Capella G. Recent advances in cancer therapy: an overview. Current pharmaceutical design. 2010;16:3-10.

[65] Herbst RS. Review of epidermal growth factor receptor biology. International journal of radiation oncology, biology, physics. 2004;59:21-6.

[66] Kuan CT, Wikstrand CJ, Bigner DD. EGF mutant receptor vIII as a molecular target in cancer therapy. Endocrine-related cancer. 2001;8:83-96.

[67] Gomperts BD, Kramer IM, Tatham PE. Signal transduction: Academic Press; 2009.

[68] Yewale C, Baradia D, Vhora I, Patil S, Misra A. Epidermal growth factor receptor targeting in cancer: a review of trends and strategies. Biomaterials. 2013;34:8690-707.

[69] Voldborg BR, Damstrup L, Spang-Thomsen M, Poulsen HS. Epidermal growth factor receptor (EGFR) and EGFR mutations, function and possible role in clinical trials. Annals of oncology : official journal of the European Society for Medical Oncology / ESMO. 1997;8:1197-206.

[70] Nyati MK, Morgan MA, Feng FY, Lawrence TS. Integration of EGFR inhibitors with radiochemotherapy. Nature reviews Cancer. 2006;6:876-85.

[71] Spano JP, Fagard R, Soria JC, Rixe O, Khayat D, Milano G. Epidermal growth factor receptor signaling in colorectal cancer: preclinical data and therapeutic perspectives. Annals of oncology : official journal of the European Society for Medical Oncology / ESMO. 2005;16:189-94.

[72] Lee J, Moon C. Current status of experimental therapeutics for head and neck cancer. Experimental biology and medicine. 2011;236:375-89.

[73] Zhang Z, Stiegler AL, Boggon TJ, Kobayashi S, Halmos B. EGFR-mutated lung cancer: a paradigm of molecular oncology. Oncotarget. 2010;1:497-514.

[74] Gan HK, Cvrljevic AN, Johns TG. The epidermal growth factor receptor variant III (EGFRvIII): where wild things are altered. The FEBS journal. 2013;280:5350-70.

[75] Heimberger AB, Hlatky R, Suki D, Yang D, Weinberg J, Gilbert M, et al. Prognostic effect of epidermal growth factor receptor and EGFRvIII in glioblastoma multiforme patients. Clinical Cancer Research. 2005;11:1462-6.

[76] Gan HK, Kaye AH, Luwor RB. The EGFRvIII variant in glioblastoma multiforme. Journal of clinical neuroscience : official journal of the Neurosurgical Society of Australasia. 2009;16:748-54.

[77] Hatanpaa KJ, Burma S, Zhao DW, Habib AA. Epidermal Growth Factor Receptor in Glioma: Signal Transduction, Neuropathology, Imaging, and Radioresistance. Neoplasia. 2010;12:675-84.

[78] Taylor TE, Furnari FB, Cavenee WK. Targeting EGFR for treatment of glioblastoma: molecular basis to overcome resistance. Current cancer drug targets. 2012;12:197-209.

[79] Ciardiello F, Tortora G. A novel approach in the treatment of cancer: targeting the epidermal growth factor receptor. Clinical cancer research : an official journal of the American Association for Cancer Research. 2001;7:2958-70.

[80] Prados MD, Chang SM, Butowski N, DeBoer R, Parvataneni R, Carliner H, et al. Phase II

Study of Erlotinib Plus Temozolomide During and After Radiation Therapy in Patients With Newly Diagnosed Glioblastoma Multiforme or Gliosarcoma. Journal of Clinical Oncology. 2009;27:579-84.

[81] Zhu JJ, Wong ET. Personalized medicine for glioblastoma: current challenges and future opportunities. Current molecular medicine. 2013;13:358-67.

[82] Sertel S, Plinkert PK, Efferth T. Natural Products Derived from Traditional Chinese Medicine as Novel Inhibitors of the Epidermal Growth Factor Receptor. Comb Chem High T Scr. 2010;13:849-54.

[83] Chen BJ, Wu YL, Tanaka Y, Zhang W. Small molecules targeting c-Myc oncogene: promising anti-cancer therapeutics. International journal of biological sciences. 2014;10:1084-96.

[84] Hoffman B, Amanullah A, Shafarenko M, Liebermann DA. The proto-oncogene c-myc in hematopoietic development and leukemogenesis. Oncogene. 2002;21:3414-21.

[85] Tansey WP. Mammalian MYC Proteins and Cancer. New Journal of Science. 2014;2014:27.

[86] Meyer N, Penn LZ. Reflecting on 25 years with MYC. Nature reviews Cancer. 2008;8:976-90.

[87] Dang CV, O'Donnell KA, Zeller KI, Nguyen T, Osthus RC, Li F. The c-Myc target gene network. Seminars in cancer biology. 2006;16:253-64.

[88] Zajac-Kaye M. Myc oncogene: a key component in cell cycle regulation and its implication for lung cancer. Lung cancer. 2001;34 Suppl 2:S43-6.

[89] McKeown MR, Bradner JE. Therapeutic strategies to inhibit MYC. Cold Spring Harbor perspectives in medicine. 2014;4.

[90] Delgado MD, Albajar M, Gomez-Casares MT, Batlle A, Leon J. MYC oncogene in myeloid neoplasias. Clinical & translational oncology : official publication of the Federation of Spanish Oncology Societies and of the National Cancer Institute of Mexico. 2013;15:87-94.

[91] Delgado MD, Leon J. Myc roles in hematopoiesis and leukemia. Genes & cancer. 2010;1:605-16.

[92] Harris AW, Pinkert CA, Crawford M, Langdon WY, Brinster RL, Adams JM. The E mu-myc transgenic mouse. A model for high-incidence spontaneous lymphoma and leukemia of early B cells. The Journal of experimental medicine. 1988;167:353-71.

[93] Varmus HE. The molecular genetics of cellular oncogenes. Annual review of genetics. 1984;18:553-612.

[94] Fauriat C, Olive D. AML drug resistance: c-Myc comes into play2014.

[95] Pan XN, Chen JJ, Wang LX, Xiao RZ, Liu LL, Fang ZG, et al. Inhibition of c-Myc overcomes cytotoxic drug resistance in acute myeloid leukemia cells by promoting differentiation. Plos One. 2014;9:e105381.

[96] Xia B, Tian C, Guo S, Zhang L, Zhao D, Qu F, et al. c-Myc plays part in drug resistance mediated by bone marrow stromal cells in acute myeloid leukemia. Leukemia research. 2015;39:92-9.

[97] Kiessling A, Sperl B, Hollis A, Eick D, Berg T. Selective inhibition of c-Myc/Max dimerization and DNA binding by small molecules. Chemistry & biology. 2006;13:745-51.

[98] Yap JL, Chauhan J, Jung K-Y, Chen L, Prochownik EV, Fletcher S. Small-molecule inhibitors of dimeric transcription factors: Antagonism of protein-protein and protein-DNA interactions. MedChemComm. 2012;3:541-51.

[99] Hammoudeh DI, Follis AV, Prochownik EV, Metallo SJ. Multiple independent binding

sites for small-molecule inhibitors on the oncoprotein c-Myc. Journal of the American Chemical Society. 2009;131:7390-401.

[100] Yap JL, Wang H, Hu A, Chauhan J, Jung KY, Gharavi RB, et al. Pharmacophore identification of c-Myc inhibitor 10074-G5. Bioorganic & medicinal chemistry letters. 2013;23:370-4.

[101] Albihn A, Johnsen JI, Henriksson MA. MYC in oncogenesis and as a target for cancer therapies. Advances in cancer research. 2010;107:163-224.

[102] Marampon F, Ciccarelli C, Zani BM. Down-regulation of c-Myc following MEK/ERK inhibition halts the expression of malignant phenotype in rhabdomyosarcoma and in non muscle-derived human tumors. Molecular cancer. 2006;5:31.

[103] Jain M, Arvanitis C, Chu K, Dewey W, Leonhardt E, Trinh M, et al. Sustained loss of a neoplastic phenotype by brief inactivation of MYC. Science. 2002;297:102-4.

[104] Wu C-H, van Riggelen J, Yetil A, Fan AC, Bachireddy P, Felsher DW. Cellular senescence is an important mechanism of tumor regression upon c-Myc inactivation. Proceedings of the National Academy of Sciences of the United States of America. 2007;104:13028-33.

[105] Shachaf CM, Kopelman AM, Arvanitis C, Karlsson A, Beer S, Mandl S, et al. MYC inactivation uncovers pluripotent differentiation and tumour dormancy in hepatocellular cancer. Nature. 2004;431:1112-7.

[106] Buck E, Eyzaguirre A, Brown E, Petti F, McCormack S, Haley JD, et al. Rapamycin synergizes with the epidermal growth factor receptor inhibitor erlotinib in non-small-cell lung, pancreatic, colon, and breast tumors. Mol Cancer Ther. 2006;5:2676-84.

[107] Borisy AA, Elliott PJ, Hurst NW, Lee MS, Lehar J, Price ER, et al. Systematic discovery of multicomponent therapeutics. Proceedings of the National Academy of Sciences of the United States of America. 2003;100:7977-82.

[108] Buck E, Eyzaguirre A, Brown E, Petti F, McCormack S, Haley JD, et al. Rapamycin synergizes with the epidermal growth factor receptor inhibitor erlotinib in non-small-cell lung, pancreatic, colon, and breast tumors. Mol Cancer Ther. 2006;5:2676-84.

[109] Schulte A, Liffers K, Kathagen A, Riethdorf S, Zapf S, Merlo A, et al. Erlotinib resistance in EGFR-amplified glioblastoma cells is associated with upregulation of EGFRvIII and PI3Kp110delta. Neuro-oncology. 2013;15:1289-301.

[110] Gebhart GF. Comments on the Isobole Method for Analysis of Drug-Interactions. Pain. 1992;51:381-.

[111] Zhang X, Pickin KA, Bose R, Jura N, Cole PA, Kuriyan J. Inhibition of the EGF receptor by binding of MIG6 to an activating kinase domain interface. Nature. 2007;450:741-4.

[112] Wiench B, Eichhorn T, Paulsen M, Efferth T. Shikonin Directly Targets Mitochondria and Causes Mitochondrial Dysfunction in Cancer Cells. Evid-Based Compl Alt. 2012.

[113] Zhu J, Blenis J, Yuan J. Activation of PI3K/Akt and MAPK pathways regulates Myc-mediated transcription by phosphorylating and promoting the degradation of Mad1. Proceedings of the National Academy of Sciences of the United States of America. 2008;105:6584-9.

[114] Zhang W, Liu HT. MAPK signal pathways in the regulation of cell proliferation in mammalian cells. Cell research. 2002;12:9-18.

[115] Gramling MW, Eischen CM. Suppression of Ras/Mapk pathway signaling inhibits Myc-induced lymphomagenesis. Cell death and differentiation. 2012;19:1220-7.

[116] Cui XR, Tsukada M, Suzuki N, Shimamura T, Gao L, Koyanagi J, et al. Comparison of the cytotoxic activities of naturally occurring hydroxyanthraquinones and hydroxynaphthoquinones. European journal of medicinal chemistry. 2008;43:1206-15.

[117] Ahn BZ, Baik KU, Kweon GR, Lim K, Hwang BD. Acylshikonin analogues: synthesis and inhibition of DNA topoisomerase-I. J Med Chem. 1995;38:1044-7.

[118] Lu Q, Liu W, Ding J, Cai J, Duan W. Shikonin derivatives: synthesis and inhibition of human telomerase. Bioorganic & medicinal chemistry letters. 2002;12:1375-8.

[119] Huang C, Luo Y, Zhao J, Yang F, Zhao H, Fan W, et al. Shikonin kills glioma cells through necroptosis mediated by RIP-1. Plos One. 2013;8:e66326.

[120] Singh F, Gao DY, Lebwohl MG, Wei HC. Shikonin modulates cell proliferation by inhibiting epidermal growth factor receptor signaling in human epidermoid carcinoma cells. Cancer Lett. 2003;200:115-21.

[121] Garcia-Claver A, Lorente M, Mur P, Campos-Martin Y, Mollejo M, Velasco G, et al. Gene expression changes associated with erlotinib response in glioma cell lines. Eur J Cancer. 2013;49:1641-53.

[122] Yamasaki F, Zhang D, Bartholomeusz C, Sudo T, Hortobagyi GN, Kurisu K, et al. Sensitivity of breast cancer cells to erlotinib depends on cyclin-dependent kinase 2 activity. Mol Cancer Ther. 2007;6:2168-77.

[123] Sirotnak FM, Zakowski MF, Miller VA, Scher HI, Kris MG. Efficacy of cytotoxic agents against human tumor xenografts is markedly enhanced by coadministration of ZD1839 (Iressa), an inhibitor of EGFR tyrosine kinase. Clinical Cancer Research. 2000;6:4885-92.

[124] Wakeling AE, Guy SP, Woodburn JR, Ashton SE, Curry BJ, Barker AJ, et al. ZD1839 (Iressa): an orally active inhibitor of epidermal growth factor signaling with potential for cancer therapy. Cancer Res. 2002;62:5749-54.

[125] Glaysher S, Bolton LM, Johnson P, Atkey N, Dyson M, Torrance C, et al. Targeting EGFR and PI3K pathways in ovarian cancer. Brit J Cancer. 2013;109:1786-94.

[126] Karpel-Massler G, Westhoff MA, Zhou S, Nonnenmacher L, Dwucet A, Kast RE, et al. Combined inhibition of HER1/EGFR and RAC1 results in a synergistic antiproliferative effect on established and primary cultured human glioblastoma cells. Mol Cancer Ther. 2013;12:1783-95.

[127] Bijnsdorp IV, Kruyt FA, Fukushima M, Smid K, Gokoel S, Peters GJ. Molecular mechanism underlying the synergistic interaction between trifluorothymidine and the epidermal growth factor receptor inhibitor erlotinib in human colorectal cancer cell lines. Cancer Sci. 2010;101:440-7.

[128] Li T, Ling YH, Perez-Soler R. Tumor dependence on the EGFR signaling pathway expressed by the p-EGFR:p-AKT ratio predicts erlotinib sensitivity in human non-small cell lung cancer (NSCLC) cells expressing wild-type EGFR gene. Journal of Thoracic Oncology. 2008;3:643-7.

[129] Klein S, Levitzki A. Targeting the EGFR and the PKB pathway in cancer. Current opinion in cell biology. 2009;21:185-93.

[130] Chen Y, Zheng L, Liu J, Zhou Z, Cao X, Lv X, et al. Shikonin inhibits prostate cancer cells metastasis by reducing matrix metalloproteinase-2/-9 expression via AKT/mTOR and ROS/ERK1/2 pathways. International immunopharmacology. 2014;21:447-55.

[131] Wiench B, Chen YR, Paulsen M, Hamm R, Schroder S, Yang NS, et al. Integration of Different "-omics" Technologies Identifies Inhibition of the IGF1R-Akt-mTOR Signaling Cascade Involved in the Cytotoxic Effect of Shikonin against Leukemia Cells. Evidence-based complementary and alternative medicine : eCAM. 2013;2013:818709.

[132] Kanzawa T, Germano IM, Kondo Y, Ito H, Kyo S, Kondo S. Inhibition of telomerase activity in malignant glioma cells correlates with their sensitivity to temozolomide. Br J Cancer. 2003;89:922-9.

[133] Nakaya K, Miyasaka T. A shikonin derivative, beta-hydroxyisovaleryishikonin, is an

ATP-non-competitive inhibitor of protein tyrosine kinases. Anticancer Drugs. 2003;14:683-93.

[134] Calonghi N, Pagnotta E, Parolin C, Mangano C, Bolognesi ML, Melchiorre C, et al. A new EGFR inhibitor induces apoptosis in colon cancer cells. Biochemical and Biophysical Research Communications. 2007;354:409-13.

[135] Efferth T, Koch E. Complex interactions between phytochemicals. The multi-target therapeutic concept of phytotherapy. Current drug targets. 2011;12:122-32.

[136] Bieker R, Lerchenmuller C, Wehmeyer J, Serve HL, Mesters RM, Buchner T, et al. Phase I study of liposomal daunorubicin in relapsed and refractory acute myeloid leukemia. Oncol Rep. 2003;10:915-20.

[137] Gorin NC, Estey E, Jones RJ, Levitsky HI, Borrello I, Slavin S. New Developments in the Therapy of Acute Myelocytic Leukemia. Hematology / the Education Program of the American Society of Hematology American Society of Hematology Education Program. 2000:69-89.

[138] Jeong K-C, Ahn K-O, Yang C-H. Small-molecule inhibitors of c-Myc transcriptional factor suppress proliferation and induce apoptosis of promyelocytic leukemia cell via cell cycle arrest. Molecular BioSystems. 2010;6:1503-9.

[139] Sanchez-Duffhues G, Calzado MA, de Vinuesa AG, Appendino G, Fiebich BL, Loock U, et al. Denbinobin inhibits nuclear factor-kappaB and induces apoptosis via reactive oxygen species generation in human leukemic cells. Biochemical pharmacology. 2009;77:1401-9.

[140] Thangapazham RL, Singh AK, Seth P, Misra N, Mathad VT, Raj K, et al. Shikonin analogue (SA) 93/637 induces apoptosis by activation of caspase-3 in U937 cells. Frontiers in bioscience : a journal and virtual library. 2008;13:561-8.

[141] Bretones G, Delgado MD, Leon J. Myc and cell cycle control. Biochimica et biophysica acta. 2015;1849:506-16.

[142] Heikkila R, Schwab G, Wickstrom E, Loke SL, Pluznik DH, Watt R, et al. A c-myc antisense oligodeoxynucleotide inhibits entry into S phase but not progress from G0 to G1. Nature. 1987;328:445-9.

[143] Wickstrom EL, Bacon TA, Gonzalez A, Freeman DL, Lyman GH, Wickstrom E. Human promyelocytic leukemia HL-60 cell proliferation and c-myc protein expression are inhibited by an antisense pentadecadeoxynucleotide targeted against c-myc mRNA. Proceedings of the National Academy of Sciences of the United States of America. 1988;85:1028-32.

[144] Zhao L, Ye P, Gonda TJ. The MYB proto-oncogene suppresses monocytic differentiation of acute myeloid leukemia cells via transcriptional activation of its target gene GFI1. Oncogene. 2014;33:4442-9.

[145] Pattabiraman DR, Gonda TJ. Role and potential for therapeutic targeting of MYB in leukemia. Leukemia. 2013;27:269-77.

[146] Kutok JL, Yang X, Folkerth R, Adra CN. Characterization of the expression of HTm4 (MS4A3), a cell cycle regulator, in human peripheral blood cells and normal and malignant tissues. Journal of cellular and molecular medicine. 2011;15:86-93.

[147] Donato JL, Ko J, Kutok JL, Cheng T, Shirakawa T, Mao XQ, et al. Human HTm4 is a hematopoietic cell cycle regulator. J Clin Invest. 2002;109:51-8.

[148] Piao JL, Cui ZG, Furusawa Y, Ahmed K, Rehman MU, Tabuchi Y, et al. The molecular mechanisms and gene expression profiling for shikonin-induced apoptotic and necroptotic cell death in U937 cells. Chemico-biological interactions. 2013;205:119-27.

[149] Thompson EB. The many roles of c-Myc in apoptosis. Annual review of physiology.

1998;60:575-600.

[150] Hoffman B, Liebermann DA. Apoptotic signaling by c-MYC. Oncogene. 2008;27:6462-72.

[151] Ayala-Torres S, Zhou F, Thompson EB. Apoptosis induced by oxysterol in CEM cells is associated with negative regulation of c-myc. Experimental cell research. 1999;246:193-202.

[152] Lerga A, Belandia B, Delgado MD, Cuadrado MA, Richard C, Ortiz JM, et al. Down-regulation of c-Myc and Max genes is associated to inhibition of protein phosphatase 2A in K562 human leukemia cells. Biochem Biophys Res Commun. 1995;215:889-95.

[153] Kimura S, Maekawa T, Hirakawa K, Murakami A, Abe T. Alterations of c-myc expression by antisense oligodeoxynucleotides enhance the induction of apoptosis in HL-60 cells. Cancer Res. 1995;55:1379-84.

[154] Huang MJ, Cheng YC, Liu CR, Lin S, Liu HE. A small-molecule c-Myc inhibitor, 10058-F4, induces cell-cycle arrest, apoptosis, and myeloid differentiation of human acute myeloid leukemia. Experimental hematology. 2006;34:1480-9.

[155] Cheng YW, Chang CY, Lin KL, Hu CM, Lin CH, Kang JJ. Shikonin derivatives inhibited LPS-induced NOS in RAW 264.7 cells via downregulation of MAPK/NF-kappaB signaling. Journal of ethnopharmacology. 2008;120:264-71.

[156] Mao X, Yu CR, Li WH, Li WX. Induction of apoptosis by shikonin through a ROS/JNK-mediated process in Bcr/Abl-positive chronic myelogenous leukemia (CML) cells. Cell research. 2008;18:879-88.

[157] Ahn J, Won M, Choi JH, Kim YS, Jung CR, Im DS, et al. Reactive oxygen species-mediated activation of the Akt/ASK1/p38 signaling cascade and p21(Cip1) downregulation are required for shikonin-induced apoptosis. Apoptosis : an international journal on programmed cell death. 2013;18:870-81.

[158] Sears R, Nuckolls F, Haura E, Taya Y, Tamai K, Nevins JR. Multiple Ras-dependent phosphorylation pathways regulate Myc protein stability. Genes & development. 2000;14:2501-14.

[159] Alarcon-Vargas D, Ronai Z. c-Jun-NH2 kinase (JNK) contributes to the regulation of c-Myc protein stability. The Journal of biological chemistry. 2004;279:5008-16.

[160] Hofmann JW, Zhao X, De Cecco M, Peterson AL, Pagliaroli L, Manivannan J, et al. Reduced expression of MYC increases longevity and enhances healthspan. Cell. 2015;160:477-88.

[161] Rajagopalan V, Vaidyanathan M, Janardhanam VA, Bradner JE. Pre-clinical analysis of changes in intra-cellular biochemistry of glioblastoma multiforme (GBM) cells due to c-Myc silencing. Cellular and molecular neurobiology. 2014;34:1059-69.

[162] Tan Y, Sementino E, Pei J, Kadariya Y, Ito TK, Testa JR. Co-targeting of Akt and Myc inhibits viability of lymphoma cells from Lck-Dlx5 mice. Cancer biology & therapy. 2015;16:580-8.

[163] Arita K, Tsuzuki S, Ohshima K, Sugiyama T, Seto M. Synergy of Myc, cell cycle regulators and the Akt pathway in the development of aggressive B-cell lymphoma in a mouse model. Leukemia. 2014;28:2270-2.

[164] Saeed M, Greten H, Efferth T. Collateral Sensitivity in Drug-Resistant Tumor Cells. In: Bonavida B, editor. Molecular Mechanisms of Tumor Cell Resistance to Chemotherapy: Springer New York; 2013. p. 187-211.

[165] Damianakos H, Kretschmer N, Syklowska-Baranek K, Pietrosiuk A, Bauer R, Chinou I. Antimicrobial and cytotoxic isohexenylnaphthazarins from Arnebia euchroma (Royle) Jonst. (Boraginaceae) callus and cell suspension culture. Molecules. 2012;17:14310-22.

[166] Kretschmer N, Rinner B, Deutsch AJA, Lohberger B, Knausz H, Kunert O, et al. Naphthoquinones from Onosma paniculata Induce Cell-Cycle Arrest and Apoptosis in Melanoma Cells. Journal of natural products. 2012;75:865-9.

[167] Jones G, Machado J, Jr., Merlo A. Loss of focal adhesion kinase (FAK) inhibits epidermal growth factor receptor-dependent migration and induces aggregation of nh(2)-terminal FAK in the nuclei of apoptotic glioblastoma cells. Cancer Res. 2001;61:4978-81.

[168] Castro F, Dirks WG, Fahnrich S, Hotz-Wagenblatt A, Pawlita M, Schmitt M. High-throughput SNP-based authentication of human cell lines. International journal of cancer Journal international du cancer. 2013;132:308-14.

[169] O'Brien J, Wilson I, Orton T, Pognan F. Investigation of the Alamar Blue (resazurin) fluorescent dye for the assessment of mammalian cell cytotoxicity. European journal of biochemistry / FEBS. 2000;267:5421-6.

[170] Lee SI. Drug interaction: focusing on response surface models. Korean journal of anesthesiology. 2010;58:421-34.

[171] Zhao W, Sachsenmeier K, Zhang LJ, Sult E, Hollingsworth RE, Yang H. A New Bliss Independence Model to Analyze Drug Combination Data. Journal of biomolecular screening. 2014;19:817-21.

[172] Lee JJ, Kong M, Ayers GD, Lotan R. Interaction index and different methods for determining drug interaction in combination therapy. J Biopharm Stat. 2007;17:461-80.

[173] Zhang W, Peyton M, Xie Y, Soh J, Minna JD, Gazdar AF, et al. Histone deacetylase inhibitor romidepsin enhances anti-tumor effect of erlotinib in non-small cell lung cancer (NSCLC) cell lines. Journal of thoracic oncology : official publication of the International Association for the Study of Lung Cancer. 2009;4:161-6.

[174] Eberwine J, Yeh H, Miyashiro K, Cao Y, Nair S, Finnell R, et al. Analysis of gene expression in single live neurons. Proceedings of the National Academy of Sciences of the United States of America. 1992;89:3010-4.

[175] Zhao Q, Zeino M, Eichhorn T, Herrmann J, Müller R, Efferth T. Molecular docking studies of myxobacterial disorazoles and tubulysins to tubulin. The Journal of Bioscience and Medicine. 2013;3.

8 Appendix

8.1 Publications

Original publications as lead author

➢ Zhao Q, Kretschmer N, Bauer R and Efferth T. Shikonin and its derivatives inhibit the epidermal growth factor receptor signaling and synergistically kill glioblastoma cells in combination with erlotinib. International journal of cancer Journal international du cancer. 2015; 137(6):1446-1456.

Original publications as co-author

➢ M. Zeino, Q. Zhao, T. Eichhorn, J. Hermann, and R. Müller, "Molecular docking studies of myxobacterial disorazoles and tubulysins to tubulin," *Journal of Bioscience and Medicine,* vol. 3, pp. 31-43, 2013

Submitted manuscripts (meanwhile accepted)

➢ Zhao Q, Assimopoulou A, Klauck S, Damianakos H, Chinou I, Kretschmer N, Rios J, Papageorgiou V, Bauer R and Efferth T. Inhibition of c-MYC with involvement of ERK/JNK/MAPK and AKT pathways as a novel mechanism for shikonin and its derivatives in killing leukemia cells. *Oncotarget*. 2015

Poster

➢ Zhao Q, Kretschmer N, Bauer R and Efferth T. "Shikonin and its derivatives inhibit the epidermal growth factor receptor signaling and synergistically kill glioblastoma cells in combination with erlotinib" [Poster], 128th meeting of the Gesellschaft Deutscher Naturforscher und Ärzte (GDNÄ) "Vorbild Natur: Faszination Mensch und Technologie", Mainz, 2014.

8.2 Curriculum Vitae